LA--12020

DE91 008497

Structure of Shocks in Solids and Liquids: Six Reprints with an Introduction

Duane C. Wallace

Los Alamos National Laboratory
Los Alamos, New Mexico 87545

ABSTRACT

This monograph consists of six papers on the theory of shocks in solids and iiquids, reprinted from *Physical Review*, together with an introduction summarizing the complete shock theory and its limitations.

ACKNOWLEDGMENT

The six papers from *Physical Review* are reprinted with permission of the American Physical Society.

CONTENTS

NOTATION

ρ = mass density

$V = \rho^{-1}$ = volume per unit mass

T = temperature

U = internal energy per unit mass

S = entropy per unit mass

i, j = Cartesian coordinates

τ_{ij} = stresses

ε^{e}_{ij} = elastic strains

ε^{p}_{ij} = plastic strains

τ = effective shear stress (non-negative)

ψ = effective plastic strain (non-negative)

NOTATION FOR PLANEWAVE GEOMETRY

σ = normal stress

τ = shear stress

ε = total compression

ψ = plastic strain

1 INTRODUCTION

In the early 1980s, six papers concerning the nature of shocks in solids and liquids appeared in *Physical Review*. These papers, constituting a comprehensive analysis of the shock structure in dense materials, are reprinted in this monograph. The theoretical basis of this analysis, and its limitations, are described in this Chapter, and a brief summary of the main points of each paper is provided in Chapter 2.

In the classic text of Courant and Friedrichs,[1] a shock is treated as a discontinuity surface, across which physical properties change discontinuously. In order to elucidate the complete shock process, which is hidden within the mathematical discontinuity of Courant and Friedrichs, one has to begin from an opposite point of view: a shock is a continuous process, and in fact no discontinuity is allowable in the physical solution for a shock. In the present work, the term shock is used to mean the concrete continuous process of a compressive wave, from the initial state to the final (Hugoniot) state.

The material considered is a crystalline solid or a liquid, initially isotropic, but passing through a sequence of anisotropic states during the shock. The material is treated as homogeneous, corresponding to local averages over microscopic heterogeneities, as observed in experiments such as VISAR measurements of shock profiles. Plastic flow is defined as any total dissipative volume-conserving rearrangement of the atoms in a solid, which does not affect the thermoelastic material parameters. While macroscopic heterogeneities, such as cracks, are not explicitly accounted for, there are two ways to do so by extension of the present shock theory. The accurate way is to account for all material boundaries and interfaces, and resolve the macroscopically heterogeneous flow. The alternative is to treat the heterogeneities in an average way, and hence account for their presence by an appropriate modification of the thermoelastic and plastic material parameters.

The shock theory of this monograph is based on the principles of irreversible thermodynamics, characterized as follows. First, in equilibrium thermodynamics, materials are required to pass through states which lie on the equilibrium surface. In irreversible thermodynamics, materials pass through nonequilibrium states, but only those states which are close to the equilibrium surface, specifically, those states for which the equilibrium properties of temperature and entropy are still reasonably well defined. To construct an irreversible thermodynamic theory it is necessary to define the variables which measure the departure from equilibrium, to express the effect of these variables by a modification of the equilibrium thermodynamic equations, and to write an equation for the (irreversible) entropy generation. These principles are applied to planar shocks in the reprints collected here. Further discussions, covering many small details, can be found in the monograph *Thermoelastic-Plastic Flow in Solids*,[2] and in the 1985 Shock Conference.[3]

---

[1] R. Courant and K. O. Friedrichs, *Supersonic Flow and Shock Waves* (Interscience, New York, 1948).

[2] D.C. Wallace, *Thermoelastic-Plastic Flow in Solids* (LA 10119, Los Alamos National Laboratory, Los Alamos, 1985).

[3] D. C. Wallace, "Computer Simulation of Nonequilibrium Processes," in *Shock Waves in Condensed Matter*, ed. by Y. M. Gupta (Plenum, New York, 1986), p. 37.

In an analysis such as this, the question arises as to whether or not irreversible thermodynamics is indeed valid. A technique for answering this question consists of the following three steps.

(a) Assume irreversible thermodynamics is valid, and use it to construct a theory for the nonequilibrium process in question.

(b) For a given material, evaluate the theory, and calculate the spatial and temporal rates-of-change which occur in the process.

(c) From the appropriate relaxation times and mean free paths, estimate whether or not the material will actually remain close to equilibrium at the calculated rates of change.

For shocks in solids and liquids, steps (a) and (b) are carried out in the reprints collected here. The last step can be formulated in terms of the electron-phonon picture of condensed matter, leading to the following conclusions. Relaxation times among electrons and phonons are very short, and do not indicate a failure of irreversible thermodynamics (for a detailed discussion, see Section V of the first reprint). With increasing shock strength, the first near-equilibrium conditions to fail are the mean-free-path conditions, namely that the relative change in temperature be small in the distance of an electron, or phonon, mean free path. This failure results from the massive demand for heat transport in the leading edge of the shock, for strongly overdriven shocks in solids and liquids. In metals, where heat is carried mainly by the electrons, the irreversible thermodynamic theory remains valid for shocks up to several Mbar. For stronger shocks, nonequilibrium hot electrons will stream forward in the leading edge; the theory for this shock process is beyond the scope of the present monograph.

2 SUMMARIES OF THE REPRINTS

Irreversible Thermodynamics of Flow in Solids

Phys. Rev. B **22**, 1477 (1980).

The purpose of this paper is to construct the complete set of equations which govern thermoelastic-plastic flow in solids. The complete set of equations comprises three theoretical disciplines, whose physical contents are summarized as follows.

(1) Continuum mechanics. This theory provides differential equations expressing conservation of mass, of momentum, and of total energy, throughout a continuous moving material. The total energy consists of thermoelastic internal energy, measured in center-of-mass coordinates, plus translational kinetic energy.

(2)Thermoelasticity. This theory gives the equilibrium relations among the thermoelastic state variables, in the form of equations for dU, $d\tau_{ij}$, and dT, in terms of $d\varepsilon^e_{ij}$ and dS. The coefficients in these equations are the heat capacity, Grüneisen parameters, and stress-strain coefficients.

(3)Thermoplasticity. There are three equations, each approximate.

(i) The Prandtl-Reuss flow rule (eq. (19)) relates all components of $d\varepsilon^p_{ij}$ to the single increment $d\psi$, hence eliminates ε^p_{ij} in terms of ψ. Under this rule, plastic strain is volume conserving.

(ii) The constitutive equation is supposed to express the actual flow surface of a given material. It is written in eq. (20) as an expression for τ, but is more transparent when inverted to an equation for the plastic strainrate $\dot{\psi}$:

$$\dot{\psi} = f(\tau, \psi, V, S) .$$

This tells us, for example, that $\dot{\psi} = 0$ for an elastic process, and $\dot{\psi} > 0$ when plastic flow is being driven.

(iii) The entropy production equation (eq. (23)) assumes plastic work is entirely dissipated:

$$TdS = 2V\tau d\psi .$$

This is the key to the complete theory, since it closes the system of equations, and makes the three disciplines mutually consistent.

The formalism is valid for large strains, both elastic and plastic. When the complete set of equations is specialized to planewave geometry, so as to apply to shocks, the only part of the Prandtl-Reuss flow rule which enters is the volume conservation of plastic flow; hence no assumptions are made about the flow surface, the geometry of strain hardening, and so on.

Flow Process of Weak Shocks in Solids

Phys. Rev. B22, 1487 (1980).

From the thermoelastic-plastic theory of the previous paper, and knowing the appropriate material parameters, namely the thermoelastic coefficients and the plastic constitutive data, it is possible to calculate a deformation process for the material in question. For example, one can calculate the evolving structure of a shock as it propagates. On the other hand, given experimental data on the shock structure, and knowing the thermoelastic coefficients, one can use the thermoelastic-plastic theory to extract the plastic constitutive data. This is the point of the present paper.

The weak-shock profile data of Johnson and Barker,[4] for 6061-T6 Al, are analyzed. The profiles are approximately fitted with a uniform three-wave structure, consisting of (1) the elastic precursor, a steady wave traveling at a constant velocity; (2) the plastic precursor, a nonsteady region connecting two steady waves; and (3) the plastic wave, a steady wave moving at velocity D, where D depends on the shock strength. The fitting procedure serves two purposes: it allows us to average some small scatter in the data, and it makes the analysis simple enough so that the basic concepts are fully revealed.

First, the equations of motion (equations for conservation of mass and momentum) are integrated to give σ and ε through each profile. Second, the thermoelastic equations are integrated to give σ and τ as power series in the strains ε and ψ, to second order, and these equations are solved for τ and ψ through each profile. Third, making use of the VISAR time data, $\dot{\psi}$ is calculated through each profile. And finally, again from thermoelasticity, T and S are calculated through each profile. It should be noted that the expansions developed here, being limited to second order in strains, should in general be accurate for strains to around 0.1. To apply the shock theory at larger strains, one needs data for the elastic constants at the corresponding large strains.

The analysis yields plastic constitutive data for ψ in the range 0 - 0.05, for $\dot{\psi}$ in the range $10^3 \cdot 10^7\ s^{-1}$, for T in the range 295 - 380K, and for pressures up to 90 kbar. As in any analysis of experimental data, the results are subject to uncertainties. However, the important point is that the results reveal the genuine plastic behavior of the material studied, and are not constrained by any apriori modeling of this behavior.

Equation of State from Weak Shocks in Solids

Phys. Rev. B22, 1495 (1980).

The purpose of this paper is to define and study the locus of equilibrium thermodynamic states reached behind weak shocks in an initially isotropic solid. These states are elastically anisotropic, and their locus is called the anisotropic Hugoniot.

Shock experiments have been extensively used to determine equations of state of solids. The experiments measure shock velocity and particle velocity, and the data are analyzed in terms of liquid Hugoniot theory. This theory is based on two assumptions: the shock is a single steady wave, and the material behind the shock is in a state of isotropic pressure. With these assumptions, the Rankine-Hugoniot jump conditions hold, relating changes in ε, σ, and U across the shock, and the stress-strain variables on the Hugoniot are merely pressure and volume.

For a weak shock in a solid, both of the above assumptions fail seriously. Since the weak shock is not a steady wave, the changes in ε, σ, and U have to be found by integrating the conservation equations along the path of the shock process. Further, states behind the shock are characterized by *two* stress variables, σ and τ, and by *two* strain variables, ε and ψ. Since these states are equilibrium thermoelastic states, it is appropriate to replace ε and ψ by an equivalent pair of purely elastic strains (eqs. (5) and (6)).

[4] J.N. Johnson and L.M. Barker, J. Appl. Phys. **40**, 4321 (1969).

With the results of the weak shock analysis for 6061-T6 Al, the anisotropic Hugoniot is constructed for σ in the range 0 - 102 kbar. From this Hugoniot, by integrating out the elastic anisotropy, and integrating out the shock entropy, the principal adiabat is constructed. Though these results are subject to uncertainties, as in any analysis of experimental data, the solid theory is in principle more accurate than is liquid Hugoniot theory.

A significant result is that entropy on the Hugoniot, in the small strain region, is of second order in strains for a solid, but is third order in the strain for a liquid. The reason is that a solid has nonzero yield strength at zero strain-rate, whereas a liquid does not.

Irreversible Thermodynamics of Overdriven Shocks in Solids

Phys. Rev. B24, 5597 (1981).

This paper constitutes a theoretical study of the structure of overdriven shocks in solids. The shock is assumed to be a steady wave, and the solid is considered capable of transporting heat, and of undergoing dissipative plastic flow. Hence the appropriate theory is thermoelastic-plastic flow in solids, with heat transport included. This work is the logical extension, to solids, of Rayleigh's study of the structure of shocks in gases.[5]

The steady-wave condition makes it possible to integrate the conservation equations, and thus to express ε, σ, and U through the shock. The $\sigma(\varepsilon)$ relation for a shock is called the Rayleigh line, and for a steady wave it is a straight line:

$$\sigma = \rho_a D^2 \varepsilon$$

where ρ_a is the initial density and D is the shock velocity. The following theorem is proved: *For an overdriven shock in a solid, no solution is possible without heat transport.* The physical reason for this theorem is, for an overdriven shock in the small-ε region, the Rayleigh line lies above the value of σ corresponding to a uniaxial elastic compression, so heat must be transported to the shock front to increase σ there.

The coupled set of equations for thermoelastic-plastic and heat transport variables is analyzed on the Rayleigh line, and several theorems are proved regarding the solution. Upper and lower bounds for these variables on the Rayleigh line are established, when heat transport is governed by ordinary conduction. The entire analysis rests on qualitative properties of thermoelastic coefficients of solid materials, and nothing is assumed about the plastic constitutive data. A final theorem is proved: *For an overdriven shock in a solid with heat conduction, no solution is possible without plastic dissipation.* The physical reason for this theorem is, the heat which must be transported to the shock front, according to the first theorem, has to be generated by plastic dissipation in the later part of the shock.

Nature of the Process of Overdriven Shocks in Metals

Phys. Rev. B24, 5607 (1981).

The purpose of this paper is to estimate the actual structure of overdriven shocks in metals, for shocks up to melting on the Hugoniot.

If sufficient materials data are known, it is possible to calculate the shock structure for a solid, by numerically integrating the thermoelastic-plastic flow equations. The required data are the thermoelastic coefficients, the plastic constitutive data, and for overdriven shocks, the thermal conductivity. Since plastic constitutive data are unknown for the high plastic strainrates involved in shocks, a different approach has to be taken. In this paper, with the help of

---

[5]Lord Rayleigh, Proc. Roy. Soc. London, Ser.A84, 247(1910).

the theoretical analysis of the preceding paper, an approximate solution is constructed, independent of the plastic constitutive behavior.

An extensive study of the thermoelastic coefficients, in the region of the Rayleigh line for shocks up to a few Mbar, is summarized. These coefficients are the heat capacity, including lattice and electronic contributions, the Grüneisen parameter, and the bulk and shear moduli. Numerical calculations of temperature, entropy, shear stress, and plastic strain, as functions of compression, are shown for shocks up to around melting for 2024 Al, and for Pt. The time dependence of the process is controlled by dissipation, and two dissipation mechanisms are going on simultaneously, namely plastic flow and heat conduction. Because the whole process is a steady wave, both dissipation mechanisms have to operate at the same rate. Hence an estimate of the thermal conductivity, which is not difficult for metals, gives an estimate of the previously inaccessible plastic strainrate within the shock.

Strongly overdriven shocks in metals have the following characteristics: the shock entropy is generated by heat conduction in the leading part of the shock, the heat is generated by plastic flow in the last part of the shock, and the shock rise time is of order 10^{-12}s.

Theory of the Shock Process in Dense Fluids

Phys. Rev. A25, 3290 (1982).

In his pioneering study of shocks in gases, Rayleigh[5] established two important conclusions: (a) When the gas has heat conduction but no viscosity, a continuous steady wave is possible only for weak shocks, and (b) When the gas has viscosity but no heat conduction, a continuous steady wave is always possible.

The present paper extends Rayleigh's analysis to liquids (dense fluids). Irreversible thermodynamics is assumed valid, and the liquid is characterized by heat conduction, and by viscoelastic response. Such response is viscous at low strainrates, and elastic at high strainrates. The following three results are established for liquids.

(1)There is a maximum shock strength, the inviscid limit, for which a continuous steady solution can exist with heat conduction but without viscosity. This is Rayleigh's first result, and for liquids the inviscid limit corresponds to very weak shocks.

(2)For shocks at the overdriven threshold and above, no continuous steady solution is possible without both heat conduction and viscosity. The physical reason is that heat must be transported to the shock front, to increase σ there, and this heat must be generated by viscous flow behind the shock front.

(3)For shocks near the viscous fluid limit and above the liquid response at the leading edge of the shock is elastic. The physical reason is that the strainrate increases as shock strength increases, and at some strainrate the liquid response ceases to be viscous, and becomes elastic.

The three thresholds are calculated for water, and for mercury.

3 REPRINTS

Irreversible thermodynamics of flow in solids

Duane C. Wallace
Los Alamos Scientific Laboratory, Los Alamos, New Mexico 87545
(Received 17 April 1979)

Dynamic deformation of solid materials is described in terms of nonuniform material motion and simultaneous thermoelastic strain and plastic flow. For deformations of arbitrary form and magnitude in an initially isotropic solid, an approximate expression for the entropy production is given, and the interrelations among the thermodynamic variables of stresses, elastic and plastic strains, and temperature and entropy are derived. The theory is specialized to plane-wave geometry, appropriate for describing a weak planar shock, and is compared with the relaxing solid model which has previously been used to analyze plane shocks in solids. A qualitative examination of the mechanics of elastic strain and plastic flow indicates that a thermodynamic description is accurate for many fast deformation processes in solids.

I. INTRODUCTION

The dynamic flow processes of solids have come under careful study in recent years with the development and use of high-speed, high-stress diagnostic capabilities [for a recent review see Ref. 1(a)]. The resulting data have in turn provided the main basis for new developments in both microscopic and macroscopic theories for the equation-of-state, transport, and flow properties of solids at high stresses. Dislocation theory for example has been extensively used in modeling the flow properties of crystalline and polycrystalline materials. However, it is first of all necessary to obtain a clear macroscopic characterization of material flow properties exhibited in the experimental data. This necessitates an extended continuum mechanic flow formalism for solids, whose general formulation and thermodynamic validity is studied in this paper.

The purpose of this paper is to present a physical description of fast deformation processes in solids. The description is mechanic and thermodynamic; it is embodied in a coupled set of equations which governs the motion of the material and the simultaneous thermoelastic and flow processes. Before going into the formal theory, some discussion of the nature of these processes is useful.

In a thermoelastic process, the material passes through a sequence of equilibrium states, i.e., states characterized by zero entropy production, and the process is reversible. The variables are the anisotropic stresses and elastic strains, the energy, temperature, entropy, and so on; these variables are related in differential form by the standard equations of thermoelasticity.[1(b),2] The question arises: What are the limitations on the space and time rates at which system variables may change and still be treated by reversible thermodynamics? An answer in the spirit of statistical mechanics is that in space the system variables must change by a small amount over a region large enough to contain many atoms, and in time the variables must change slowly in comparison with the characteristic rate (or rates) at which the system approaches equilibrium. Such restrictions do not rule out some rather fast thermoelastic processes; in transmitting an adiabatic sound disturbance with wavelength of order 10^{-3} cm and period of order 10^{-6} s, a solid can be described as a large number of material elements, each passing through a sequence of near-equilibrium states under the influence of slowly varying stresses imposed by neighboring material elements.

For the second type of process, a general and for the moment not complete definition is as follows: Flow is any dissipative rearrangement of the atoms within a material. When thinking of solids, we usually call this plastic flow. Such a process is by definition irreversible. It can still be described in thermodynamic terms, however, if the rate-of-change limitations mentioned above are satisfied. Then the material passes through a sequence of states which are close to thermodynamic equilibrium states and, hence, the state of the material is always described to a sufficient approximation by thermodynamic variables. To complete the description of the process, it is required to devise an explicit expression for the entropy production. These two requirements are at the base of the theory of irreversible thermodynamics.[3,4] For example, imagine a polycrystalline material with a shear stress τ applied and slowly increased from zero. At first the material deforms elastically, and when τ reaches the appropriate static yield value the flow, as measured by a plastic shear strain ψ, begins. The flow is irreversible and entropy production is positive. A phenomenological relation[3] of the form $\tau \propto \psi$ does not hold because τ reaches a finite value while ψ is still zero. This essential nonlinearity cannot be treated by standard irreversible thermodynamics; nevertheless there

is a driving force and there *is* a reciprocal flow, and it is possible in principle to relate these quantities to the entropy production. Further, such a relation can be determined, or verified, by experiment.

It is interesting to compare time-rate effects for the two types of process discussed. A thermoelastic process is rate independent (up to some limit), which means for example the stresses change "instantly" in response to changes in the elastic strains and the entropy. Flow, however, is intrinsically rate dependent. In the plastic shear experiment mentioned above, there is a functional relation, generally called the plastic constitutive relation, among the variables τ, ψ, and $\dot{\psi}$, where $\dot{\psi}$ is the time derivative of ψ at a fixed material point. Formally it is $f(\tau, \psi, \dot{\psi}) = 0$, which means the driving stress τ depends explicitly on how fast the flow is being driven. We note in passing that the indicated dependence on ψ is to account for strain hardening, and that the plastic constitutive relation depends also on the thermoelastic state variables.

Now with regard to time-rate effects, a point of some significance is as follows. A thermoelastic process can be very fast and still be, to a good approximation, reversible. On the other hand, again with reference to the plastic shear experiment, it is possible to control τ so that $\dot{\psi}$ is arbitrarily small, but the flow is still irreversible. Entropy production accompanies the process no matter how slowly it proceeds. Hence the thermodynamic reversibility of a process is not determined by its rate.

In the following section the general theory of dynamic deformation processes in an initially isotropic solid is presented. The theory is specialized in Sec. III to plane-wave geometry, appropriate for describing a planar shock, and the theory is compared in Sec. IV with the relaxing solid model. In Sec. V we discuss in qualitative terms the question of local thermodynamic equilibrium. In applying the present theory to shocks in solids, we limit consideration to weak shocks, i.e., ones in which the shock velocity is not greater than the elastic precursor velocity, which means shock stresses up to one hundred kbar or so.

II. GENERAL THEORY

A. Equations of motion

We consider a spatially continuous isotropic solid. The definition of isotropic solid is given in Sec. IV, but it should be noted in advance that such a material can support anisotropic elastic strain and in such a configuration the material is physically anisotropic. At any time t the location of a given infinitesimal element of the material is $\vec{x}(t)$ in laboratory coordinates; at some initial (reference) time t_0 it is $\vec{x}(t_0) = \vec{X}$, so that $\vec{X}$ is the Lagrangian coordinate of the mass element. The field variable which denotes the whole material configuration is $\vec{x}(\vec{X}, t)$ for all $\vec{X}, t$. The velocity field $\vec{v}(\vec{X}, t)$ is the velocity in laboratory coordinates of each mass element:

$$\vec{v} = \left(\frac{\partial \vec{x}}{\partial t}\right)_{\vec{X}}. \tag{1}$$

We also use $\vec{x}$ as an independent variable denoting location in laboratory coordinates; for example, $\mathrm{div}\vec{v}$ in the laboratory system is $(\partial v_i/\partial x_i)_t$, where $i = 1, 2, 3$ are Cartesian indices and repeated indices are summed.

The material density is ρ, the stress tensor components are τ_{ij}, and both are functions of $\vec{X}, t$, or equivalently of $\vec{x}, t$. The equations of motion are conveniently expressed in mixed Lagrangian-Eulerian form as follows[5]:

Conservation of mass:

$$\left(\frac{\partial \rho}{\partial t}\right)_{\vec{X}} = -\rho\left(\frac{\partial v_i}{\partial x_i}\right)_t. \tag{2}$$

Conservation of linear momentum:

$$\rho\left(\frac{\partial v_i}{\partial t}\right)_{\vec{X}} = \left(\frac{\partial \tau_{ij}}{\partial x_j}\right)_t. \tag{3}$$

Conservation of angular momentum:

$$\tau_{ij} = \tau_{ji}. \tag{4}$$

There is also an equation for conservation of energy. We can write the total energy of each mass element as a sum of two parts, the translational kinetic energy and the center-of-mass energy. It is easy to show that the translational kinetic energy is equal to the translational work done by the stresses, because of Newton's law which is Eq. (3); the energy balance for each mass element is then reduced to center-of-mass contributions, which are discussed below.

B. Thermoelasticity[1(b),2]

Consider an incremental process, in which the material goes from the current state to the next state in an incremental time dt. The incremental displacement (motion) of each mass element is given by the field variable $d\vec{u}(\vec{X}, t)$; the incremental displacement gradients are

$$du_{ij} = \left(\frac{\partial du_i}{\partial x_j}\right)_t, \tag{5a}$$

related to the velocity gradients by

$$du_{ij} = v_{ij}\,dt, \tag{5b}$$

where $v_{ij} = (\partial v_i/\partial x_j)_t$. The du_{ij} are precisely the

same as the displacement gradients $u_{i,j}$ of Refs. 1(b) and 2, when those $u_{i,j}$ are limited to infinitesimal magnitude and are always measured from the (continually changing) current configuration, instead of from a fixed Lagrangian configuration. In the incremental process, the work done by stresses in a local center-of-mass system is $dW = \rho^{-1}\tau_{i,j}\,du_{i,j}$ per unit mass of material, and by conservation of energy this equals the increase dU of thermodynamic internal energy per unit mass (we are neglecting heat transport):

$$dU = dW = \rho^{-1}\tau_{i,j}\,du_{i,j}. \tag{6}$$

This equation, as with all thermodynamic equations, is Lagrangian in the sense that it holds for a given mass element, no matter how the mass element moves; hence (6) is equivalent to

$$\dot{U} = \rho^{-1}\tau_{i,j}\dot{u}_{i,j} = \rho^{-1}\tau_{i,j}v_{i,j},$$

where the dot signifies a Lagrangian time derivative: $\dot{U} = (\partial U/\partial t)_{\chi}$.

The strains may be expressed as symmetric plus antisymmetric parts, where the symmetric part

$$d\epsilon_{i,j} = \tfrac{1}{2}(du_{i,j} + du_{j,i}) \tag{7}$$

measures the pure strain and the antisymmetric part

$$d\omega_{i,j} = \tfrac{1}{2}(du_{i,j} - du_{j,i}) \tag{8}$$

measures the pure (rigid) rotation. Further, the pure strain is presumed to result from a combination of elastic strain $d\epsilon^{e}_{i,j}$, and some "flow" or "plastic" strain $d\epsilon^{p}_{i,j}$ which is due to an internal rearrangement of the atoms of the material. As long as the process is infinitesimal, the two strain contributions are additive:

$$d\epsilon_{i,j} = d\epsilon^{e}_{i,j} + d\epsilon^{p}_{i,j}. \tag{9}$$

The meaning of the $d\epsilon^{p}_{i,j}$ will be made precise a little later. We first set out the thermodynamic theory which is coupled to the elastic strains $d\epsilon^{e}_{i,j}$, ignoring the explicit presence of the plastic strains.

In the theory of thermoelasticity, a complete set of variables which specify the thermodynamic state of a material (the state variables) are the elastic configuration and the entropy. In differential form these variables are $d\epsilon^{e}_{i,j}$ and dS, where S is the entropy per unit mass. Then the differential of any thermodynamic function, e.g., U, can be written as

$$dU = \frac{\partial U}{\partial \epsilon^{e}_{i,j}}\,d\epsilon^{e}_{i,j} + \frac{\partial U}{\partial S}\,dS. \tag{10a}$$

Repeated indices are summed; in each partial derivative with respect to a given variable, all other independent variables are held fixed. Thermoelastic definitions of the stresses and the temperature T are[1(b),2]

$$\tau_{i,j} = \rho\,\frac{\partial U}{\partial \epsilon^{e}_{i,j}} \tag{10b}$$

at constant S, and

$$T = \left(\frac{\partial U}{\partial S}\right) \tag{10c}$$

at constant $\epsilon^{e}_{i,j}$. Hence Eq. (10a) is

$$dU = \rho^{-1}\tau_{i,j}\,d\epsilon^{e}_{i,j} + T\,dS. \tag{11}$$

In a similar way the variations $d\tau_{i,j}$ and dT may be calculated and expressed as

$$d\tau_{i,j} = B_{i,j,k,l}\,d\epsilon^{e}_{k,l} + \frac{\partial \tau_{i,j}}{\partial \omega_{k,l}}\,d\omega_{k,l} - \rho\gamma_{i,j}\,T\,dS, \tag{12}$$

$$dT = -T\gamma_{i,j}\,d\epsilon^{e}_{i,j} + (T/C_{\eta})\,dS, \tag{13}$$

where C_{η} is the heat capacity at constant elastic configuration, $B_{i,j,k,l}$ are the adiabatic stress-strain coefficients, which can be measured in stress-strain experiments or in adiabatic sound-wave experiments, and $\gamma_{i,j}$ are the anisotropic Grüneisen parameters defined by[2]

$$\rho\gamma_{i,j} = -T^{-1}\,\frac{\partial \tau_{i,j}}{\partial S}. \tag{14a}$$

Derivatives at constant elastic configuration equivalent to (14a) are

$$\rho\gamma_{i,j} = -C_{\eta}^{-1}\,\frac{\partial \tau_{i,j}}{\partial T} = -\,\frac{\partial \tau_{i,j}}{\partial U}. \tag{14b}$$

The rotation coefficient $(\partial\tau_{i,j}/\partial\omega_{k,l})$ in (12) is given in Ref. 1(b); this term in $d\tau_{i,j}$ accounts for simultaneous incremental rigid rotation of a mass element and the stress tensor.

The thermoelastic equations (11)–(13) are not all independent. In fact, they form a hierarchy of coupled equations: The coefficients in dU, namely, $\tau_{i,j}$ and T, are first derivatives of U with respect to independent variables; the coefficients in $d\tau_{i,j}$ and dT, namely, $B_{i,j,k,l}$, $\gamma_{i,j}$, and C_{η}, are second derivatives of U with respect to independent variables; and so on. In order to break the hierarchy at this point, we regard the second-order coefficients as known functions of the state variables.

A comment is in order concerning the convenient choice of thermodynamic state variables. In a theory which includes both elastic and plastic strains, the elastic configuration is a complicated nonlinear integral function of the total and the plastic-strain increments, $d\epsilon_{i,j}$ and $d\epsilon^{p}_{i,j}$. While it is easy to use $d\epsilon^{e}_{i,j}$ and dS for differential state variables, as above, if integrated state variables are desired, it is most convenient to use the equivalent complete set $\tau_{i,j}$ and S (equivalent because stresses are elastically supported). The stresses are easily

calculated by integrating $d\tau_{ij}$, and with τ_{ij} and S specified, all other thermodynamic functions, including the elastic configuration, are uniquely determined. To complete the thermodynamics, we need an equation for dS; this is obtained below.

C. Thermoplasticity

The mechanical theory of plastic flow is well described in textbooks.[6-8] It is based on two conditions on the plastic-strain increments; the first is the experimental observation that plastic strain is volume conserving. To express this, note that Eq. (2) for conservation of mass is precisely equivalent to

$$d\ln V = du_{ii} = d\epsilon_{ii}, \tag{15}$$

where $V = \rho^{-1}$ is the volume per unit mass. $d\ln V$ is then a sum of elastic and plastic contributions, and the plastic contribution is set to zero:

$$d\epsilon^p_{ii} = 0. \tag{16}$$

The second condition is the Prandtl-Reuss flow rule,[9] which requires some definitions. The average compressive stress is $\bar{P}$, and the stress deviators are s_{ij}:

$$\begin{aligned} \bar{P} &= -\tfrac{1}{3}\tau_{ii}, \\ s_{ij} &= \tau_{ij} + \bar{P}\delta_{ij}. \end{aligned} \tag{17}$$

An effective shear stress τ, which is a measure of the stress which drives the plastic flow, is defined by

$$\tau^2 = \tfrac{1}{2} s_{ij} s_{ij}, \quad \tau \geq 0. \tag{18}$$

The Prandtl-Reuss flow rule then allows the several variables $d\epsilon^p_{ij}$ to be expressed in terms of a single measure $d\psi$ of the plastic strain:

$$d\epsilon^p_{ij} = \tfrac{3}{2}(s_{ij}/\tau)d\psi. \tag{19}$$

Since the definitions (17) imply $s_{ii} = 0$, then (17) and (19) together contain (16). Equation (19) represents the intuitively reasonable idea that the plastic-strain increments ought to be isotropically proportional to the stress deviators; it has some experimental verification for cases of complex flow.[7,8] Finally, the effective plastic-strain increment $d\psi$ is determined by the von Mises criterion[10] in terms of a generalized flow function K:

$$\tau \leq K(\psi, \dot{\psi}, \tau_{ij}, S), \tag{20}$$

This equation has the following meaning: If $\tau < K$, the process is elastic and $d\psi = 0$; if τ is on the flow surface, $d\psi > 0$ and is determined by the condition $\tau = K$. $\psi = \int d\psi$ is the integrated plastic strain, and the dependences of K on ψ and $\dot{\psi}$ represent, respectively, strain-hardening and strain-rate effects. K also depends on the thermoelastic state variables τ_{ij} and S, as indicated.

The thermodynamic theory of plastic flow requires, in addition to the above equations, a thermodynamic description of the energy associated with the process. This energy can be identified as part of the total center-of-mass energy. In Eq. (6) for the conservation of total energy, because $\tau_{ij} = \tau_{ji}$, the antisymmetric parts of du_{ij} sum to zero, giving

$$dW = \rho^{-1}\tau_{ij}\, d\epsilon_{ij} = dW^e + dW^p, \tag{21}$$

where dW^e and dW^p are work increments done against elastic and plastic strains, respectively:

$$dW^e = \rho^{-1}\tau_{ij}\, d\epsilon^e_{ij}, \tag{22a}$$

$$dW^p = \rho^{-1}\tau_{ij}\, d\epsilon^p_{ij} = 2V\tau d\psi. \tag{22b}$$

The last form in (22b) follows by using (17)–(19). In a classic experiment on metals, Farren and Taylor[11] observed that 87–95% of the plastic work was dissipated; we expect this same qualitative behavior for deformations involving dislocation motion, twinning, or viscous rearrangement of atoms in amorphous solids. Because it is a good approximation, and because it simplifies the theory conceptually, we assume that the plastic work dW^p is entirely dissipated:

$$TdS = 2V\tau d\psi. \tag{23}$$

The plastic flow is now completely defined. It follows the flow rule (19) and is totally dissipative. It includes any process which approximates these conditions. Further, the combined thermoelastic and thermoplastic theory is internally consistent, since the energy partition given by (21)–(23) makes the thermoelastic equation (11) for dU identical with (6).

As a matter of fact, in a real flow process in a real solid, a small part of the plastic work may go into creating a change in the defect structure of the material; for example, energy may be stored in the elastic strain field of an increased number of dislocations. Such stored energy is presumably responsible for work hardening (strain hardening). This energy is not included in ordinary thermoelastic theory, hence an explicit accounting of it will require a redefinition of the thermoelastic coefficients. Suppose, for example, that 90% of dW^p is dissipated in a given process, while the rest is stored; the entropy-production and energy-conservation equations then read

$$\begin{aligned} TdS &= 0.9\, dW^p, \\ dU &= \rho^{-1}\tau_{ij}(d\epsilon^e_{ij} + 0.1\, d\epsilon^p_{ij}) + TdS. \end{aligned}$$

Comparison with (11) shows that the first-order coefficients τ_{ij} and T are no longer given by the thermoelastic definitions (10b) and (10c). The effect carries

on to Eqs. (12) and (13), changing the definitions of the second-order coefficients $B_{ij\beta 1}$, γ_{ij}, C_v, and so on. Thus in making the total dissipation approximation (23), we obtain a significant simplification of the theory, in exchange for introducing small errors into our thermodynamic computations. On the other hand, the major effect of hardening is properly contained in the theory, through the dependence of the flow function K on the total plastic strain ψ. It may also be noted that when a solid melts, the defect structure anneals, and the energy stored there is recovered as equivalent heat.

III. PLANE-WAVE GEOMETRY

The theory is much simplified when it is specialized to the geometry appropriate for describing a plane compressive wave, such as a weak shock. This is an example of "principal axis flow": The principal axes coincide at all $\vec{X}, t$ with a single invariant orthogonal (not necessarily Cartesian) coordinate system. Since the stress tensor is diagonal in this coordinate system, then for an isotropic solid both the elastic and plastic strains are diagonal; it is then convenient to express strains in terms of the transformation matrix α which transforms the initial configuration $\vec{X}$ to the current configuration $\vec{x}$ at any time t (Refs. 1(b ,2):

$$\alpha_{ij} = \left(\frac{\partial x_i}{\partial X_j}\right)_t . \tag{24}$$

Because all strain measures are diagonal, we can use the Voigt indices $\beta = 1, 2, 3$ to replace $ij = 11, 22, 33$, respectively, and write

$$\begin{aligned} \alpha_{ij} &= \alpha_\beta \delta_{ij} , \\ d\epsilon_{ij} &= d\epsilon_\beta \delta_{ij} . \end{aligned} \tag{25}$$

We now have $du_\beta = d\epsilon_\beta$, and the relation

$$d\epsilon_\beta = d \ln \alpha_\beta . \tag{26}$$

The logarithm appears in (26) because the α_β are measured from a fixed (initial) configuration, while the ϵ_β are measured from a continually varying (current) configuration. Again because the strain measures are diagonal, the total transformation α is a matrix product of the elastic transformation α^e and the plastic transformation α^p, as the following calculation shows:

$$\begin{aligned} \ln \alpha_\beta &= \int d\epsilon_\beta = \int d\epsilon_\beta^e + \int d\epsilon_\beta^p \\ &= \ln \alpha_\beta^e + \ln \alpha_\beta^p , \end{aligned} \tag{27}$$

or in matrix form

$$\begin{aligned} \alpha &= \begin{bmatrix} \alpha_1 & 0 & 0 \\ 0 & \alpha_2 & 0 \\ 0 & 0 & \alpha_3 \end{bmatrix} \\ &= \begin{bmatrix} \alpha_1^e & 0 & 0 \\ 0 & \alpha_2^e & 0 \\ 0 & 0 & \alpha_3^e \end{bmatrix} \begin{bmatrix} \alpha_1^p & 0 & 0 \\ 0 & \alpha_2^p & 0 \\ 0 & 0 & \alpha_3^p \end{bmatrix} . \end{aligned} \tag{28}$$

In plane-wave geometry, the wave propagates along Cartesian coordinate 1, and coordinates 2, 3 are equivalent transverse directions. Hence, $\alpha_2 = \alpha_3$ and so on. The transformation of a mass element is shown in Fig. 1, from the initial configuration of density ρ_a, to an intermediate configuration of density ρ_1, to the current configuration of density ρ. No physical meaning is to be attached to the intermediate configuration: it is not reached in the physical process unless it coincides with the current configuration. The mass element has thickness d in direction 1 and width w in the two transverse directions. The initial dimensions d_a, w_a are presumed known, so there are four independent strain variables in the transformation, namely d_1, w_1, d, w. In terms of these we can write

$$\begin{aligned} &\alpha_1 = d/d_a , \quad \alpha_1^e = d_1/d_a , \quad \alpha_1^p = d/d_1 , \\ &\alpha_2 = w/w_a , \quad \alpha_2^e = w_1/w_a , \quad \alpha_2^p = w/w_1 . \end{aligned} \tag{29}$$

Plane-wave geometry requires the boundary condition that the total transverse strain of each mass element is zero:

$$w = w_a . \tag{30}$$

The volume conservation of plastic flow, Eq. (16), can be written

$$\rho = \rho_1 . \tag{31}$$

With these conditions we are left only two independent strain variables, and for these we introduce the conventional plane-wave variables ϵ, ψ, both positive in compression and defined by

$$\epsilon = 1 - \rho_a/\rho = 1 - V/V_a , \tag{32}$$

$$\psi = -\ln \alpha_1^p . \tag{33}$$

The flow strain ψ is the same as the natural or logarithmic plastic strain in simple tension or compression experiments. The transformation coefficients now become

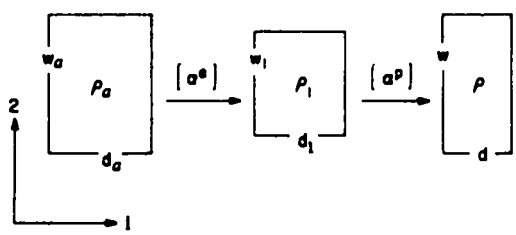

FIG. 1. Two-step transformation of a mass element in plane-wave geometry.

$$\alpha_1 = (1-\epsilon), \quad \alpha_1^e = (1-\epsilon)e^{\psi}, \quad \alpha_1^p = e^{-\psi},$$
$$\alpha_2 = 1, \quad \alpha_2^e = e^{-\psi/2}, \quad \alpha_2^p = e^{\psi/2}. \tag{34}$$

The stress system is also simple in plane-wave geometry. The conventional variables are the normal stress σ and the shear stress τ, both positive in compression and defined by

$$\sigma = -\tau_1,$$
$$\tau = -\tfrac{1}{2}(\tau_1 - \tau_2). \tag{35}$$

These stresses are shown in Fig. 2. Note that the above definitions are completely consistent with the general thermoplastic theory of Sec. II: We have incorporated the volume-conserving condition (16), the shear stress τ of (35) satisfies the definition (18), and the plastic strains $d\epsilon_\beta^p = d\ln\alpha_\beta^p$ satisfy the flow rule (19). In fact the Prandtl-Reuss rule is superfluous in the case of plane-wave geometry because here we have only one independent plastic-strain variable.

Under the stress system (35), an originally isotropic solid has tetragonal symmetry, and the stress-strain coefficients $B_{\alpha\beta}$ (Voigt indices) have the symmetry

$$\begin{pmatrix} B_{11} & B_{12} & B_{12} & & & \\ B_{21} & B_{22} & B_{23} & & 0 & \\ B_{21} & B_{23} & B_{22} & & & \\ & & & B_{44} & 0 & 0 \\ & 0 & & 0 & B_{66} & 0 \\ & & & 0 & 0 & B_{66} \end{pmatrix}. \tag{36}$$

The Grüneisen parameters, Eqs. (14), have the symmetry $\gamma_{ij} = \gamma_\alpha \delta_{ij}$, and the thermoelastic equations for stresses and temperature reduce to

$$d\sigma = \rho\gamma_1 T dS - B_{11} d\ln(1-\epsilon) - (B_{11} - B_{12}) d\psi, \tag{37}$$

$$d\tau = \tfrac{1}{2}\rho(\gamma_1 - \gamma_2) T dS - \tfrac{1}{2}(B_{11} - B_{21}) d\ln(1-\epsilon) - \tfrac{1}{2}(B_{11} + \tfrac{1}{2}B_{22} + \tfrac{1}{2}B_{23} - B_{12} - B_{21}) d\psi, \tag{38}$$

$$dT = C_\eta^{-1} T dS - T\gamma_1 d\ln(1-\epsilon) - T(\gamma_1 - \gamma_2) d\psi. \tag{39}$$

The equations of motion (2) and (3) for conservation of mass and linear momentum, respectively, are

$$\left(\frac{\partial\rho}{\partial t}\right)_x = -\rho\left(\frac{\partial v}{\partial x}\right)_t, \tag{40}$$

$$\rho\left(\frac{\partial v}{\partial t}\right)_x = -\left(\frac{\partial\sigma}{\partial x}\right)_t, \tag{41}$$

where x is the laboratory coordinate and v the material velocity, both in the propagation direction. The Eqs. (37)–(41), together with the entropy production equation (23) and the flow criterion (20), are sufficient to calculate any dynamic flow process in plane-wave geometry, provided the coefficients $C_\eta, \gamma_\beta, B_{\alpha\beta}$ and the flow function $K(\psi, \dot\psi, \sigma, \tau, S)$ are known. The conservation of energy equation, which is uncoupled from the above system unless U is taken as a state variable, reduces to

$$dU = -\sigma dV = \sigma V_a d\epsilon. \tag{42}$$

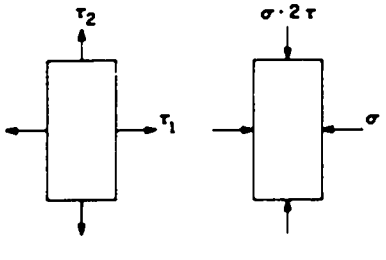

FIG. 2. Stresses in plane-wave geometry.

IV. COMPARISON WITH RELAXING SOLID MODEL

A. Expansions for small anisotropy

In order to make a comparison with other models, we need to approximate the thermoelastic coefficients in the present theory. A systematic approximation can be based on the condition that the stress system is always close to isotropic, or equivalently that the anisotropic part of the elastic strain is small. We first construct a working definition of isotropic solid.

Consider an isotropic solid under arbitrary isotropic pressure P; take V, S for state variables, so P, T, U, and so on are functions of V, S. Throughout this thermodynamic space, the solid is physically isotropic. Now from any state, say state 1, in the isotropic thermodynamic space, change the stress system to an anisotropic τ_{ij} at constant S; this brings the solid to a state of anisotropic elastic strains η_{ij}^e, where $\eta_{ij}^e = \frac{1}{2}(\alpha_{ki}^e \alpha_{kj}^e - \delta_{ij})$ and all strains are measured from state 1. The dependence of any thermodynamic function on the strain matrix η^e can be expressed in terms of the three rotation invariants of η^e, which are

$$I_1 = \eta_{ii}^e,$$
$$I_2 = \sum_j \mathrm{cof}\eta_{jj}^e, \tag{43}$$
$$I_3 = \det\eta^e,$$

where $\mathrm{cof}\eta_{jj}^e$ stands for the cofactor of η_{jj}^e. The above observations constitute a definition of isotropic solid. A strain expansion of the internal energy is given in Ref. 1(b), and this serves to define the second-order adiabatic Lamé coefficients λ, μ, and the third-order adiabatic Murnaghan coefficients ζ, ξ, ν:

$$\rho_1 U(V,\eta_1^e,S)=\rho_1 U(V,0,S)-PI_1+\left[\tfrac{1}{2}(\lambda+2\mu)I_1^2-2\mu I_2\right]+\left[\tfrac{1}{3}(\zeta+2\xi)I_1^3-2\xi I_1I_2+\nu I_3\right]+\cdots, \tag{44}$$

where ρ_1 is the density at state 1, and the coefficients (of the strain functions) are all evaluated at state 1. The adiabatic bulk and shear moduli, B and G, respectively, at state 1 are[1(b)]

$$B=-V(\partial P/\partial V)_S=\lambda+\tfrac{2}{3}\mu+\tfrac{1}{3}P, \tag{45}$$

$$G=B_{44}=\tfrac{1}{2}(B_{11}-B_{12})=\mu-P. \tag{46}$$

For application to the present theory of dynamic flow processes, it is convenient to restrict expansions such as (44) to the condition of fixed V; then V,S are the same in the elastically anisotropic state (the current state), as in state 1 where all coefficients are evaluated. Hence V,S evaluated in the current state serve as state variables for the coefficients. For the case of plane-wave geometry, we have expanded the second-order thermoelastic coefficients at constant V,S, and expressed the results in powers of τ/G, which should always be small. Results for the stress-strain coefficients are

$$\begin{aligned}
&B_{11}=(B+\tfrac{4}{3}G)-\tfrac{1}{3}(2\lambda+5\mu+2\xi-P)(\tau/G)+\cdots,\\
&\tfrac{1}{2}(B_{11}-B_{12})=G-(\lambda+4\mu+\xi+\tfrac{1}{6}\nu-\tfrac{4}{3}P)(\tau/G)+\cdots,\\
&\tfrac{1}{2}(B_{12}-B_{21})=\tau,\\
&\tfrac{1}{3}(B_{11}+\tfrac{1}{2}B_{22}+\tfrac{1}{2}B_{23}-B_{12}-B_{21})\\
&\qquad=G-(\mu+\tfrac{1}{6}\nu-\tfrac{1}{3}P)(\tau/G)+\cdots,
\end{aligned} \tag{47}$$

where $+\cdots$ means terms of relative order τ^2/G^2 and higher. For the remaining coefficients, with terms of order τ/G represented by $O(\tau/G)$,

$$\begin{aligned}
&C_\eta=C_v[1+O(\tau/G)],\\
&\gamma_1-\gamma_2=O(\tau/G),\\
&\gamma_1=\gamma[1+O(\tau/G)],
\end{aligned} \tag{48}$$

where C_v is the heat capacity at constant volume, and γ is the ordinary Grüneisen parameter,

$$\rho\gamma=\left(\frac{\partial P}{\partial U}\right)_v. \tag{49}$$

We now gather up the thermoelastic and thermoplastic equations of the preceding section for plane-wave geometry, put in the above expansions, and write each equation explicitly to leading order only as follows:

$$d\sigma=-(B+\tfrac{4}{3}G)d\ln(1-\epsilon)-2Gd\psi+O(\tau d\ln(1-\epsilon),\tau d\psi), \tag{50}$$

$$d\tau=-G[d\ln(1-\epsilon)+\tfrac{3}{2}d\psi]+O(\tau d\ln(1-\epsilon),\tau d\psi), \tag{51}$$

$$\tau\le K(\psi,\dot\psi,V,S). \tag{52}$$

$$TdS=2V\tau d\psi. \tag{53}$$

$$dT=[C_v^{-1}TdS-\gamma Td\ln(1-\epsilon)][1+O(\tau/G)]. \tag{54}$$

Note $\rho TdS=O(\tau d\psi)$; the terms $O(\tau d\ln(1-\epsilon))$ and $O(\tau d\psi)$ in (50) and (51) are the TdS terms from Eqs. (37) and (38), and the terms of first order in τ from Eqs. (47).

B. Relaxing solid model

In 1867, Maxwell[12] wrote a constitutive equation for a material which shows instantaneous elastic response plus stress relaxation according to a relaxation time. Malvern,[13] in studying plane-wave propagation in infinitesimal strain theory, generalized the Maxwell model by introducing a stress relaxation function. Taylor[14] investigated the shape of weak plane shocks with a constitutive equation which is a special case of Malvern's. Herrmann[15] has used the relaxing solid model extensively in analyzing plane shocks; his equations are the most general since they allow for finite strain and include the shear stress τ. Equations (6) or (7) and (9) or (10) of Ref. 15, transcribed to the present notation,[16] are

$$d\sigma=-(B+\tfrac{4}{3}G)d\ln(1-\epsilon)-2Gd\psi, \tag{55}$$

$$d\tau=-G[d\ln(1-\epsilon)+\tfrac{3}{2}d\psi], \tag{56}$$

$$\dot\psi=g'(\sigma,\epsilon), \tag{57}$$

where $g'(\sigma,\epsilon)$ is the stress relaxation function, with g^+ for compressive loading and g^- for unloading.

By comparison with Eqs. (50)–(54), it is seen that the system (55)–(57) neglects all effects due to entropy, and neglects all terms $O(\tau d\ln(1-\epsilon))$ and $O(\tau d\psi)$ in $d\sigma, d\tau$. In plane shocks we generally have $\tau\ll\sigma$; this means the terms of order τ neglected in (55) are formally small, and (55) should integrate to give a reasonably accurate value of σ throughout the process. Terms of the same order are not negligible in (56), however, and the integral of that equation will give a value of τ with an error formally of order τ. With regard to the plastic-flow constitutive equations, it is interesting to note there is a formal equivalence between the von Mises condition and the relaxation function. Equation (52) can be inverted to $\dot\psi=f(\tau,\psi,V,S)$, and since τ,ψ,V are coupled by one equation, they can be replaced by two variables, say σ,ϵ, giving $\dot\psi=f(\sigma,\epsilon,S)$; finally, if S is neglected as an independent variable, a relation of the form (57) is obtained.

V. THE QUESTION OF EQUILIBRIUM

A macroscopic treatment of a material process without thermodynamics is conceptually difficult.

Theory has to be founded in mechanical variables, which are specified in terms of atomic motions and interactions. For a given mass element containing a fixed assembly of atoms, or at least a fixed number in the case where mass transfer is allowed, the mechanical energy is always defined, and so are mechanical stresses in the form of forces acting across surfaces. Mechanical work is defined, but temperature and entropy are not. In order to examine the question of thermodynamic equilibrium, we have to imagine that we are first able to find a complete mechanical solution to the problem of motion; then we can study the space and time variations of the solution.

We begin by constructing a picture of continuum mechanics. The material is divided into mass elements which are macroscopically small but which still contain many atoms. The mass elements are considered as interacting mechanical systems, and the entire flow problem is expressed in terms of variables which give total mechanical properties of each mass element, for example, the position of the center of mass, the configuration, the energy, momentum, and stresses. These are macroscopic variables because they average the atomic properties over all the atoms in a mass element; they are functions of the time. To help bridge the gap between mechanics and thermodynamics it is useful to divide the deformation into two separate parts, defined as follows at any instant of time. The homogeneous deformation is that part of the deformation which is essentially constant over a mass element; this means the measure of strain varies by only a small amount over a region large enough to contain many atoms (at a fixed time), and hence it applies to the strain in any reversible thermoelastic process such as an adiabatic one, or a nonadiabatic one where the heat flux is spatially slowly varying. The other part of the deformation, that due to plastic flow, is heterogeneous on an atomic scale; this heterogeneity does not appear in detail in the macroscopic mechanical variables, only the average appears, but it is nevertheless important in the question of thermodynamic equilibrium. Incremental contributions to stresses, strains, and energies from the two types of deformation are additive.

The next step is to construct a physical model of an individual mass element as a mechanical system. A solid material is composed of ions and band electrons; the choice of which electrons are to be put in the ion cores and which in the bands is somewhat arbitrary and does not affect the present discussion. The mechanical states are quantum states. The ground state is a function only of the configuration, which is specified by the positions of the ions, and it is the $T = 0$ thermodynamic state. For a given configuration, we may think of a distribution of quantum states with a unique ground state, such that the system's mechanical properties are represented by some average over the distribution. The mechanical variables are then written as a ground-state contribution plus an excitation contribution. For a thermodynamic equilibrium distribution of states, the excitation contribution becomes a thermodynamic quantity, generally called the thermal contribution, and is characterized by the temperature and the configuration. Thermodynamic variables are then written as a ground-state ($T = 0$) contribution plus a thermal contribution.

We now ask the following question: If the configuration is suddenly changed, at what strain rate can the ground state still be considered a thermodynamic state? Or, how fast do the ground-state electrons respond to a sudden motion of the ions? If the ion motion is a homogeneous strain, i.e., it is characterized by a wavelength long compared to the interionic distance. The band electrons respond collectively in a time of the order of an inverse plasma frequency,[17,18] say in about 10^{-16} s. The polarization response of the ion cores should in principle be faster, but it will in practice be limited to the same rate as the collective response. Finally, for a short-wavelength (localized) motion of the ions, we expect the ground-state electron response to be equally fast, so for all practical purposes thermodynamic equilibrium can be assumed for the ground-state contributions to system variables.

The response of the excited states can also be estimated for near-equilibrium conditions. In the customary approximations of solid-state physics, the excitation modes of the ion-electron system are the phonons and the one-electron Fermi-Dirac excitations. Among the phonons, in a distribution which is anywhere near thermodynamic equilibrium at room temperature and above, practically all of the excitation energy is carried by short-wavelength motions, i.e., wavelengths of the order of one or two interionic spacings. We may assume that at room temperature and above, the lifetime of such phonons is limited by phonon-phonon collisions; experimental measurements for metals[19] give $\tau_{pp} \approx 10^{-12}$ s, and Peierls[20] has estimated $\tau_{pp} \approx 10^{-13}$ s for nonmetals at room temperature. These lifetimes should decrease as temperature increases. Long-wavelength phonons have much longer lifetimes, but we should be able to neglect their influence as long as we avoid low-temperature problems. For metals there are also electronic excitations. From the theory of thermal conduction at temperatures of the order and above the Debye temperature,[20-22] and from the measured

thermal-conductivity values, the relaxation time which describes the approach to equilibrium of the electrons due to collisions with phonons in equilibrium is estimated as $\tau_{ep} \sim 10^{-14}$–10^{-13} s. This should decrease with increasing temperature. The electron-electron relaxation time is rather long at room temperature,[18,20,21] $\tau_{ee} \sim 10^{-12}$ s, but it is expected to decrease with temperature as T^{-2}.

We can now draw the following conclusion: For a homogeneous deformation process, the electron-phonon system ought to be able to maintain itself near equilibrium as long as the deformation at any material point changes little in a time of order 10^{-13} s; this means strain rates of order 10^{10} s^{-1} are easily allowed. Such strain rates are well beyond those induced by weak shocks. This result is helpful because in many fast deformation processes the homogeneous part gives the major contribution to thermal functions, and together with the ground state it represents the dominant contribution to thermodynamic functions. For the example of a 100-kbar shock in Al, the ground-state deformation and the thermal adiabatic homogeneous deformation account for 90% of the increase in internal energy and 99% of the increase in the stresses.

The last barrier to a complete thermodynamic description of dynamic deformation processes is the heterogeneous nature of plastic flow. On the finest scale, the flow is localized to atomic-sized regions, as in dislocations, which act as dispersed moving sources of mechanical excitations. The problem is to determine how long it takes this mechanical energy to become thermalized. We might imagine that the higher the rate at which plastic flow is driven, the finer the scale of this heterogeneity, and that near thermal equilibrium could be maintained for plastic strain rates up to the same order as those which limit homogeneous deformation processes. This argument then implies approximately local equilibrium in the presence of heterogeneities on a larger scale. Evidence for large scale thermal and mechanical inhomogeneities in the fast deformations of very brittle solids has been discussed.[23]

If the assumption of thermodynamic equilibrium fails, it is possible to identify the errors which can result. To illustrate, consider the passage of a plane compressive shock through a polycrystalline material; assume the material remains in local thermodynamic equilibrium except for those mechanical excitations generated by plastic flow. The initial and final states are equilibrium states, and we will use the thermodynamic theory of Sec. III to calculate thermodynamic variables in the final state. The first step is to integrate the conservation equations (40) and (41), to find the normal stress σ as a function of the normal strain ϵ through the process. The result for $\sigma(\epsilon)$ is the proper thermodynamic value in the final state. The same is true for $U(\epsilon)$ in the final state, computed by integrating Eq. (42). Through the process, however, $\sigma(\epsilon)$ is a mechanical variable; its value is given correctly by the conservation equations, but it does not represent material in thermodynamic equilibrium. We thus make an error when we use thermodynamics to calculate τ and ψ from $\sigma(\epsilon)$. But the error should be small, at most of the same order as the contribution of the entropy to the stresses. For a 100-kbar shock in Al, this is not greater than 1%. This now becomes the measure of the error in all thermodynamic quantities we calculate. As for the increase in the temperature from the initial to the final state, most is due to homogeneous adiabatic compression. The calculation of the entropy in the final state, and of the temperature increase due to dissipative heating, is based on integrating the inexact differential $\tau d\psi$ [see Eqs. (22b) and (23)] along a path defined by τ and ψ, so the error in the integral is at most of the same order as that in τ and ψ along the path. From this point of view the assumption of thermodynamic equilibrium is seen as an approximation of very good accuracy.

VI. CONCLUSION

In this work we have shown that within the conventional assumptions of plasticity theory, the complete thermoelastic-plastic equations of flow can be expected to have a wide range of applicability. Evaluation of these equations for general flow problems would require a large computer.[24] However, for one-dimensional strain problems a relatively simple system of equations results. These equations will be applied in the following two papers to experimental data on an extensively studied Al alloy in order to obtain model-independent information concerning its flow function and equation of state.

---

[1] (a) L. Davison and R. A. Graham, Phys. Rep. 55, 255 (1979); (b) D. C. Wallace, in *Solid State Physics*, edited by H. Ehrenreich, F. Seitz, and D. Turnbull (Academic, New York, 1970), Vol. 25, p. 301.

[2] D. C. Wallace, *Thermodynamics of Crystals* (Wiley, New York, 1972).

[3] I. Prigogine, *Thermodynamics of Irreversible Processes*, 2nd ed. (Interscience, New York, 1961).

[4] S. R. deGroot, *Thermodynamics of Irreversible Processes* (North-Holland, Amsterdam, 1958).

[5]For a derivation of the equations of motion see, e.g., W. Prager, *Introduction to Mechanics of Continua* (Ginn, Boston, 1961).
[6]R. Hill, *The Mathematical Theory of Plasticity* (Clarendon, Oxford, 1950).
[7]A. Mendelson, *Plasticity: Theory and Application* (Macmillan, New York, 1968).
[8]L. M. Kachanov, *Foundations of the Theory of Plasticity* (North-Holland, Amsterdam, 1971).
[9]L. Prandtl, in *Proceedings of the First International Congress for Applied Mechanics*, edited by C. Biezeno and J. Burgers (Waltman, Delft, 1925), p. 43; A. Reuss, Z. Angew. Math. Mech. 10, 266 (1930).
[10]R. von Mises, Gött. Nachrichten, Math-Phys. 1913, 582.
[11]W. S. Farren and G. I. Taylor, Proc. R. Soc. London 107, 422 (1925).
[12]J. C. Maxwell, Philos. Trans. R. Soc. London 157, 49 (1867).
[13]L. E. Malvern, Q. Appl. Math. 8, 405 (1951).
[14]J. W. Taylor, in *Dislocation Dynamics*, edited by A. R. Rosenfield *et al.* (McGraw-Hill, New York, 1968), p. 573.
[15]W. Herrmann, in *Propagation of Shock Waves in Solids*, edited by E. Varley (ASME, New York, 1976), p. 1.
[16]Herrmann uses a different definition of the Lamé coefficients; I have transcribed his $\lambda + 2\mu$ and μ, respectively, as $B + \frac{4}{3}G$ and G.
[17]C. Kittel, *Quantum Theory of Solids* (Wiley, New York, 1963).
[18]D. Pines, *Elementary Excitations in Solids* (Benjamin, New York, 1963).
[19]B. N. Brockhouse *et al.*, in *Inelastic Scattering of Neutrons in Solids and Liquids*, (IAEA, Vienna, 1961), p. 531; R. Stedman and G. Nilsson, Phys Rev. 145, 492 (1966); R. Stedman *et al.*, *ibid.* 162, 545 (1967).
[20]R. E. Peierls, *Quantum Theory of Solids* (Clarendon, Oxford, 1955).
[21]J. M. Ziman, *Electrons and Phonons* (Oxford University Press, Oxford, 1960).
[22]J. Callaway, *Quantum Theory of the Solid State* (Academic, New York, 1974), part B.
[23]D. E. Grady, in *High-Pressure Research*, edited by M. H. Manghnani and S. Akimoto (Academic, New York, 1977), p. 389.
[24]A similar system of equations, in which plastic-strain-rate effects are modeled with artificial viscosity, has been studied numerically by M. L. Wilkins, in *Methods in Computational Physics*, edited by B. Alder *et al.* (Academic, New York, 1964), Vol. 3, p. 211; also Y. M. Chen and M. L. Wilkins, in *Mechanics of Fracture*, edited by G. C. Sih (Noordhoff, Leyden, 1977), Vol. 4, p. 295.

Flow process of weak shocks in solids

Duane C. Wallace
Los Alamos Scientific Laboratory, Los Alamos, New Mexico 87545
(Received 17 April 1979)

Experimental measurements of weak-shock profiles in the alloy 6061-*T*6 Al are analyzed by irreversible-thermodynamic finite-strain theory to obtain a complete description of the flow process through the shock compression, including the entropy production and the relations among the flow variables of shear stress, plastic strain, and plastic strain rate. The primary quantities, the normal stress and the normal strain, are determined entirely from the equations of motion and the shock-profile data; the secondary quantities, the shear stress, plastic strain, temperature, and entropy, are then determined by thermodynamics. It is shown that infinitesimal strain theory gives unreliable results as soon as the plastic strain becomes of the same order of magnitude as the elastic strain.

I. INTRODUCTION

A rich source of experimental information on dynamic deformation processes in solids is shock profiles in the weak-shock region[1]; the term *weak shock* is here used to mean a shock whose velocity is not greater than the elastic precursor velocity. The profile measurements are capable of determining the particle velocity as a function of position and time in a solid through which a planar shock is propagating. This gives a one-variable map of the shock-induced deformation process, since the particle velocity is one of the several variables which are coupled into the process. The complete process is governed by three coupled subsets of equations[2]: the equations of motion, which express conservation of mass, momentum, and energy; the thermoelastic equations, which are relation among stresses, elastic strains, temperature, and so on, and whose coefficients are reasonably well known experimentally in the weak-shock region; and the plastic constitutive equation which relates the plastic-flow variables. The plastic constitutive relation is experimentally the least-known material property involved in the whole process. Experimental shock profiles have generally been analyzed by constructing parametrized dislocation models to represent the plastic flow. The decay of the elastic precursor in iron[3] was so analyzed by Taylor[4] and by Rohde,[5] and in aluminum by Arvidsson *et al.*[6] In a series of papers on single-crystal LiF, the Washington State University group developed a model based on nucleation and growth of dislocation loops.[7] A detailed numerical study of dislocation multiplication effects on profile shapes has been carried out by Herrmann and co-workers at Sandia.[8]

In the present work we take an alternative approach: Given the weak-shock profiles and the relevant thermoelastic properties of the solid under consideration, we set out to extract from this information the constitutive relations governing the plastic flow. The results so obtained can be considered experimental results, independent of a dislocation-dynamics theory. A profile analysis of the present kind is made possible by the great increase in experimental precision in recent years, as illustrated by the example of 6061-*T*6 Al: The 1963 measurements of Lundergan and Herrmann,[9] with a time resolution of approximately 2 μs, gave a value of 6.4 ± 0.7 kbar for the Hugoniot elastic limit; the 1969 measurements of Johnson and Barker[10] with resolution of a few ns gave 4.1 kbar.

The Johnson and Barker data are analyzed in the following section, and the flow variables, which are the shear stress, plastic strain, and plastic strain rate, are determined with respectable precision through each shock profile.

II. PROFILE ANALYSIS

A. Shock velocity *v*. particle velocity

We have chosen to study 6061-*T*6 Al because there are available a set of shock profiles and also measurements of the polycrystal third-order elastic constants. The profile data of Johnson and Barker[10] are shown in Fig. 1, in the form of the particle velocity as a function of time t, where $t=0$ when the elastic precursor arrives at the aluminum surface. The measurements were accomplished with a laser velocity interferometer looking at the aluminum through a fused-quartz window; a small impedance-difference correction was applied to transform surface velocity to particle velocity.

The qualitative character of the profiles is illustrated in Fig. 2, where the various states in the shock compression process are lettered, from the initial state a at zero stress and room temperature to the final state e. The experi-

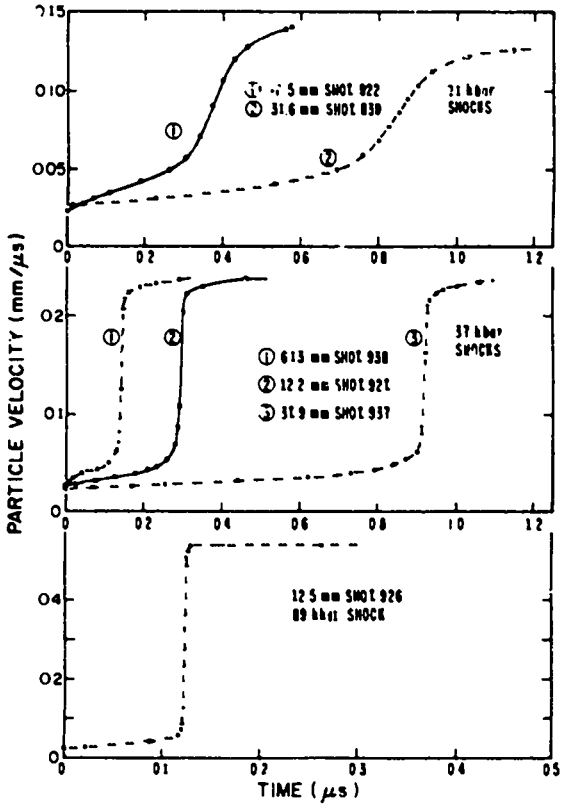

FIG. 1. Data of Johnson and Barker (Ref. 10) for six impact experiments on 6061-*T*6 Al.

ment supports the following description: The front from state a to state b, called the elastic precursor, is a steady wave; the region from state b to state c, which we call the plastic precursor, is nonsteady; the plastic wave from state c to state e is steady with velocity D. We generally refer to D as the shock velocity.

A precision method for measuring all three of the adiabatic polycrystal third-order elastic constants ζ, ξ, ν was described by Clifton.[11] His results for these for 6061-*T*6 Al, and also for the two adiabatic second-order elastic constants λ, μ (the Lamé constants), and for the initial-state density ρ_e, are

$$\rho_e = 2.703\ \text{g/cm}^3, \quad \zeta = -1.40\ \text{Mbar},$$
$$\lambda = 0.544\ \text{Mbar}, \quad \xi = -2.82\ \text{Mbar}, \qquad (1)$$
$$\mu = 0.276\ \text{Mbar}, \quad \nu = -4.69\ \text{Mbar}.$$

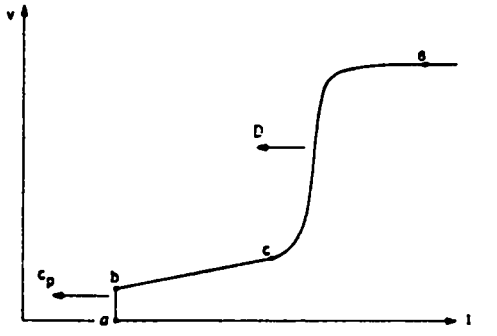

FIG. 2. Schematic representation of a shock profile moving as two steady waves and an intervening unsteady region. Particle velocity v as a function of time t.

The first step in the analysis is to determine the shock velocity for each profile. For the first five shots of Fig. 1 (all but 926), the original data time record runs from impact time; hence it is possible to compute for these shots the elastic precursor velocity c_p (in mm/μs):

$$c_p = 6.46 \pm 0.01, \qquad (2)$$

where the ± 0.01 represents merely the experimental scatter. This velocity is considerably faster (1.4% faster) than Clifton's value[11] of the longitudinal sound speed c_l (in mm/μs):

$$c_l = 6.37. \qquad (3)$$

The difference is mostly due to finite-strain effects in the elastic precursor: The normal strain on the precursor is $\epsilon_b = 0.0037$ and this is not exactly infinitesimal. With the elastic constants of Eq. (1), I calculate a velocity of 6.43 mm/μs in finite-strain theory for a steady wave of this strain amplitude.

Since the profile analysis is going to be based on the treatment of the plastic wave of each profile as a steady wave, the appropriate velocity D has to be computed from the difference in arrival times of two similar steady waves. This procedure eliminates any nonsteady effects which may have been present in the time immediately following impact. In this way we obtain one velocity from the two shocks at 21 kbar and two independent velocities from the three shocks at 37 kbar. Comparing these results with velocities determined from the arrival time of each separate plastic wave shows small differences (of order 1%) for the 21-kbar shocks and no differences (random scatter of order 0.2%) for the 37 kbar shocks. It is therefore safe to compute the shock velocity for the 89-kbar shock from the precursor velocity (2) together with the profile time record shown in Fig. 1.

A well-established experimental result for shocks up to the Mbar range is that shock velocity is proportional to the final-state particle velocity v_e.[12] In the present work, where one D is computed from two profiles, we assign the corresponding value v_e as the average for the two profiles; there is no averaging for shot 926. The resulting collection of four $D(v_e)$ points is

plotted in Fig. 3, along with the least-squares-fitted straight line

$$D = 5.26 + 1.47 v_e \text{ mm}/\mu\text{s} . \quad (4)$$

Also shown for comparison is the result of Marsh and McQueen[13] for 6061 Al of unspecified hardness; they measured D for shocks of 70 to 680 kbar and fitted the data to the line $D = 5.29 + 1.38 v_e$. The agreement is good in the pressure region of comparison. In the subsequent analysis, we take D from the relation (4).

B. Integration of the equations of motion

The equations for conservation of mass and conservation of linear momentum in plane-wave geometry are given in Ref. 2, Eqs. (40) and (41), in a mixed Eulerian-Lagrangian form; it is convenient here to use the Lagrangian forms

$$\frac{\partial \epsilon}{\partial t} = -\frac{\partial v}{\partial X} , \quad (5)$$

$$\frac{\partial \sigma}{\partial X} = -\rho_0 \frac{\partial v}{\partial t} , \quad (6)$$

where X is the Lagrangian coordinate, i.e., the position in the initial configuration of a material plane, $\epsilon = 1 - \rho_0/\rho$ is the normal strain, σ is the normal stress, all variables are functions of X and t, and $v(X, t)$ is the particle velocity, i.e., the velocity in the shock propagation direction of that material plane whose Lagrangian coordinate is X.

We define a steady wave as one which propagates at a fixed velocity without changing its shape; in mathematical terms this means $v(X, t)$ is a function of only one variable, namely $X - ct$, where c is the propagation velocity:

$$v(X, t) = v(X - ct) . \quad (7)$$

If a wave is steady, or if any portion of the wave in a fixed range of the particle velocity is steady, then we can argue that the flow process is steady in that range, i.e., each successive planar slab of material passes along the same physical path while the steady wave passes over the material plane. This means each thermodynamic variable is also a function of only $X - ct$, and in particular

$$\epsilon = \epsilon(X - ct) , \quad \sigma = \sigma(X - ct) . \quad (8)$$

Under the conditions (7) and (8), the equations of motion (5) and (6) become the total differential equations

$$d\epsilon = c^{-1} dv , \quad (9)$$

$$d\sigma = \rho_0 c\, dv . \quad (10)$$

Equations (5) and (6) can now be integrated through the profile illustrated in Fig. 2, as follows.

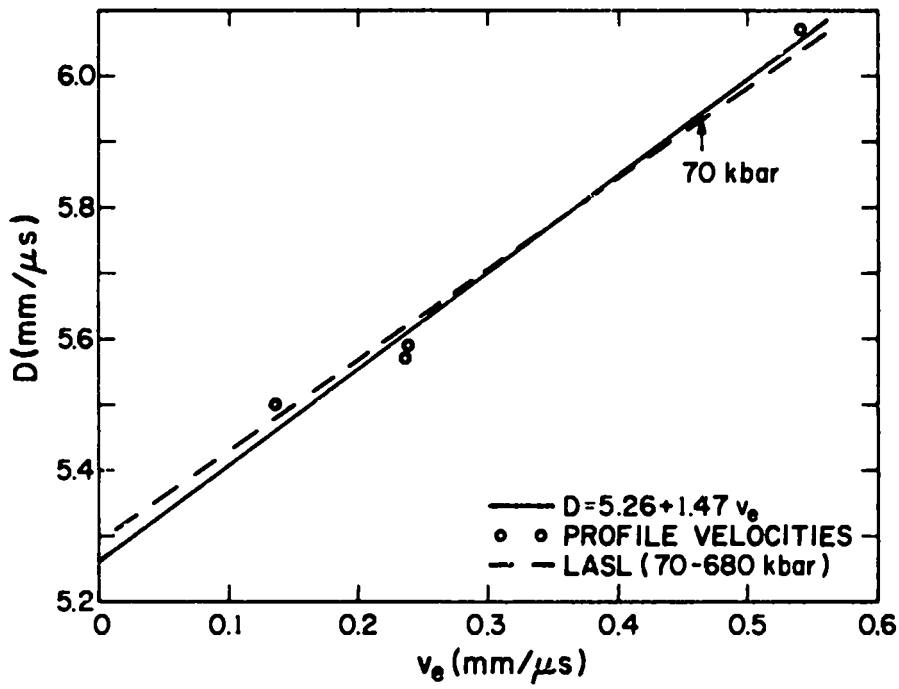

FIG. 3. Shock velocity versus particle velocity for 6061-T6 Al. Data points are from the Johnson and Barker profiles, the straight line is a least-squares fit to these points, the dashed line is the fitted result of Marsh and McQueen (Ref. 13).

Elastic precursor. The front is steady and moves at velocity c_p; the initial conditions are $\epsilon_a = 0$, $\sigma_a = 0$; Eqs. (9) and (10) then give

$$\epsilon_b = v_b/c_p, \tag{11}$$

$$\sigma_b = \rho_a c_p v_b. \tag{12}$$

Plastic precursor. States b and c are characterized by constant values of v_b and v_c moving at the velocities c_p and D, respectively; an approximation compatible with the experimental data for $v(X, t)$ between states b and c is the straight line

$$v = v_b + (v_c - v_b)\left(\frac{c_p t - X}{X\delta}\right), \quad \delta = \frac{c_p - D}{D}. \tag{13}$$

For this function, (5) and (6) integrate to

$$\epsilon = \epsilon_b + \frac{v - v_b}{c_p}\left(1 + \frac{\delta(v - v_b)}{2(v_c - v_b)}\right), \tag{14}$$

$$\sigma = \sigma_b + \rho_a c_p\left(\frac{v_c - v_b}{\delta}\right)\ln\left(1 + \frac{\delta(v - v_b)}{(v_c - v_b)}\right). \tag{15}$$

Plastic wave. We can again use the steady wave forms (9) and (10) to integrate from c toward e and find

$$\epsilon = \epsilon_c + D^{-1}(v - v_c), \tag{16}$$

$$\sigma = \sigma_c + \rho_a D(v - v_c). \tag{17}$$

It may be noted that we have relied heavily on the experimental data in devising the above integration procedure. For the six profiles of Fig. 1, v_b lies in the range 0.023–0.026 mm/μs, with nothing in the data to indicate a dependence on either the shock strength or the propagation distance. As for the value of v_c, this can be chosen somewhat arbitrarily, but all the profiles are consistent with $v_c = 0.050$ mm/μs, which was used in the present calculations. For the $v(X, t)$ curve in the unsteady region from b to c, we are fortunate that experiment provides a simple analytic approximation. This also allows us to see clearly a result which may be expected to hold in general: For the unsteady flow region, the Rayleigh line, which is the $\sigma(\epsilon)$ relation, is not a straight line. The Rayleigh line is straight for a steady wave; this is obvious from the combination of Eqs. (9) and (10) to give $d\sigma = \rho_a c^2 d\epsilon$. But for σ and ϵ on the plastic precursor, the combination of (14) and (15) produces a $\sigma(\epsilon)$ relation which is slightly curved (concave downward) in this region.

We used the above equations to calculate σ and ϵ as functions of v for each of the six profiles. The raw data points for v were used. The results for the two profiles at 21 kbar, and for the three at 37 kbar are in excellent internal agreement.

C. The flow behavior

The thermoelastic differential equations for the normal stress σ and the shear stress τ for plane-wave geometry are given in Ref. 2, Eqs. (37) and (38). The independent strain variables are the total normal strain ϵ and the plastic strain ψ. Since the strains are small in weak shocks, it is convenient here to integrate $d\sigma$, $d\tau$ and express σ, τ as power series in ϵ, ψ. This can be done in either of the following two ways: (a) Expand the stress-strain coefficients in powers of elastic strains, convert to ϵ, ψ, and integrate $d\sigma$, $d\tau$ or (b) expand the internal energy in powers of elastic strains and calculate stresses from their thermoelastic definition as strain derivatives of the internal energy.[14,15] We carry the expansion of σ, τ only to second order in strains because coefficients of third-order terms involve the fourth-order elastic constants, whose values we do not know.

In addition to the strain terms, the equations for $d\sigma$, $d\tau$ contain the following terms in the entropy: $\rho\gamma_1 T dS$ in $d\sigma$ and $\frac{1}{2}\rho(\gamma_1 - \gamma_2)T dS$ in $d\tau$, where T is the temperature, S is the entropy per unit mass, and γ_β are the anisotropic Grüneisen parameters. Since $T dS$ is proportional to $\tau d\psi_1^2$ and since τ is of lowest-order linear in strains, $T dS$ is a second-order quantity. Hence to express the above $T dS$ terms correct to second order, γ_β may be evaluated to lowest order in strains, which means γ_β may be taken as the ordinary Grüneisen parameter evaluated in the initial state γ_a. The completed results for σ and τ to second order in strains are

$$\begin{aligned}\sigma = {} & (\lambda + 2\mu)\epsilon - 2\mu\psi - (\tfrac{3}{2}\lambda + 3\mu + \zeta + 2\xi)\epsilon^2 \\ & + (4\lambda + 10\mu + 4\xi)\epsilon\psi - (\tfrac{3}{2}\lambda + 6\mu + \tfrac{3}{2}\xi + \tfrac{1}{4}\nu)\psi^2 \\ & + 2\gamma_a \int_0^{\epsilon,\psi} \tau(\epsilon', \psi')d\psi',\end{aligned} \tag{18}$$

$$\begin{aligned}\tau = {} & \mu(\epsilon - \tfrac{3}{2}\psi) - (\lambda + \tfrac{3}{2}\mu + \xi)\epsilon^2 \\ & + (\tfrac{3}{2}\lambda + \tfrac{9}{2}\mu + \tfrac{3}{2}\xi + \tfrac{1}{4}\nu)\epsilon\psi - (\tfrac{9}{4}\mu + \tfrac{3}{8}\nu)\psi^2.\end{aligned} \tag{19}$$

The integral in (18) is the entropy contribution to σ; an entropy contribution to τ would appear in third order.

By integrating the equations of motion, we have already determined the variables σ, ϵ through each shock profile; note for a given profile the variables correspond to a fixed Lagrangian coordinate, i.e., to a fixed planar slab of material. With σ, ϵ given, Eqs. (18) and (19) were then solved for τ, ψ. Because of the $\int \tau d\psi$ in (18), it was necessary to solve (18) and (19) simultaneously by numerical iteration. For γ_a, we used the value for pure aluminum,[14]

$$\gamma_a = 2.16 . \qquad (20)$$

The results for τ as a function of ψ through each shock profile are shown in Figs. 4–6. Since the time variable through each profile is also known from experiment, it is possible to calculate $\dot{\psi}$, the Lagrangian time derivative of ψ. These results are also shown in Figs. 4–6. The shaded area at the top of each $\dot{\psi}$ curve is meant to indicate the experimental scatter there; this scatter is not significant in the overall analysis since we have $\dot{\psi}$ spanning a range of four orders of magnitude.

It is seen from Figs. 4–6 that the shear stress increases rapidly, and drives up the flow rate, at the beginning of the flow process; toward the end of the process the plastic flow slows, and it finally stops when the material reaches the static state e, where ψ reaches its maximum. For the 89-kbar shock the rise of the plastic wave was possibly too fast to be followed by the instrumentation, so the observed rise time of 5 ns is an upper limit (see Fig. 1); therefore the maximum plastic strain rate of 10^7 s^{-1} in Fig. 6 may be only a lower limit. The flow curves of Figs. 4–6 support two qualitative conclusions for 6061-*T*6 Al, as follows:

(a) The rapid increase of the shear stress at the flow front is due mainly to strain-rate effects.

(b) Except for possibly the weakest shocks, the shear stress decreases in the approach to static equilibrium behind the shock.

We comment now on the errors in the τ, ψ curves. At the front of each curve the error in τ is small since the total strain there is mostly elastic. Later, however, τ no longer increases even though ϵ continues to increase strongly. This is because the metal is flowing in such a way as to keep the shear stress from increasing, i.e., plastic flow is canceling out much of the increase in the anisotropic part of the purely

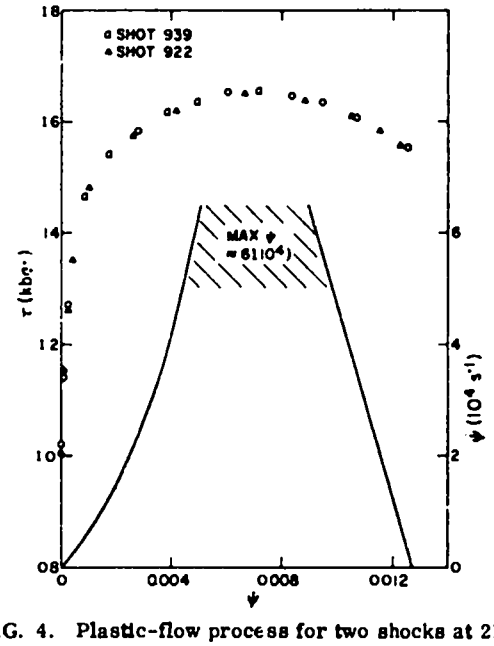

FIG. 4. Plastic-flow process for two shocks at 21 kbar.

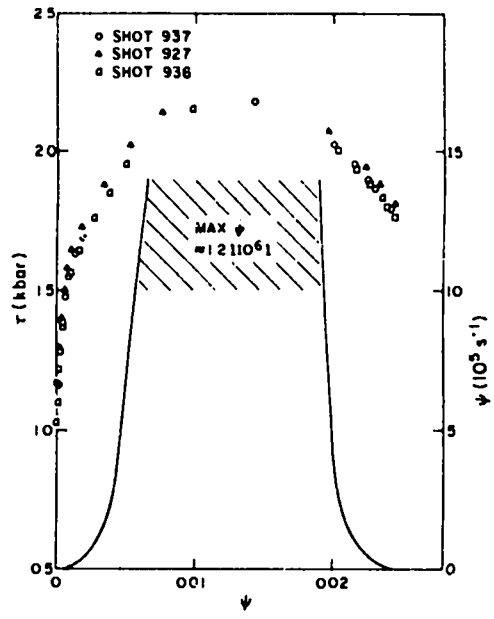

FIG. 5. Plastic-flow process for three shocks at 37 kbar.

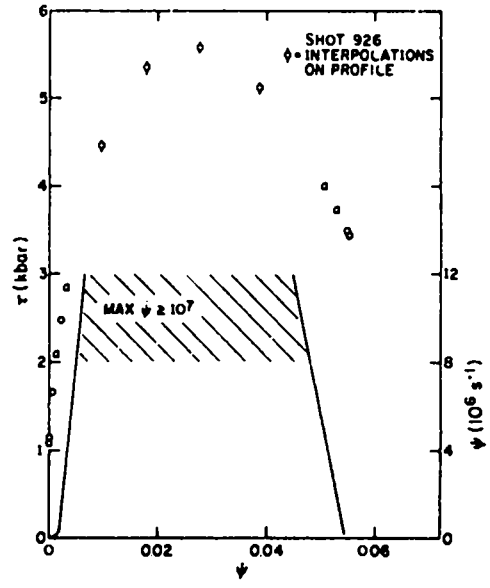

FIG. 6. Plastic-flow process for the 89-kbar shock. The four points indicated were interpolated as a straight line in particle velocity versus time on the plastic wave front (see Fig. 1).

elastic strain. Because of this subtle cancellation, the error in our computed ψ, which comes ultimately from errors in our thermoelastic stress-strain relations, can be significant in the late stage of each shock compression profile (near the final state). The effect depends in a complicated way on the coupling between the errors for ψ and τ. To learn something about this we computed ψ and τ at the final state in infinitesimal strain theory; that is, from equations (18) and (19) with the second-order strain terms omitted. The results are compared with the second-order calculations in Table I. It is seen that infinitesimal strain theory produces unacceptable results for all the shock groups. It is further obvious that inclusion of the next-higher-order strain terms, corresponding to fourth-order elastic constants, would be desirable for the 89-kbar shock.

D. Constitutive relations

In addition to the steady-wave profiles analyzed above, Johnson and Barker[10] also presented a series of 9.5-kbar profiles which show the decay of the elastic precursor through a material distance X of 4 to 38 mm. In these experiments they measured the free surface velocity, which gives quite accurately the particle velocity at the profile point b through the relation: v_b equals half the free surface velocity at b. These data can be analyzed by Taylor's theory,[4] which is based on the observations that the elastic precursor travels on the lead C_+ characteristic and that $\psi = C$ there. With the characteristic velocity c_p, the equations of Ref. 4 give

$$\psi_b = 0, \qquad \dot{\psi}_b = -\frac{\rho_0 c_p^2}{\mu}\frac{dv_b}{dX}. \tag{21}$$

From this and (19), the shear stress is

$$\tau_b = \mu\epsilon_b - (\lambda + \tfrac{2}{3}\mu + \xi)\epsilon_b^2, \tag{22}$$

where ϵ_b is given in leading order by (11). Thus from the elastic precursor data for $v_b(X)$, we can find the $\tau, \dot{\psi}$ relation on the line $\psi = 0$.

TABLE I. Final-state values ψ_e, τ_e as calculated in infinitesimal strain theory and in second-order theory, averaged for each shock group. Also the entropy contributions to ψ_e, τ_e. τ_e is in kbar.

Shock group (kbar)	Infinitesimal ψ_e	Infinitesimal τ_e	Second order ψ_e	Second order τ_e	Entropy contribution ψ_e	Entropy contribution τ_e
21	0.010	2.6	0.013	1.6	1%	−4%
37	0.016	5	0.024	1.8	1%	−9%
89	0.016	18	0.055	3.5	3%	−25%

The flow relations we have determined are shown in Fig. 7 as curves of τ vs $\dot{\psi}$ at fixed ψ. The $\psi = 0$ curve is from the elastic precursor decay, Eqs. (21) and (22). The curves for $\psi = 0.001, 0.002, 0.004$ are each composed of three points; one from the 21-kbar shocks (Fig. 4), one from the 37-kbar shocks (Fig. 5), and one from the 89-kbar shock (Fig. 6). Though the values of ψ are very small, all of these curves are quite accurate; recall that cancellation errors in τ are not important when ψ is small. A set of points at the largest plastic strains we could determine were taken from near the end of the 89-kbar shock; these have ψ values of 0.048–0.054, and we expect them to be accurate in ψ and $\dot{\psi}$ but possibly in significant error in τ. It should also be noted that these points represent material under a pressure of approximately 84 kbar and at a temperature of about 380 K. Results reported recently by Herrmann,[16] based on analysis of part of the same experimental data through a relaxation function formalism, differ significantly from the present results, presumably due to the inclusion here of third-order elastic constants and entropy effects (the two methods are compared analytically in Ref. 2). The plastic-flow behavior of 6061-*T*6 Al was measured by Holt *et al.*[17] for ψ up to 0.08 and $\dot{\psi}$ from 10^{-3} to 10^{3} s^{-1}: they observed essentially no strain-rate dependence at all, and a mild strain hardening. The curves of Fig. 7, extrapolated to low strain rates, are consistent with the measurements of Holt *et al.* Note that in the extrapolation to low strain rates, the four curves for small ψ values will all cross, giving τ as an increasing function of ψ at a fixed $\dot{\psi}$ of say $\dot{\psi} = 10^{3}$ s^{-1}.

E. Temperature and entropy

The theory of Ref. 2 also enables us to calculate the temperature and entropy through the shock profiles by means of the equations

$$T\,dS = 2V\tau\,d\psi, \tag{23}$$

$$T\,dS = C_\eta[dT + T\gamma_1\,d\ln(1-\epsilon) + T(\gamma_1 - \gamma_2)d\psi], \tag{24}$$

where $V = \rho^{-1}$ is the volume per unit mass and C_η is the heat capacity at constant elastic configuration. The anisotropic Grüneisen parameters may be expressed as derivatives of the stresses τ_β with respect to the internal energy U at constant elastic configuration[2,14]:

$$\rho\gamma_\beta = -\left(\frac{\partial\tau_\beta}{\partial U}\right)_\eta. \tag{25}$$

A set of approximations which simplify the numerical integration of (23) and (24), and which

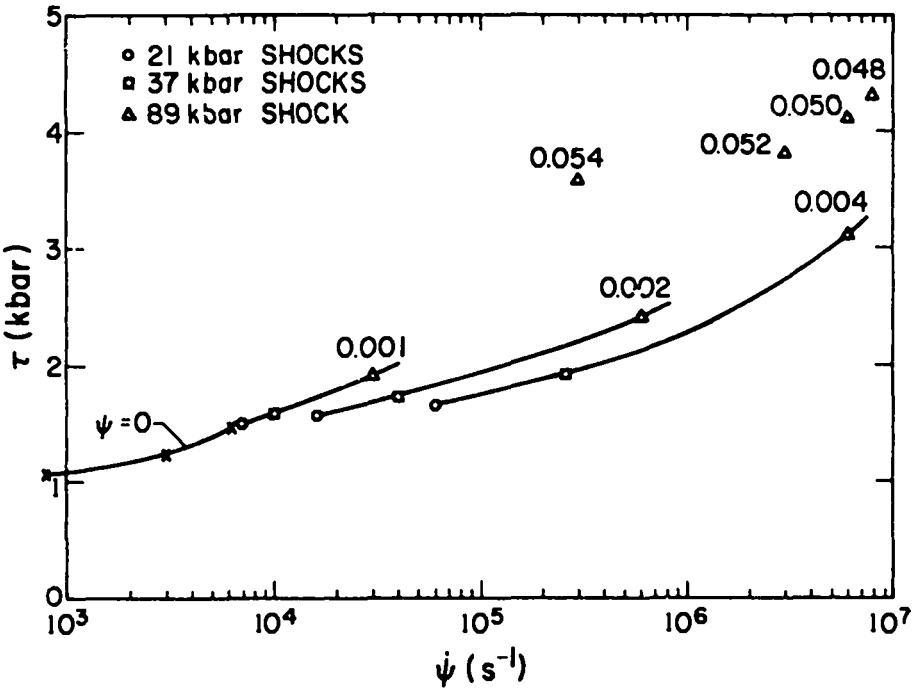

FIG. 7. Shear stress τ as a function of plastic strain rate $\dot{\psi}$ for lines of constant ψ. The numbers label the value of ψ for the lines and points.

are of acceptable accuracy for the present calculations, are

$$\gamma_1=\gamma_2=\gamma\,,\qquad C_\eta=C_V\,,\qquad C_V=0.88\times10^7\,,\qquad \rho\gamma=\text{constant}=\rho_a\gamma_a\,, \tag{26}$$

where the C_V for 6061-$T6$ Al is measured in erg/gm K. The first approximation expresses the idea that the thermal energy exerts outward forces in an essentially isotropic way, i.e., it contributes nearly equally to all three principal stresses [see Eq. (25)]. $C_\eta=C_V$ is the same sort of approximation. To support taking C_V constant, we note that for any characteristic temperature theory, as e.g., the Debye theory, with characteristic temperature Θ a function only of the volume, the relations hold:

$$S=S(\Theta/T),\quad \Theta=\Theta(V)\,;$$

then $S=$ constant implies $\Theta/T=$ constant, which implies $C_V=$ constant. Since entropy generation is small in the weak-shock region, the thermodynamic states are not far from $S=S_a$, and C_V is not far from its value in the initial state, which is the value given for 6061-$T6$ Al in (26). Finally the approximation $\rho\gamma=$ constant is in keeping with $d\ln\gamma/d\ln V\approx-1$ for pure Al,[14] and with the extensive shock-related study of Neal[18] for Al and Al alloys for compressions up to a factor of 2.

The initial temperature for our calculations was taken as $T_a=295$ K. The values of T and $S-S_a$ in the final state, along with stresses and strains at some intermediate profile points, are listed for each shock group in Table II.

III. DISCUSSION

The application of the general thermoelastic–plastic-flow theory to accurate one-dimensional strain experiments on 6061-$T6$ Al has been shown to be relatively simple. With the velocity profiles

TABLE II. Thermodynamic quantities at state b and at the final state e. Averages are listed for each shock group. Stress is in kbar, temperature in K, entropy in 10^5 erg/gm K. $T_a=295$ K. The number in parentheses is the last significant digit.

Quantity	21 kbar	37 kbar	89 kbar
ϵ_b	0.0036	0.0038	0.0038
σ_b	4.0	4.1	4.1
τ_b	1.0	1.0(6)	1.0(6)
ϵ_e	0.0240	0.0414	0.089
σ_e	21.0	36.7	89
ψ_e	0.0127	0.0244	0.055
τ_e	1.6	1.8	3.5
T_e	313	327	380
S_e-S_a	0.5	1.2	5.3

divided into steady and self-similar parts in the stress range 20–90 kbar, only algebraic computations are required. For more general profiles the analysis will be more complicated. A more complex space- and time-dependent representation of material velocities is required for the initial evolution of shock profiles, as illustrated by the data of Johnson and Barker[10] at approximately 9 kbar.

Lipkin and Asay[19] have recently reported velocity measurements on 6061-*T*651 Al at 20 kbar which are approximately self-similar throughout, implying a very weak flow-rate dependence for τ. The present analysis also shows a small strain-rate dependence at the 21-kbar stress level (Figs. 4 and 7). In addition, Asay and Lipkin[20] used the same reshock and release measurements to estimate the shear stress for 6061-*T*651 Al in the shocked state at 20 kbar. Their result for $Y = 2\tau$ is 2.6 kbar; the present result from Fig. 4 at 21 kbar is $2\tau = 3.1$ kbar. The difference is not unreasonable in view of uncertainties in either analysis. A new experimental method for propagating large one-dimensional shear waves at high stresses[21] should provide valuable new data for improving our knowledge of the flow functions of metals.

ACKNOWLEDGMENT

I am grateful to Jim Johnson for providing me with his original data notebook from which to work.

[1]J. W. Taylor, in *Dislocation Dynamics*, edited by A. R. Rosenfield *et al.* (McGraw-Hill, New York, 1968), p. 573.
[2]D. C. Wallace, Phys. Rev. B 22, 1477 (1980) (preceding paper).
[3]J. W. Taylor and M. H. Rice, J. Appl. Phys. 34, 364 (1963).
[4]J. W. Taylor, J. Appl. Phys. 36, 3146 (1965).
[5]R. W. Rohde, Acta Metall. 17, 353 (1969).
[6]T. E. Arvidsson, Y. M. Gupta, and G. E. Duvall, J. Appl. Phys. 46, 4474 (1975).
[7]Y. M. Gupta, G. E. Duvall, and G. R. Fowles, J. Appl. Phys. 46, 532 (1975); J. R. Asay, D. L. Hicks, and D. B. Holdridge, *ibid.* 46, 4316 (1975).
[8]W. Herrmann, D. L. Hicks, and E. G. Young, in *Shock Waves and the Mechanical Properties of Solids*, edited by J. J. Burke and V. Weiss (Syracuse University Press, Syracuse, 1971), p. 23.
[9]C. D. Lundergan and W. Herrmann, J. Appl. Phys. 34, 2046 (1963).
[10]J. N. Johnson and L. M. Barker, J. Appl. Phys. 40, 4321 (1969).
[11]R. J. Clifton, in *Shock Waves and the Mechanical Properties of Solids*, edited by J. J. Burke and V. Weiss (Syracuse University Press, Syracuse, 1971), p. 73.
[12]R. G. McQueen, S. P. Marsh, J. W. Taylor, J. N. Fritz, and W. J. Carter, in *High Velocity Impact Phenomena*, edited by R. Kinslow (Academic, New York, 1970), p. 293.
[13]S. P. Marsh and R. G. McQueen, Los Alamos Scientific Laboratory (LASL) file data (unpublished). An updated shock velocity-particle relation for 6061 Al is $D = 5.35 - 1.34v_p$ (LASL Shock Hugoniot Data, University of California Press, Berkeley, 1980).
[14]D. C. Wallace, *Thermodynamics of Crystals* (Wiley, New York, 1972).
[15]D. C. Wallace, in *Solid State Physics*, edited by H. Ehrenreich, F. Seitz, and D. Turnbull (Academic, New York, 1970), Vol. 25, p. 301.
[16]W. Herrmann, in *Propagation of Shock Waves in Solids*, edited by E. Varley (ASME, New York, 1976), p. 1.
[17]D. L. Holt, S. G. Babcock, S. J. Green, and C. J. Maiden, Trans. Am. Soc. Met. 60, 152 (1967).
[18]T. Neal, Phys. Rev. B 14, 5172 (1976).
[19]J. Lipkin and J. R. Asay, J. Appl. Phys. 48, 182 (1977).
[20]J. R. Asay and J. Lipkin, J. Appl. Phys. 49, 4242 (1978).
[21]A. S. Abou-Sayed and R. J. Clifton, J. Appl. Mech. 44, 79 (1979); 44, 85 (1979).

Erratum: Text in Reference 13 should read, "An updated shock velocity - particle velocity relation..."

Equation of state from weak shocks in solids

Duane C. Wallace
Los Alamos Scientific Laboratory, Los Alamos, New Mexico 87545
(Received 17 April 1979)

The Rankine-Hugoniot jump conditions for the increases across a shock of the normal stress, normal strain, and internal energy are not valid for weak shocks in solids. Correct jump equations for a solid can be obtained by integrating the equations for conservation of mass, momentum, and energy along the Rayleigh line through the shock process; these jump equations then depend on the details of the shock profile. Further, because a uniaxially compressed solid supports a nonzero shear stress, the locus of thermodynamic states reached behind planar shocks, which we call the anisotropic Hugoniot, requires for its description two stress variables and two strain variables. In the present paper the thermodynamic description of the anisotropic Hugoniot is given, and for the example of 6061-*T*6 Al the shock-profile jump equations are derived, the weak-shock equation of state is computed, and the pressure on the principal adiabat is found to differ from the results of Rankine-Hugoniot theory by several percent in the range 0–100 kbar.

I. INTRODUCTION

Shock experiments have been extensively used to determine equations of state of solids.[1–4] The quantities measured are the shock and particle velocities, and from these the Hugoniot equation of state, a pressure-volume-energy curve, is computed by means of the Rankine-Hugoniot jump conditions. Since these jump conditions were constructed specifically to describe shocks in gases or liquids,[5–7] their use to analyze shocks in solids represents the neglect of differences in solid and liquid behavior. This situation has been recognized in the past,[1–4] but the theory and the experimental data needed to correct for solid-liquid differences were not available. In the present paper we present the needed theory for the case of weak planar shocks in initially isotropic solids.

It is helpful at the outset to identify the characteristics of shocks in solids which are to be accounted for in this work. The Rankine-Hugoniot jump conditions and related thermodynamic analyses[5–7] will be referred to as "liquid Hugoniot theory." This theory assumes that the shock is a single steady wave, which means the jump conditions can be calculated by the black box treatment: The entire shock front is considered a black box of fixed thickness which moves at the shock speed; ahead of the box is material in the initial equilibrium state and behind the box is uniformly moving material in the final equilibrium state. Without knowing any details of the shock structure it is still possible to apply conservation laws: Whatever flows into the box must flow out. In this way conservation of mass, momentum, and energy give relations among the following three quantities: the normal strain from initial to final state, the corresponding change in the normal stress, and the change in the internal energy. Since these are thermodynamic quantities, by the assumption of initial and final equilibrium, it is then possible to calculate the increase in entropy through the shock, a very appealing result of the theory. Unfortunately, however, the black-box treatment does not work for a weak shock in a solid. For since the elastic precursor travels faster than the plastic wave, the entire shock front is not a steady wave; it spreads continuously and takes in an ever increasing mass of material, and momentum and energy. This means the shock is a sink for these quantities, and the steady Rankine-Hugoniot jump conditions across the shock do not hold: All of what flows in does not flow out. Conservation of mass, momentum, and energy still hold on the local scale, but the total change in these quantities across the shock will depend on the spreading of the shock profile.

The other approximation of liquid Hugoniot theory is that the material behind the shock is in a state of isotropic pressure. This means there is only one stress variable and one strain variable on the Hugoniot, namely the pressure and the volume, and the liquid jump conditions are sufficient to specify these uniquely. A solid, however, after uniaxial compression by a planar shock, presumably supports a nonzero shear stress, so the final state is characterized by two stress variables and two strain variables; jump conditions on the normal stress and the normal strain are insufficient to determine all four of these stress and strain variables.

In Sec. II we set up a thermodynamic description of the anisotropic (tetragonal) Hugoniot for a solid; this description is not limited to weak shocks. In Sec. III we show how the weak-shock Hugoniot can be constructed from shock profiles,

and carry out the construction for 6061-*T*6 Al. Once the anisotropic Hugoniot is determined, it is possible to calculate isotropic pressure curves, including the principal adiabat; the theory for this is also derived in Sec. III, and the adiabat for 6061-*T*6 Al is compared with the corresponding curve calculated from liquid Hugoniot theory.

II. ANISOTROPIC HUGONIOT THERMODYNAMICS

The term Hugoniot will be used here to mean the sequence of thermodynamic equilibrium states reached behind each shock for a sequence of different-strength shocks from a given initial state. Our first job is to specify the Hugoniot in terms of thermodynamic variables. Since they are equilibrium states, they may be reached by a thermoelastic (reversible) process from the intial state. For an initially isotropic solid in plane-shock geometry, the stress and configuration variables are shown in Fig. 1. Cartesian coordinate 1 is the normal (propagation) direction and coordinates 2 and 3 are equivalent transverse directions. An element of mass in the initial configuration has dimensions d_a, w_a, and density ρ_a, and zero applied stress; in the final configuration it has dimensions d, w, density ρ, and normal compressive stress σ and transverse compressive stress $\sigma - 2\tau$. The final shear stress is τ. The configuration transformation from initial to final state is given by the elastic transformation matrix $\underline{\alpha}^e$,[8,9] whose elements for the simple transformation of Fig. 1 are (Voigt notation)

$$\alpha_1^e = d/d_a, \quad \alpha_2^e = \alpha_3^e = w/w_a, \qquad \alpha_4^e = \alpha_5^e = \alpha_6^e = 0. \tag{1}$$

The conservation of mass equation for $\underline{\alpha}^e$ is[8]

$$\rho_a/\rho = V/V_a = \det\underline{\alpha}^e = \alpha_1^e\alpha_2^e\alpha_3^e, \tag{2}$$

where $V = \rho^{-1}$ is the volume per unit mass. As shown in Fig. 1, there is also an increase in the entropy, from S_a in the initial state to S in the final state.

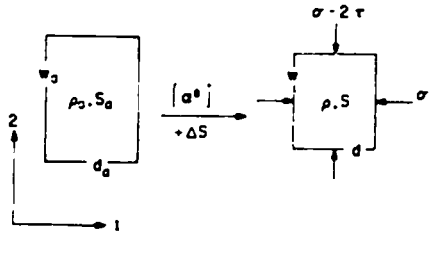

FIG. 1. Thermoelastic transformation of a mass element from the initial state to a final state which is on the anisotropic Hugoniot.

There is a different process by which the material can be brought from the same initial to final states shown in Fig. 1. This is the dynamic (irreversible) process which occurs during planar shock compression.[9-11] It is characterized by simultaneous elastic strain $\underline{\alpha}^e$ and plastic flow $\underline{\alpha}^p$, so there are four strain variables, but with the restrictions that the total transverse strain is zero and the plastic flow is volume conserving, there are only two independent strain variables, which can be taken as the total normal strain ϵ and the plastic strain ψ:

$$\epsilon = 1 - V/V_a, \tag{3}$$

$$\psi = -\ln\alpha_2^p. \tag{4}$$

The elastic strains are then related to ϵ and ψ by

$$\alpha_1^e = (1-\epsilon)e^{\psi}, \tag{5}$$

$$\alpha_2^e = e^{-\psi/2}. \tag{6}$$

For the moment, however, let us forget about shocks. We consider the Hugoniot to be an equilibrium thermodynamic curve of states reached through anisotropic *elastic* compression by a tetragonal stress system, while some reversible heat $dQ = TdS$ is put in from an external source. For stress-strain variables on the Hugoniot we take the set $\sigma, \tau, \alpha_1^e, \alpha_2^e$, or what is equivalent through Eqs. 2 and 3, σ, τ, V or ϵ, α_2^e. Then we proceed to find relations between these and other thermodynamic functions. Note the use of the variable V does not imply that the compression is isotropic or that the stress system is isotropic. Also note that there is no plastic flow on the Hugoniot; nevertheless the material must be presumed to be hardened in some way, so as to support elastically the shear stress τ. This point will be examined at the end of this section.

The thermodynamics of elastically anisotropic materials is well described in textbooks.[8,11] For the geometry of Fig. 1, the combined first and second laws are

$$TdS = dU + \sigma dV - 4V\tau d\ln\alpha_2^e, \tag{7}$$

where U is the internal energy per unit mass, S is the entropy per unit mass, and T is the temperature. An independent equation for dS is the identity which results from considering T as a function of S and the elastic strains,

$$TdS = C_\eta dT + TC_\eta[\gamma_1 d\ln V - 2(\gamma_1 - \gamma_2)d\ln\alpha_2^e], \tag{8}$$

where C_η is the heat capacity at constant elastic configuration and γ_1, γ_2 are the anisotropic Grüneisen parameters (Voigt indices, see Ref. 9 or 11 for definitions). Between Eqs. (7) and (8), T and S can be calculated by integrating up the Hugoniot if the other quantities are known on the

Hugoniot. The entropy is small in weak shocks, but not as small as in liquid Hugoniot theory. In particular, because σ and τ are of lowest-order linear in strains [Eqs. (9) and (10) below], the lowest-order terms in (7) and (8) are of second order, and these terms do not cancel in $\int dS$, so $S-S_a$ on the Hugoniot is of second order in strains. In liquid Hugoniot theory,[3] because $\tau=0$ on the Hugoniot, the second-order terms cancel and $S-S_a$ is of order ϵ^3 at small ϵ.

Another useful set of equations results from considering σ and τ as functions of S and the elastic strains, and calculating variations:

$$d\sigma=\rho\gamma_1 T dS-B_{11}d\ln V+2(B_{11}-B_{12})d\ln\alpha_2^e, \tag{9}$$

$$d\tau=\tfrac{1}{2}\rho(\gamma_1-\gamma_2)TdS-\tfrac{1}{2}(B_{11}-B_{21})d\ln V+(B_{11}+\tfrac{1}{2}B_{22}+\tfrac{1}{2}B_{23}-B_{12}-B_{21})d\ln\alpha_2^e, \tag{10}$$

where $B_{\beta\gamma}$ are the adiabatic stress-strain coefficients. Equations (9) and (10) hold everywhere for the configuration change of Fig. 1, i.e., they hold for arbitrary strains and entropy, or for arbitrary stresses and entropy. For the present tetragonal geometry, two of the $B_{\beta\gamma}$ are related by

$$B_{21}=B_{12}-2\tau. \tag{11}$$

If enough were known of the quantities on the Hugoniot, Eqs. (9) and (10) could be used to find information about the $B_{\beta\gamma}$ coefficients; this is analogous to the calculation of the bulk modulus in liquid Hugoniot theory.[3]

In the small strain region the $B_{\beta\gamma}$ can be expanded at constant S in terms of the two adiabatic second-order elastic constants λ, μ and the three adiabatic third-order elastic constants ζ, ξ, ν, as[8]

$$B_{11}=\lambda+2\mu-(4\lambda+8\mu+2\zeta+4\xi)\epsilon-(8\lambda+20\mu+8\xi)\ln\alpha_2^e, \tag{12}$$

$$B_{11}-B_{12}=2\mu-(4\lambda+10\mu+4\xi)\epsilon-(6\lambda+24\mu+6\xi+\nu)\ln\alpha_2^e, \tag{13}$$

$$B_{11}-B_{21}=2\mu-(4\lambda+8\mu+4\xi)\epsilon-(6\lambda+18\mu+6\xi+\nu)\ln\alpha_2^e, \tag{14}$$

$$B_{11}+\tfrac{1}{2}B_{22}+\tfrac{1}{2}B_{23}-B_{12}-B_{21}=3\mu-(3\lambda+9\mu+3\xi+\tfrac{1}{2}\nu)\epsilon-(18\mu+3\nu)\ln\alpha_2^e. \tag{15}$$

Equations (12)–(15) are correct to first order in strains at constant entropy; they are also correct to first order in strains in the region of the Hugoniot, because entropy contributions are formally of second order there.

We can now clarify the point of work hardening on the Hugoniot. The Hugoniot described by Eqs. (7)–(10) is entirely thermoelastic; the elastic strains are presumed homogeneous (or at least slowly varying on an atomic scale), and the energy stored in these strains is recoverably by reducing the stresses to zero. In the conservation of energy, Eq. (7), no energy has been allotted to work hardening. However, when a real solid is shocked to the Hugoniot, a small amount of energy is used to accomplish the work hardening and remains stored in the defect structure of the solid. Such energy is elastic in nature, inhomogeneous on an atomic scale, and recoverable by annealing; it does not correspond to the same stress-strain relation, or any other thermoelastic relation, as does the energy stored in homogeneous elastic strain. Now in our dynamic theory of the shock process, the energy associated with work hardening is accounted for through conservation of energy, but it is not stored in any "recoverable" form; it is instead assigned as part of the dissipation. Hence if we use the dynamic theory and shock data to calculate the thermodynamic variables in the shock-compressed state, we construct a Hugoniot which is the same as the one described by Eqs. (7)–(10) and which approximates the real physical Hugoniot by replacing energy stored in the defect structure by heat. The error is small, as discussed in Ref. 9.

III. THE SHOCK EQUATION OF STATE

A. Construction of the Hugoniot

We proceed now specifically for the case of 6061-*T*6 Al and base our calculations on the profile measurements of Johnson and Barker[12] and on the methods previously developed for analyzing them.[10] The experimental profiles are described by three regions on the graph of particle velocity v as a function of time (Fig. 2):

(1) The front from state a to state b is the elas-

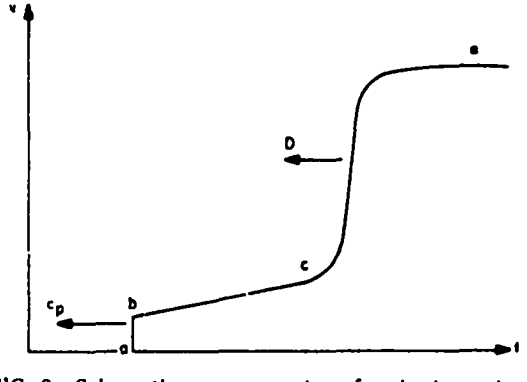

FIG. 2. Schematic representation of a shock moving as two steady waves and an intervening unsteady region. Particle velocity v as a function of time t.

tic precursor, a steady wave moving at velocity c_p; v_b = constant.

(2) The plastic precursor is an unsteady region from state b to state c; v_c = constant.

(3) The plastic wave extends from state c to the final Hugoniot state e, is steady, and moves at velocity D.

The experimental profile data needed here are

$$\begin{aligned} &v_a = \epsilon_a = \sigma_a = 0, \\ &v_b = 0.0236 \text{ mm}/\mu\text{s}, \quad v_c = 0.050 \text{ mm}/\mu\text{s}, \\ &c_p = 6.46 \text{ mm}/\mu\text{s}, \\ &D = 5.26 + 1.47 v_e \text{ mm}/\mu\text{s}. \end{aligned} \tag{16}$$

The jump conditions for ϵ, σ, U are obtained by integrating the conservation equations through the profile with the following results.[10]

At b:

$$\begin{aligned} &\epsilon_b = v_b / c_p, \\ &\sigma_b = \rho_a c_p v_b, \\ &U_b - U_a = \tfrac{1}{2} c_p^2 \epsilon_b^2. \end{aligned} \tag{17}$$

At c:

$$\begin{aligned} &\epsilon_c = c_p^{-1} v_c + \tfrac{1}{2} c_p^{-1} (v_c - v_b)\delta, \\ &\sigma_c = \rho_a c_p v_c - \tfrac{1}{2} \rho_a c_p (v_c - v_b)\delta + \cdots. \\ &U_c - U_a = \tfrac{1}{2} c_p^2 \epsilon_c^2 - \tfrac{1}{3} D c_p (\epsilon_c - \epsilon_b)^2 \delta + \cdots. \end{aligned} \tag{18}$$

At e:

$$\begin{aligned} &\epsilon_e = \epsilon_c + D^{-1}(v_e - v_c), \\ &\sigma_e = \sigma_c + \rho_a D (v_e - v_c), \\ &U_e - U_a = \tfrac{1}{2} D^2 (\epsilon_e^2 - \epsilon_c^2) + \tfrac{1}{2} c_p^2 \epsilon_c^2 \\ &\qquad + D c_p [(\epsilon_c + \epsilon_b)(\epsilon_e - \epsilon_c) \\ &\qquad\quad - \tfrac{1}{3}(\epsilon_c - \epsilon_b)^2]\delta + \cdots. \end{aligned} \tag{19}$$

The small quantity $\delta (\delta \ll 1)$ is

$$\delta = (c_p - D)/D. \tag{20}$$

and in (18) and (19) the $+\cdots$ represent terms of second and higher order in δ which arise from a series expansion of $\sigma(v)$ in the unsteady region from state b to state c. The expansion was made to facilitate analytic integration of the internal energy $dU = V_a \sigma d\epsilon$. The final-state particle velocity v_e may be eliminated from Eqs. (19) in favor of the shock velocity D by the experimental relation (16). The shock velocity is not defined for $v_e < v_c$.

Equations (17)–(19) constitute the jump conditions for ϵ, σ, U, from the initial state a to the final Hugoniot state e. Final-state values for 6061-$T6$ Al up to $\sigma \approx 100$ kbar are listed in Table I.

The equations for the shear stress τ and the plastic strain ψ through the profile are the same as Eqs. (9) and (10), with TdS replaced by the dynamic entropy production $2V\tau d\psi$ and with $d\ln\alpha_2^e$ replaced by $-\frac{1}{2}d\psi$ according to (6). It is not possible in principle to find jump conditions for τ and ψ because the equations for them at state e contain $\int_a^e \tau d\psi$, the integral to be evaluated along the path of the process. In practice this problem can be eliminated by constructing an approximate jump condition for the integral itself. We expect the integral to be roughly proportional to ϵ_e^2, since $S_e - S_a$ is of second order in strains. For 6061-$T6$ Al the integral was evaluated numerically in Ref. 10 for six shock profiles ranging from 21 to 89 kbar; a check of these integrations shows

$$\int_a^e \tau d\psi = (32 \pm 3)\epsilon_e^2. \tag{21}$$

(in kbar) for all the profiles. We therefore calculated τ and $\ln\alpha_2^e = -\frac{1}{2}\psi$ on the Hugoniot, from integrals of Eqs. (9) and (10) with the expansions (12)–(15) for the $B_{\beta\gamma}$ coefficients, the resulting equations being the same as (18) and (19) of Ref. 10. We also used the function $32\epsilon_e^2$ kbar as an interpolation approximation for the integral (21) and the experimental elastic constants of Clifton.[13]

TABLE I. The anisotropic Hugoniot for 6061-$T6$ Al in the weak-shock region.

ϵ	D (mm/μs)	σ (kbar)	$U-U_a$ (10^9 erg/g)	$-\ln\alpha_2^e$	τ (kbar)	T (K)	$S-S_a$ (10^5 erg/g K)	$S-S_4$ (Liquid theory)
0		0	0	0	0	295	0	0
0.0037[a]		4.1	0.003	0	1.1	297	0	0
0.0082[b]	5.3335	8.2	0.013	0.0009	1.6	300	0.07	0.003
0.020	5.364	17.7	0.072	0.0049	1.7	310	0.4	0.04
0.040	5.596	35.4	0.274	0.0117	1.8	326	1.2	0.31
0.060	5.775	55.4	0.63	0.0183	2.2	345	2.4	1.1
0.080	5.966	77.9	1.17	0.0247	3.1	368	4.3	2.7
0.100	6.169	103.4	1.92	0.0305	4.7	398	7.4	5.4

[a] Corresponds to profile point b.
[b] Corresponds to profile point c.

The results are listed in Table I.

With the energy and the stresses and strains known, it is possible to integrate Eqs. (7) and (8) up the Hugoniot to find T and S. The thermodynamic coefficients in these equations were evaluated by a set of approximations whose justification was discussed in the profile analysis,[10] and which are of sufficient accuracy here as well:

$$\gamma_1 = \gamma_2 = \gamma, \quad \rho\gamma = \rho_a\gamma_a, \quad \gamma_a = 2.16, \tag{22}$$

$$C_v = C_p = 0.88 \times 10^7 \text{ erg/g K}.$$

Values of temperature and entropy on the Hugoniot are also listed in Table I.

B. Construction of isotropic pressure curves

The next problem is the following: Given σ, τ, α_1^e, α_2^e on the Hugoniot, construct a P-V curve. This can be done in different ways by carrying out a thermoelastic strain from the anisotropic Hugoniot to conditions of isotropic pressure. We could, for example, hold σ constant and increase the transverse compressive stress until it equals σ, adiabatically. An alternate process, which we use here because of its simplicity in plane-wave geometry, is to bring the shear stress to zero under conditions of constant density and entropy. The thermoelastic process is described by equations of the preceding section, in particular (7)–(10), specialized to $dV = 0$ and $dS = 0$:

$$dU = 4V d\ln\alpha_2^e, \tag{23}$$

$$dT = 2T(\gamma_1 - \gamma_2) d\ln\alpha_2^e, \tag{24}$$

$$d\sigma = 2(B_{11} - B_{12}) d\ln\alpha_2^e, \tag{25}$$

$$d\tau = b\, d\ln\alpha_2^e, \tag{26}$$

where b is the combination

$$b = B_{11} + \tfrac{1}{2}B_{22} + \tfrac{1}{2}B_{23} - B_{12} - B_{21}. \tag{27}$$

For abbreviation, the P-V curve to be constructed will be called the isotrope. Equations (23)–(26) are to be integrated from a point on the Hugoniot (denoted by subscript H) to the corresponding point on the isotrope (denoted by subscript I). The independent variable of the integration is τ, which goes from τ_H to 0; Eq. (26) may be used to eliminate $d\ln\alpha_2^e$ in favor of $d\tau$ in (23)–(25). Since the integration ranges are small increments (the isotrope is close to the Hugoniot), the $B_{\beta\gamma}$ are taken constant for each integral. To integrate dT, the approximations (22) for the anisotropic Grüneisen parameters are used, which implies $dT = 0$. The isotrope may then be calculated from the Hugoniot by the equations

$$S_I = S_H, \tag{28}$$

$$V_I = V_H, \tag{29}$$

$$U_I = U_H - 2(V/b)\tau_H^2, \tag{30}$$

$$T_I = T_H, \tag{31}$$

$$P_I = \sigma_H - 2|(B_{11} - B_{12})/b|\tau_H. \tag{32}$$

The difference $\sigma_H - P_I$ at a common value of V and S is approximately $\frac{1}{3}\tau_H$; Eqs. (12)–(15) can be used to make a small-strain expansion of (32) to find

$$\begin{aligned}\sigma_H - P_I &= \tfrac{1}{3}\tau_H\left[1 - \mu^{-1}(\lambda + 2\mu + \xi - \tfrac{1}{2}\nu)\right.\\ &\qquad \left.\times(\epsilon + 3\ln\alpha_{2H}^e) + \cdots\right]\\ &= \tfrac{1}{3}\tau_H\left[1 - \mu^{-1}(\lambda + 2\mu + \xi - \tfrac{1}{2}\nu)\right.\\ &\qquad \left.\times(\tau_H/\mu) + \cdots\right].\end{aligned} \tag{33}$$

The term of order τ_H/μ should usually be quite small.

To evaluate the isotrope for 6061-$T6$ Al, we used the expressions (12)–(15) for the $B_{\beta\gamma}$ and the elastic-constant data of Clifton.[13] This constitutes a neglect of contributions to the $B_{\beta\gamma}$ from the entropy on the Hugoniot and from fourth-order elastic constants. The thermodynamic functions so calculated are listed in Table II. Regarding the principal elastic strains α_1^e and α_2^e, we have available two equations from which they may be evaluated on the isotrope: the integral of Eq. (26),

$$\ln(\alpha_{2H}^e/\alpha_{2I}^e) = b^{-1}\tau_H, \tag{34}$$

and Eq. (2) for conservation of mass,

$$\ln\rho_I/\rho_a = -\ln\alpha_{1I}^e - 2\ln\alpha_{2I}^e. \tag{35}$$

However, as there is only one stress measure to the isotrope, namely P_I, there is for an isotropic material only one strain measure, say V_I or ρ_I, and it is not necessary to evaluate α_1^e and α_2^e. In other words, α_1^e and α_2^e become equal on the isotrope, and (34) and (35) are not independent.[14] The change in the material configuration in going from the Hugoniot to the isotrope is

TABLE II. The isotrope and the principal adiabat for 6061-$T6$ Al.

	Isotrope		Adiabat	
ρ (g/cm³)	P (kbar)	T (K)	P (kbar)	T (K)
2.703	0	295	0	295
2.713	2.7	297	2.7	297
2.725	6.1	300	6.1	300
2.758	15.5	310	15.4	308
2.816	32.9	326	32.7	322
2.876	52.4	345	51.9	336
2.938	73.7	368	72.8	351
3.003	97.0	398	95.4	366

shown in Fig. 3.

It is now straightforward to calculate the principal adiabat, which is the pressure-volume curve at constant entropy $S = S_0$. A convenient process for going from isotrope to adiabat is to reduce S from S_I to S_0 at constant V by extracting reversible heat from the material. Ordinary P-V thermodynamics gives[11]

$$dU = TdS - PdV, \tag{36}$$

$$TdS = C_V dT + \rho\gamma C_V T dV, \tag{37}$$

$$\rho\gamma = \left(\frac{\partial P}{\partial U}\right)_V. \tag{38}$$

From these equations, the differentials at constant V are

$$dU = TdS = C_V dT = (\rho\gamma)^{-1} dP. \tag{39}$$

In going from the isotrope to the adiabat, the independent integration variable is S. Again since the integration ranges are small increments, the coefficients C_V and $\rho\gamma$ can be set constant for each integral. The adiabat, denoted by subscript A, may then be calculated from the isotrope by the equations

$$S_A = S_0, \tag{40}$$

$$V_A = V_I, \tag{41}$$

$$T_A = T_I \exp[-(S_I - S_0)/C_V], \tag{42}$$

$$P_A = P_I + \rho\gamma C_V (T_A - T_I), \tag{43}$$

$$U_A = U_I + C_V (T_A - T_I). \tag{44}$$

The principal adiabat for 6061-T6 Al is listed in Table II. The stresses on the anisotropic Hugoniot and the pressure on the isotrope and the adiabat, as functions of the compression, are compared graphically in Fig. 4.

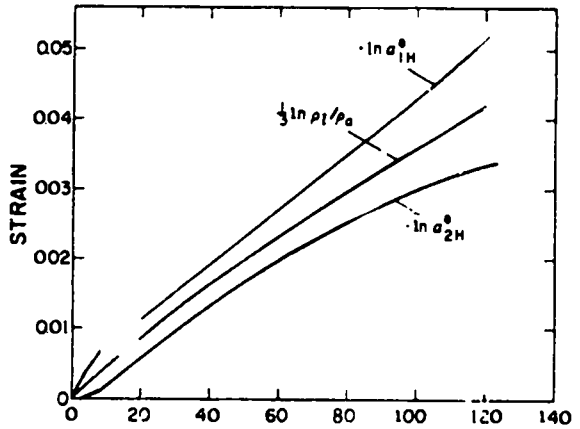

FIG. 3. Change in the elastic-strain variables in going from the anisotropic Hugoniot to the isotropic pressure curve. The density ρ_I on the isotrope is related to the elastic strains on the isotrope by Eq. (35).

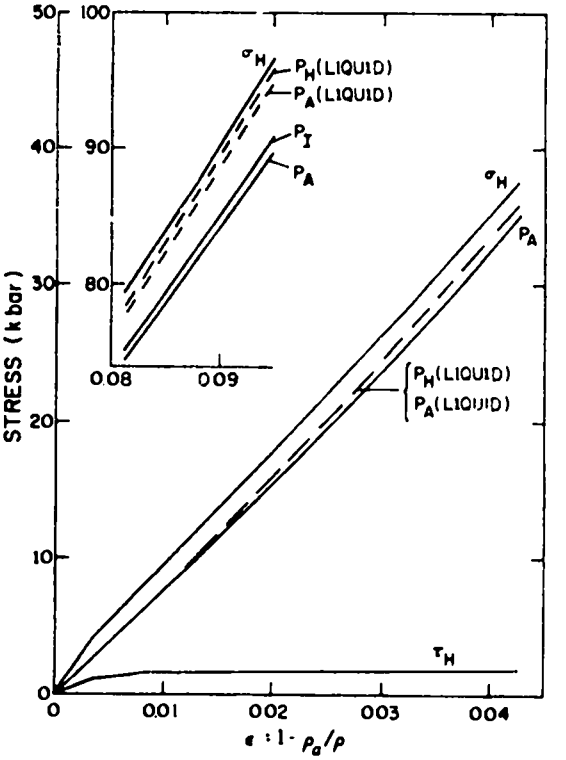

FIG. 4. Stresses as a function of elastic strain: σ_H and τ_H are on the anisotropic Hugoniot, P_I is on the isotrope, and P_A is on the principal adiabat, and representing liquid Hugoniot theory, P_H (liquid) is on the Hugoniot and P_A (liquid) is on the principal adiabat.

C. Approximate P-V curves

Having carried out an accurate calculation of the weak-shock equation of state for 6061-T6 Al, it is interesting to calculate the same property by means of liquid Hugoniot theory based on the same experimental data. The difference of liquid Hugoniot theory[5-7] from the present anisotropic Hugoniot theory can be made clear in two separate steps.

(1) Liquid Hugoniot theory says the elastic and plastic precursors do not exist; jump conditions for a single steady wave then follow. These jump conditions may be obtained as a special case of Eqs. (19) by eliminating the elastic and plastic precursors, i.e., by setting $v_b = v_c = 0$:

$$\epsilon_e = D^{-1} v_e,$$

$$\sigma_e = \rho_0 D v_e, \tag{45}$$

$$U_e - U_0 = \tfrac{1}{2} D^2 \epsilon_e^2.$$

(2) Liquid Hugoniot theory then says $\tau_e = 0$, which means the Eqs. (45) determine an isotropic pres-

sure curve with

$$\sigma_e = P_e . \tag{46}$$

When the shock velocity is a linear function of the final-state particle velocity, the above equations of liquid Hugoniot theory simplify to[3]

$$\begin{aligned} D &= c + s\epsilon_e , \\ P_e &= \rho_0 c^2 \epsilon_e (1 - s\epsilon_e)^{-2} , \\ U_e - U_a &= \tfrac{1}{2} V_a P_e \epsilon_e . \end{aligned} \tag{47}$$

We used the experimental shock-velocity–particle-velocity relation (16) to calculate the pressure and energy as functions of compression on the liquid Hugoniot for 6061-*T*6 Al. We also calculated T and S on the liquid Hugoniot by integrating Eqs. (7) and (8) and then constructed the principal adiabat by means of Eqs. (40)–(44), all using the same approximations (22) for γ and C_V as before. The liquid results are compared with results of the anisotropic theory in Fig. 4.

A well-known approximation for the P-V curve is due to Murnaghan[15]; this is simply a first-order Maclaurin expansion in pressure for the bulk modulus and we will apply it here for the adiabatic bulk modulus on the line of constant entropy:

$$B(P, S_a) = B_0 + B_0' P , \tag{48}$$

where B is the adiabatic bulk modulus, B_0 is B at $P = 0$ and $S = S_a$, and B_0' is $(\partial B/\partial P)_S$ at $P = 0$ and $S = S_a$. Equation (48) integrates to the Murnaghan form for $P(V)$ in the present case along the principal adiabat,

$$P(V, S_a) = \frac{B_0}{B_0'}\left[\left(\frac{V_a}{V}\right)^{B_0'} - 1\right] . \tag{49}$$

For 6061-*T*6 Al at room temperature and zero pressure, Clifton's[13] measurements give

$$\begin{aligned} B_0 &= 728 \text{ kbar} , \\ B_0' &= 5.275 . \end{aligned} \tag{50}$$

The differences from our accurate adiabat of the Murnaghan approximation and of the adiabat constructed from liquid Hugoniot theory are shown in Fig. 5, in the form of ΔP_A at a fixed volume, defined by

$$\Delta P_A = \frac{P_A(V)_{\text{approx}} - P_A(V)}{P_A(V)} . \tag{51}$$

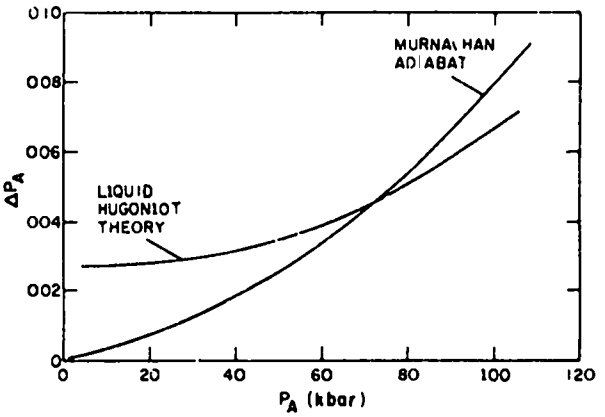

FIG. 5. Relative difference ΔP_A in the pressure P_A on the principal adiabat for two approximations as compared with the accurate calculations of the present paper. ΔP_A is defined by Eq. (51).

D. Errors

On the Hugoniot, the relations $\sigma(\epsilon)$ and $U(\epsilon) - U_a$ are determined entirely from shock-profile data, through the profile jump equations (17)–(19), and these relations as listed in Table I should be quite accurate, σ to within 1% and $U - U_a$ to 2%. The main source of error is expected to be the shock-velocity–particle-velocity data. The error most significant in specifying the Hugoniot, and in determining the isotrope and the adiabat, is the error in τ. This arises mainly from errors in the $\sigma(\epsilon)$ relation and in the $B_{\beta\gamma}$ coefficients. We have not attempted to estimate the fourth-order-elastic-constant contributions to $B_{\beta\gamma}$; it is hard to imagine, however, that the τ values listed in Table I can be in error by more than 25% up to 50 kbar and by more than 50% up to 100 kbar. The error in $S = S_a$ on the Hugoniot comes from our approximations for γ and C_η and from evaluation of the profile integral $\int_a^e \tau\, d\psi$. The latter is determined with good precision, say of order 10%, independently of larger errors in τ in the final state. $S - S_a$ should be accurate to within 20% on the Hugoniot.

In transforming from the Hugoniot to the isotrope, the process is approximately equivalent to replacing the stress system σ, τ at each density and entropy by a pressure $P_I \approx \sigma - \frac{4}{3}\tau$. Hence the error in P on the isotrope is essentially the sum of the errors in σ and τ on the Hugoniot. Finally in going to the adiabat, the pressure change $P_A - P_I$ will be in error by about the same percentage as is $S_H - S_a$, giving an error in P_A by at most a few tenths kbar at 100 kbar. All in all the pressure on the adiabat, Table II, should be accurate to 1 kbar at 50 kbar and to about 4 kbar at 100 kbar.

The error in liquid Hugoniot theory can be estimated with more precision, by comparing its results with those of the anisotropic Hugoniot theory, because the same shock-velocity–particle-velocity relation was used in both calculations, and the same approximations for γ and C_η

as well. There are two differences between the two theories: The anisotropic Hugoniot has nonzero τ (the major effect) and it has a slightly larger entropy than the liquid Hugoniot. The role of these two effects is easily seen at the point where the shock velocity is equal to the elastic precursor velocity because here the ϵ, σ, U jump conditions are the same for both theories [compare Eqs. (17)–(19) with (45) for the case $D = c_\rho$]. At this value of ϵ, then, σ is equal for the two Hugoniot curves, at about 143 kbar for 6061-$T6$ Al. Integrating out the shear stress from the anisotropic Hugoniot, say at constant ϵ, reduces the pressure by about $\frac{4}{3}\tau$ below the liquid Hugoniot Integrating out the entropy from either curve to reach the adiabat also reduces the pressure, but more so in the case of the anisotropic Hugoniot because it has the higher entropy. Both effects work in the same direction, although in the present aluminum calculations the entropy effect is only about 5% of the $\frac{4}{3}\tau$ effect. These comments, and our numerical results, are summarized as follows:

(a) For shocks in the neighborhood of $D = c_\rho$, liquid Hugoniot theory produces a pressure which is too high by about $\frac{4}{3}\tau$.

(b) For the 6061-$T6$ Al adiabat from 0 to 100 kbar, liquid Hugoniot theory produces a pressure which is too high by several percent (Fig. 5).

The Murnaghan adiabat (49) was evaluated entirely from elastic constant data, Eq. (50). In the low-pressure region this represents the most reliable determination of the $P_A(V)$ curve. It is gratifying to find that the anisotropic Hugoniot, which is mainly determined by shock data, gives a $P_A(V)$, after integrating out the sizable shear stress, in agreement with the Murnaghan curve in the low-pressure region.

E. Stronger shocks

The relative error in using liquid Hugoniot theory for solids depends primarily on the value of τ/σ on the anisotropic Hugoniot. In the present analysis this ratio is roughly constant in the range 50–100 kbar, but it is reasonable to expect it eventually to decrease as a function of shock strength, and hence to expect liquid Hugoniot theory to become more accurate for stronger shocks.

IV. CONCLUSIONS

A method for extracting true thermodynamic information from a wave-profile analysis has been illustrated with data on 6061-$T6$ Al. In addition to obtaining proper thermodynamic variables of the material undergoing fast one-dimensional deformation, an equation of state for the material can be measured at stresses intermediate between the low values obtained in static experiments and the higher values in shock experiments where strength corrections presumably become smaller.

[1] J. M. Walsh, M. H. Rice, R. G. McQueen, and F. L. Yarger, Phys. Rev. 108, 196 (1957).

[2] L. V. Al'tshuler, Usp. Fiz. Nauk 85, 197 (1965) [Sov. Phys. Usp. 8, 52 (1965)].

[3] R. G. McQueen, S. P. Marsh, J. W. Taylor, J. N. Fritz, and W. J. Carter, in *High Velocity Impact Phenomena*, edited by R. Kinslow (Academic, New York, 1970), p. 293.

[4] J. A. Morgan, High Temp.—High Pressures 6, 195 (1974); 7, 65 (1975).

[5] R. Courant and K. O. Friedrichs, *Supersonic Flow and Shock Waves* (Interscience, New York, 1948).

[6] L. D. Landau and E. M. Lifshitz, *Fluid Mechanics* (Pergamon, London, 1959).

[7] Ya. B. Zel'dovich and Yu. P. Raizer, *Physics of Shock Waves and High-Temperature Hydrodynamic Phenomena* (Academic, New York, 1966), Vol. 1.

[8] D. C. Wallace, in *Solid State Physics*, edited by H. Ehrenreich, F. Seitz, and D. Turnbull (Academic, New York, 1970), Vol. 25, p. 301.

[9] D. C. Wallace, this issue, Phys. Rev. B 22, 1477 (1980).

[10] D. C. Wallace, preceding paper, Phys. Rev. B 22, 1487 (1980).

[11] D. C. Wallace, *Thermodynamics of Crystals* (Wiley, New York, 1972).

[12] J. N. Johnson and L. M. Barker, J. Appl. Phys. 40, 4321 (1969).

[13] R. F. Stilton, in *Shock Waves and the Mechanical Properties of Solids*, edited by J. J. Burke and V. Weiss (Syracuse University Press, Syracuse, 1971), p. 73.

[14] The two principal elastic strains α_1^I and α_1^{II} would not be equal on the isotrope for a single crystal of symmetry lower than cubic, or for an anisotropically prepared polycrystal (e.g., cold rolled); hence for any real material after shock compression there will be a small effect of this nature due to the anisotropic working of the shock itself. No elastic anisotropy was found in the present analysis for aluminum.

[15] F. D. Murnaghan, Proc. Nat. Acad. Sci. U.S.A. 30, 244 (1944).

Irreversible thermodynamics of overdriven shocks in solids

Duane C. Wallace
Los Alamos Scientific Laboratory, Los Alamos, New Mexico 87545
(Received 6 February 1981)

An isotropic solid, capable of transporting heat and of undergoing dissipative plastic flow, is treated. The shock is assumed to be a steady wave, and any phase changes or macroscopic inhomogeneities which might be induced by the shock are neglected. Under these conditions it is established that for an overdriven shock, no solution is possible without heat transport, and when the heat transport is governed by the steady conduction equation, no solution is possible without plastic dissipation as well. Upper and lower bounds are established for the thermodynamic variables, namely the shear stress, temperature, entropy, plastic strain, and heat flux, as functions of compression through the shock.

I. INTRODUCTION

We have recently discussed the irreversible-thermodynamic theory of flow processes in solids.[1–3] The processes considered include simultaneous elastic strain and plastic flow, where plastic flow is any dissipative rearrangement of the atoms in a solid. The theory is expressed in three coupled subsets of equations: the continuum-mechanic equations for conservation of mass, momentum, and energy; the thermoelastic equations which relate variations in the elastic strains, stresses, entropy, temperature, and so on; the thermoplastic equations which define plastic flow and specify the entropy generation. When the thermoelastic coefficients, which are the stress-strain coefficients, the anisotropic Grüneisen parameters, and the heat capacity at constant elastic configuration, and the plastic constitutive relations are known, the equations can be integrated from initial conditions to find a general flow process of a solid.

When applied to the problem of weak shocks in solids,[4] this work provides an improvement in the description of the shock process in two ways: Entropy terms in the stress equations are properly included (instead of using Hooke's law) and the entropy production is properly expressed in terms of plastic flow (instead of using viscous fluid dissipation).[1] Further, the theory can be used to determine the plastic flow behavior in the weak-shock process, from measurements of the shock profiles and the polycrystalline thermoelastic coefficients.[2] Finally, a solid-state Hugoniot theory has been given for the first time, from which it is possible to determine accurate equation-of-state data from weak shocks in solids.[3]

For overdriven shocks,[4] there is very little experimental information about the nature of the shock process. The shock is generally too fast to be experimentally resolved; an experimental upper limit for the rise time for shocks of several hundred kbar in several metals is 3 ns.[5] However, by applying the same principles we have previously used in the weak-shock theory, it is possible to learn a great deal about the process of overdriven shocks in solids, even without knowing details of the plastic constitutive behavior of the material. The purpose of the present paper is to develop this theory of overdriven shocks in solids.

The solid material is assumed to be isotropic, according to the definition of Ref. 1, and capable of transporting heat and of undergoing dissipative plastic flow. Polycrystalline effects are neglected; some justification for this is given in the Appendix. Shock-induced phase transitions, such as melting and other structural changes, and shock-induced macroscopic inhomogeneities, such as cracks and local hot spots, are also neglected. The shock is assumed to be a steady wave. The theory has been developed with application to polycrystalline metals in mind, but it might be valid for some nonmetals as well.

II. RAYLEIGH-LINE EQUATIONS

A. The conservation equations

The shock is a plane wave which propagates in the x direction; y and z are equivalent transverse directions. Lateral edge effects are eliminated by specifying that there is no material motion in transverse directions. Mass elements of the materi-

al are planar slabs of infinitesimal thickness, normal to the propagation direction. The Lagrangian coordinate of each mass element is X, which is equal to the laboratory coordinate x of the mass element before the shock arrives, i.e., at the time $t=-\infty$. The mechanic and thermodynamic properties of each mass element are functions of t, so for the whole material these properties are functions of X and t. The density is ρ, the volume per unit mass is $V=\rho^{-1}$, the material velocity is v, compressive stresses in the normal and transverse directions are, respectively, σ and $\sigma-2\tau$, so the shear stress is τ. Quantities in the initial state (before the shock) are denoted by subscript a, and $\epsilon=1-V/V_a$ measures the total compression from the initial state. The heat flux is J.

The shock is assumed to be a steady wave, moving at constant velocity D. The steady-wave condition is that any property $F(X,t)$ depends only on the Lagrangian steady-wave variable $Z=X-Dt$: $F(X,t)=F(Z)$. Equivalently, with $z=x-Dt$ the laboratory steady-wave variable, the condition is $F(x,t)=F(z)$. The two variables are related by

$$dZ=(\rho/\rho_a)dz\ . \tag{1}$$

Because of the steady-wave condition, the entire space and time dependence of any function $F(\epsilon)$ on the Rayleigh line is specified by a single variable.

The initial conditions are that the stresses, the material velocity, and the heat flux are zero in the state ahead of the shock,

$$\sigma_a=\tau_a=v_a=J_a=0\ . \tag{2}$$

First integrals of the equations for conservation of mass and conservation of momentum are, respectively,

$$\epsilon=v/D\ . \tag{3}$$

$$\sigma=\rho_a Dv\ . \tag{4}$$

The Rayleigh line is the $\sigma(\epsilon)$ relation through the shock process; from (3) and (4) this is

$$\sigma=\rho_a D^2\epsilon\ . \tag{5}$$

Since the transverse stresses do no work, the incremental center-of-mass work done on the material is $dW=-\sigma dV$ per unit mass. The incremental heat transferred to the material is dQ per unit mass, so conservation of energy requires

$$dU=-\sigma dV+dQ\ . \tag{6}$$

This equation includes arbitrary entropy generation, corresponding to whatever part of the work dW is dissipated, in addition to the entropy generation due to heat flow. It is convenient to eliminate Q for J, because J is the function customarily related to the material heat-transport properties. For a steady wave the continuity equation is simply $dQ=dJ/\rho_a D$, and the energy is integrated on the Rayleigh line to give

$$U-U_a=\tfrac{1}{2}D^2\epsilon^2+J/\rho_a D\ . \tag{7}$$

B. The thermodynamic equations

The thermodynamic equations include both thermoelastic and thermoplastic subsets; the derivation proceeds as follows.[1] Total symmetric strain measures may be taken as $\dot{\epsilon}_{ij}=\frac{1}{2}(v_{ij}+v_{ji})$, where v_{ij} are velocity gradients; ϵ_{ij} increments are composed of elastic and plastic parts: $d\epsilon_{ij}=d\epsilon^e_{ij}+d\epsilon^p_{ij}$; the $d\epsilon^e_{ij}$ are related in the usual way to variations in stresses, energy, entropy, and so on, and $d\epsilon^p_{ij}$ are related to plastic constitutive behavior and to the entropy production. Note that all these thermodynamic equations are Lagrangian, in that they relate various properties of a given mass element. In the present case of plane-wave motion there are only four independent strain variables: $d\epsilon^e_{xx}$, $d\epsilon^e_{yy}=d\epsilon^e_{zz}$, $d\epsilon^p_{xx}$, and $d\epsilon^p_{yy}=d\epsilon^p_{zz}$. The boundary condition of no transverse motion requires $d\epsilon_{yy}=d\epsilon_{zz}=0$, and the assumption that the plastic flow is volume conserving means $d\epsilon^p_{xx}+2d\epsilon^p_{yy}=0$. There remain only two independent strain variables, which may be taken as the total compression ϵ and the plastic strain ψ, where $d\psi=-d\epsilon^p_{xx}$. It is also convenient on occasion to use V or ρ in place of ϵ.

The thermoelastic equations may be derived in complete tensor form, appropriate for arbitrary elastic strains, by taking $d\epsilon^e_{ij}$ and dS as independent variables, where S is the entropy per unit mass. These equations may then be simplified for the present geometry. The results for the energy U, the stresses σ and τ, and the temperature T are the following[1]:

$$dU=TdS-\sigma dV-2V\tau d\psi\ , \tag{8}$$

$$d\sigma=\rho\gamma_1 TdS-B_{11}d\ln V-(B_{11}-B_{12})d\psi\ , \tag{9}$$

$$d\tau=\tfrac{1}{2}\rho(\gamma_1-\gamma_2)TdS-\tfrac{1}{2}(B_{11}-B_{21})d\ln V$$
$$-\tfrac{1}{2}(B_{11}+\tfrac{1}{2}B_{22}+\tfrac{1}{2}B_{23}-B_{12}-B_{21})d\psi\ , \tag{10}$$

$$dT=C_\eta^{-1}TdS-T\gamma_1 d\ln V-T(\gamma_1-\gamma_2)d\psi\ . \tag{11}$$

Here the Voigt indices are $1=xx$, $2=yy$, $3=zz$. $B_{\alpha\beta}$ are the adiabatic stress-strain coefficients, γ_β are the anisotropic Grüneisen parameters, and C_η is the heat capacity at constant elastic configuration.[6] We also have to specify the entropy production. There are two sources in the present theory: dQ contributes to TdS, and also the plastic work $dW^p=2V\tau d\psi$, which is assumed to be totally dissipative,

$$TdS=dJ/\rho_a D+2V\tau d\psi\ . \tag{12}$$

Concerning the energy equation, we note that the continuum mechanic form (6) and the thermodynamic form (8) are the same when (12) for TdS is used. Because we have used the entropy as an independent variable, the energy equation is not coupled to the other thermodynamic equations (9)–(12), and so the energy equation does not have to be solved simultaneously with them.

To complete the description of the process, two more equations describing dynamic response characteristics of the material are needed. The plastic constitutive behavior is expressible as a dependence of the stress which drives the plastic flow, namely the shear stress τ, on the plastic strain and strain rate and on the thermodynamic state, approximately

$$\tau=\tau(\psi,\dot{\psi},V,S)\ . \tag{13}$$

The heat transport behavior relates the heat current J to the temperature gradient and other variables

$$J=J(\text{grad}\,T,V,S,\ldots)\ . \tag{14}$$

The complete set of Rayleigh-line equations is then (5) together with (9)–(14). We assume the thermoelastic coefficients $B_{\alpha\beta},\gamma_\beta,C_\eta$ are known as functions of the thermoelastic state. There are then seven coupled Rayleigh-line equations in the seven variables: σ,τ,T,S,ψ,J, and one space-time variable, z, for example. These equations are in principle solvable for the shock process. On the other hand, if one of the Rayleigh-line variables were known from experiment, e.g., $z(\epsilon)$, or $T(\epsilon)$, or for example $v(t)$ at a fixed X, then these equations can in principle be used to determine the plastic constitutive relation (13) through the shock. An alternate point of view, which we pursue in the following because there is no experimental data on the Rayleigh-line variables, and because the plastic constitutive behavior in overdriven shocks is entirely unknown, is to omit the last two equations of the set, and to study Eqs. (5) and (9)–(12), which are five equations in the six variables v,τ,T,S,ψ,J. Following this, some information on the heat transport mechanism will be used to extend the study to the space-time dependence of the process.

III. THEOREMS ON THE SHOCK PROCESS

A. Necessity of heat transport

Theorem 1. For an overdriven shock in a solid, no solution is possible without heat transport.

The proof does not depend on the mechanism of heat transport. Heat transport is needed at the beginning of the shock, to bring σ up to the Rayleigh line, as shown in Fig. 1. The elastic line corresponds to adiabatic ($dS=0$) uniaxial elastic compression of the material under plane-wave boundary conditions (no transverse motion). The slope of this line at $\epsilon=0$ is $\rho_a c_l^2$, where c_l is the longitudinal sound velocity in state a. The elastic precursor velocity is $c_p\geq c_l$, where c_p can be greater than c_l by only very small finite-strain corrections. The definition of an overdriven shock is $D>c_p$, the slope of the Rayleigh line for a steady-wave shock is $\rho_a D^2$, so for an overdriven shock the Rayleigh line is steeper than the elastic line, as shown in Fig. 1. If plastic flow takes place in the small-ϵ region, it can only reduce σ below the elastic line at small ϵ. Therefore heat must be transported to the material in the initial stage of the shock.

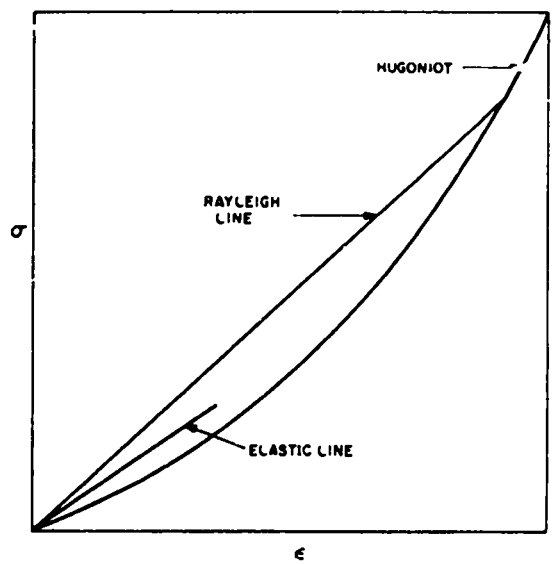

FIG. 1. Showing the proof of Theorem 1. The elastic line has a fixed slope of $\rho_a c_l^2$ at $\epsilon=0$; the Rayleigh line has slope $\rho_a D^2$ which increases with shock velocity D.

The proof may be shown directly from the Rayleigh-line equations. We set the heat transport to zero: $dJ=0$. Then from (12), $TdS=0$ at state a, since $\tau_a=0$. Also at state a, $\rho=\rho_a$, $B_{11}=\rho_a c_l^2$, $B_{11}-B_{12}=2G$, where G is the adiabatic shear modulus, so (9) at state a is

$$d\sigma=\rho_a c_l^2 d\epsilon-2Gd\psi\ .$$

Differentiating the Rayleigh-line equation (5) for a fixed D gives

$$d\sigma=\rho_a D^2 d\epsilon\ .$$

Since $d\psi\geq 0$ by definition, no solution is possible when $D>c_l$. When heat transport is included, $dJ>0$ and a solution is possible.

B. Family of partial solutions

Consider a given material with specified properties and a fixed shock strength corresponding to a shock velocity D. The state behind the shock is the thermodynamic equilibrium Hugoniot state, denoted by subscript H, where the Rayleigh line reaches the Hugoniot at ϵ_H. The thermodynamic variables have the values $\sigma_H,\tau_H,T_H,S_H,\psi_H$, and because of equilibrium the heat current vanishes:

$$J_H=0\ . \tag{15}$$

Because the shock is a continuous process, the Rayleigh-line solution is continuous, i.e., all the variables are continuous functions of ϵ for $0\leq\epsilon\leq\epsilon_H$.

We define a partial solution as a set of six functions $\sigma(\epsilon)$, $\tau(\epsilon)$, $T(\epsilon)$, $S(\epsilon)$, $\psi(\epsilon)$, and $J(\epsilon)$ which are continuous on $0\leq\epsilon\leq\epsilon_H$, which take on the correct values at $\epsilon=0$ and ϵ_H, and which satisfy the five Rayleigh-line equations (5) and (9)–(12). A partial solution can be constructed by taking any function for one of the variables, for example $S(\epsilon)$, which is continuous and which takes on the correct values at $\epsilon=0$ and ϵ_H, and by solving the five Rayleigh-line equations for the other five functions. Given $S(\epsilon)$, the solution for the other five functions is unique, because for the tetragonal symmetry of the material under plane-wave compression there are three independent thermoelastic state variables, which can be taken as S,ϵ,σ, and $\sigma(\epsilon)$ is fixed by Eq. (5). Because one function of a partial solution is arbitrary, the family of partial solutions is infinite. Among these, many will be unacceptable on simple physical grounds, as we will see shortly; among the physically acceptable partial solutions, one is the correct solution for the material under consideration.

It is possible to establish an important ordering of the partial solutions. Starting from one partial solution, we generate another one infinitesimally removed by adding to $S(\epsilon)$ an increment $\delta S(\epsilon)$, which is continuous and which does not change sign on $0\leq\epsilon\leq\epsilon_H$, and which vanishes at $\epsilon=0$ and at ϵ_H. From one given partial solution, all partial solutions can be generated in this way. Functional relations among the variations $\delta S(\epsilon)$, $\delta T(\epsilon)$, and so on, at a fixed value of ϵ, can be found from Eqs. (5) and (9)–(12) evaluated at $\delta\epsilon=0$:

$$\delta\sigma=0\ , \tag{16}$$

$$\delta\sigma=\rho\gamma_1 T\delta S-(B_{11}-B_{12})\delta\psi\ , \tag{17}$$

$$\delta\tau=\tfrac{1}{2}\rho(\gamma_1-\gamma_2)T\delta S-\tfrac{1}{2}(B_{11}+\tfrac{1}{2}B_{22}+\tfrac{1}{2}B_{23}-B_{12}-B_{21})\delta\psi\ , \tag{18}$$

$$\delta T=C_\eta^{-1}T\delta S-T(\gamma_1-\gamma_2)\delta\psi\ , \tag{19}$$

$$T\delta S=\delta J/\rho_a D+2V\tau\delta\psi\ . \tag{20}$$

These relations will eventually be useful in establishing bounds for the Rayleigh-line solution throughout the shock.

The coefficients in these equations are complicated, but a consistent use of the small-anisotropy expansion is sufficient to determine the relative signs of the variations $\delta S(\epsilon)$, $\delta T(\epsilon)$, and so on. The small-anisotropy expansion is defined as follows[1]: Throughout the shock process, the shear stress τ should be small compared to the shear modulus G, so any thermodynamic coefficient $f=f(\epsilon,S,\tau)$ can be expanded in powers of τ/G at constant ϵ,S:

$$f(\epsilon,S,\tau)=f(\epsilon,S,0)+(\text{coefficient})(\tau/G)+\cdots\ . \tag{21}$$

For the needed coefficients we write explicitly the leading term in the expansion, which is defined in isotropic thermodynamic space ($\tau=0$), and denote by $+\cdots$ all terms of relative order τ/G and higher:

$$\begin{aligned}
&\gamma_1=\gamma+\cdots\ ,\\
&\gamma_2=\gamma+\cdots\ ,\\
&B_{11}=B+\tfrac{4}{3}G+\cdots\ ,\\
&B_{11}-B_{12}=2G+\cdots\ ,\\
&\tfrac{1}{2}(B_{22}+\tfrac{1}{2}B_{22}+\tfrac{1}{2}B_{23}-B_{12}-B_{21})=\tfrac{3}{2}G+\cdots\ ,\\
&C_\eta=C_V+\cdots\ ,
\end{aligned} \tag{22}$$

where γ is the ordinary (isotropic) Grüneisen parameter. B is the adiabatic bulk modulus, and C_V is the heat capacity at constant volume.

Relative signs of the variations δS, δT, and so on, are given by the leading order evaluation of Eqs. (16)–(20). In view of (16) and (17), the first term on the right of (18) may be neglected because it is of order τ/G times the second term. Also because $TC_V \lesssim VG$ for shocks in solids,[7] the second term on the right of (19) is $\lesssim(\tau/G)$ times the first term. Then to leading order the functional variations at fixed ϵ are related by

$$\delta\psi(\epsilon)=(\rho\gamma T/2G)\delta S(\epsilon)\,, \tag{23}$$

$$\delta T(\epsilon)=(T/C_V)\delta S(\epsilon)\,, \tag{24}$$

$$\delta J(\epsilon)=\rho_a DT\delta S(\epsilon)\,, \tag{25}$$

$$\delta\tau(\epsilon)=-\tfrac{3}{4}\rho\gamma T\dot{\omega}S(\epsilon)\,. \tag{26}$$

Therefore, given any partial solution, functional variation to a new partial solution has $\delta S(\epsilon)$, $\delta T(\epsilon)$, $\delta\psi(\epsilon)$, $\delta J(\epsilon)$ of the same sign everywhere, and $\delta\tau(\epsilon)$ of the opposite sign everywhere. The next step is to introduce physical restrictions that will limit the range of partial solutions which are acceptable.

C. The minimum-τ partial solution

For a solid, τ cannot be negative during shock compression, hence $\tau=0$ is a lower bound for $\tau(\epsilon)$ on the Rayleigh line. We can construct a partial solution, the minimum-τ partial solution, by specifying $\tau(\epsilon)$ as follows: $\tau(\epsilon)=0$ for $0\le\epsilon\le\epsilon_H-\delta$, where δ is a positive infinitesimal, and $\tau(\epsilon)$ increases continuously to τ_H at ϵ_H. If we want to set $\tau_H=0$, i.e., to approximate the solid Hugoniot by a fluid Hugoniot, then the minimum-τ partial solution has $\tau(\epsilon)=0$ everywhere. Specifying $\tau(\epsilon)$ determines a partial solution, whose properties follow directly from Eqs. (5) and (9)–(12), and from the ordering of the family of partial solutions:

Theorem 2. The minimum-τ partial solution represents, in the region where $\tau(\epsilon)=0$, an inviscid fluid with heat transport, and it constitutes a bound for physically acceptable solutions, in which $T(\epsilon)$, $S(\epsilon)$, $\psi(\epsilon)$, $J(\epsilon)$ are all upper bounds.

The qualitative forms of $T(\epsilon)$ and $J(\epsilon)$ for the minimum-τ partial solution are shown in Fig. 2. The Rayleigh-line equations simplify in the region where $\tau=0$. The stress becomes an isotropic pressure P, and all the thermodynamic coefficients are evaluated at $\tau=0$, which is the state corresponding

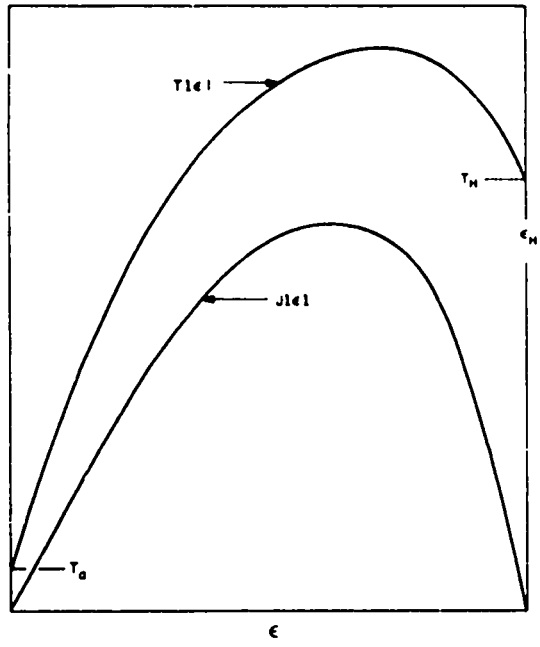

FIG. 2. Behavior of $T(\epsilon)$ and $J(\epsilon)$ on the Rayleigh line for an inviscid fluid with heat transport or a solid with $\tau(\epsilon)=0$.

to the leading terms in (22). Equation (10) is

$$0=-G(d\ln V+\tfrac{3}{2}d\psi)\,, \tag{27}$$

which allows $d\psi$ to be eliminated from the set. Equations (5), (9), (11), (12) then become

$$\sigma=P=\rho_a D^2\epsilon\,, \tag{28}$$

$$dP=\rho\gamma TdS+\rho V_a Bd\epsilon\,, \tag{29}$$

$$dT=\rho\gamma V_a Td\epsilon+C_V^{-1}TdS\,, \tag{30}$$

$$TdS=dJ/\rho_a D\,. \tag{31}$$

D. The minimum-ψ partial solution

The plastic strain must be nondecreasing by definition: $d\psi\ge 0$. Hence $\psi=0$ is a lower bound for $\psi(\epsilon)$ on the Rayleigh line. The condition $\psi=0$ represents the response of an elastic solid with heat transport and with infinite yield strength; we refer to this hypothetical material as a nonplastic solid. If we set $\psi(\epsilon)=0$ the Rayleigh-line equations can be solved. Figure 3 shows the behavior of $J(\epsilon)$ and $T(\epsilon)$ in this case: $J(\epsilon)$ has a maximum at some point ϵ_b, and $T(\epsilon)$ has a maximum at $\epsilon_d>\epsilon_b$. This solution is not a partial solution because the variables do not reach the Hugoniot values at ϵ_H; we find, in particular, $T(\epsilon_H)<T_H$ and $J(\epsilon_H)<0$.

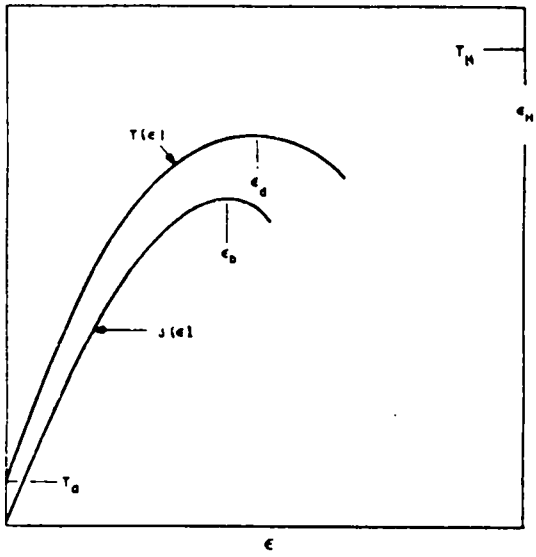

FIG. 3. Behavior of $T(\epsilon)$ and $J(\epsilon)$ on the Rayleigh line for a solid with heat transport and with $\psi=0$ (a nonplastic solid). $J(\epsilon)$ has a maximum at ϵ_b and $T(\epsilon)$ has a maximum at $\epsilon_d > \epsilon_b$.

In other words, the nonplastic solid does not possess a steady-wave shock solution. But we are only interested in this solution in the region $0 \le \epsilon \le \epsilon_d$; beyond this, one of the thermodynamic variables can be arbitrarily continued to the Hugoniot state, generating a partial solution. This partial solution, with $\psi(\epsilon)=0$ for $0 \le \epsilon \le \epsilon_d$, is called the minimum-$\psi$ partial solution. Properties which follow at once from Eqs. (5) and (9)–(12) and from the ordering of the family of partial solutions are the following.

Theorem 3. The minimum-ψ partial solution in the region where $\psi(\epsilon)=0$ represents a nonplastic solid, and constitutes a bound for physically acceptable solutions in which $T(\epsilon)$, $S(\epsilon)$, $J(\epsilon)$ are lower bounds and $\tau(\epsilon)$ is an upper bound.

The condition $d\psi=0$ simplifies the Rayleigh-line equations considerably. Combining (5) and (9) gives

$$\rho\gamma_1 T dS = (\rho_a D^2 - \rho V_a B_{11}) d\epsilon , \tag{32}$$

and (11) and (12) become

$$dT = \rho\gamma_1 V_a T d\epsilon + C_\eta^{-1} T dS, \tag{33}$$

$$T dS = dJ/\rho_a D . \tag{34}$$

These are three equations in $T(\epsilon)$, $S(\epsilon)$, $J(\epsilon)$. The equation for $\tau(\epsilon)$ is then uncoupled from the above set:

$$d\tau = \tfrac{1}{2}\rho(\gamma_1-\gamma_2) T dS + \tfrac{1}{2}\rho V_a (B_{11}-B_{12}) d\epsilon . \tag{35}$$

E. Solutions continuous in space and time

To study the space and time dependence of the shock process, we need to know something about the dynamic response characteristics of the material. There is currently no sound basis for estimating plastic flow behavior under conditions of overdriven shocks. However, a respectable estimate of the heat transport mechanism can be made, and we will do this specifically for metals.

For an ordinary metal, solid, or liquid phase, undergoing a shock to the few Mbar range, the compression is about a factor of 2, and the temperature rises to the order of 10^4 K. These changes are mild for most metals, so the nature of the electron-phonon system in its simplest approximation is not significantly changed. We can still think of electrons carrying the heat, and being scattered by electrons and phonons. Further, if irreversible thermodynamics is approximately valid, the heat current should be given approximately by the steady conduction equation $J = -\kappa \operatorname{grad} T$.

Elementary solid-state theory for electronic conduction at high temperatures ($T \gtrsim$ Debye temperature) expresses the conductivity κ as[8–11]

$$\kappa = \tfrac{1}{3} C v_F^2 t_e ,$$

where C is the electronic heat capacity per unit volume, v_F is the Fermi velocity, and t_e is the dominant electronic relaxation time. The electron-phonon relaxation time is $t_{ep} \sim 10^{-14}$ s at room temperature and should decrease through the shock approximately as T^{-1}. The electron-electron relaxation time is $T_{ee} \sim 10^{-12}$ s at room temperature and should decrease approximately as T^{-2}. Hence t_{ee} will become dominant at sufficiently strong shocks, but up to a few Mbar, t_{ep} should ordinarily be dominant. With t_{ep} as the electronic relaxation time, the above expression for κ has the following properties[8–11]: κ is independent of T, and κ has only a small density dependence of order ρ to ρ^2. So in the shocks under consideration, κ is roughly constant.

The thermodynamic variables σ, τ, T, S, ψ, J should be continuous single-valued functions of space and time through the shock, or what is equivalent, they should be continuous single-valued functions of z. This requirement leads to a condition on the behavior of $T(\epsilon)$ and $J(\epsilon)$, which we will derive. The heat-conduction equation for a steady plane wave is

$$J = -\kappa(\partial T/\partial x)_t = -\kappa(dT/dz) , \tag{36}$$

or with $d\epsilon > 0$,

$$J = -\kappa \frac{dT/d\epsilon}{dz/d\epsilon} . \tag{37}$$

For overdriven shocks, Theorem 1 implies $J(\epsilon)$ and $dT/d\epsilon$ are both positive at small ϵ. As ϵ increases Eq. (37) allows the following possibilities. If $dT/d\epsilon = 0$ on a finite interval while $J(\epsilon) > 0$, then $\epsilon(z)$ is discontinuous. If $dT/d\epsilon < 0$ on a finite interval while $J(\epsilon) > 0$, then $\epsilon(z)$ is double valued. If $J(\epsilon) = 0$ on a finite interval while $dT/d\epsilon > 0$, then $z(\epsilon)$ is undefined. If $J(\epsilon) < 0$ on a finite interval while $dT/d\epsilon > 0$, then $\epsilon(z)$ is double valued. All of these cases can be rejected, because if ϵ is discontinuous or double valued in z, then the thermodynamic variables are also discontinuous or double valued in z. Then either $J(\epsilon)$ and $dT/d\epsilon$ both remain positive on $0 < \epsilon < \epsilon_H$ or else both are zero at some $\epsilon' < \epsilon_H$.

In fact, both $J(\epsilon)$ and $dT/d\epsilon$ must remain positive, as can be shown from the Rayleigh-line equations. In (11) the last term on the right is of order τ/G relative to the second term, so the sign of the last two terms together is the sign of the second term, from which it follows that $T(dS/d\epsilon) < 0$ when $dT/d\epsilon \leq 0$. Then because $\tau(d\psi/d\epsilon) \geq 0$, (12) implies $dJ/d\epsilon < 0$ when $dT/d\epsilon \leq 0$. Now suppose J and $dT/d\epsilon$ are zero at $\epsilon' < \epsilon_H$. Then if $dT/d\epsilon \leq 0$ all the way to ϵ_H, $dJ/d\epsilon < 0$ all the way to ϵ_H, and $J(\epsilon_H) < 0$, which violates the final condition (15). If instead $dT/d\epsilon \leq 0$ for $\epsilon' \leq \epsilon \leq \epsilon''$, where $\epsilon'' < \epsilon_H$ and $dT/d\epsilon > 0$ for a finite interval of $\epsilon > \epsilon''$, then $J(\epsilon) < 0$ for a finite interval of $\epsilon > \epsilon''$ and $\epsilon(z)$ is double valued. Hence we have the following theorem.

Theorem 4. For an overdriven shock in a solid with heat conduction and dissipative plastic flow, a steady-wave solution continuous and single valued in z is possible only under the conditions $J(\epsilon) \geq 0$, $dT/d\epsilon \geq 0$, on $0 \leq \epsilon \leq \epsilon_H$, where either equality can hold on a sum of intervals whose total length is zero.

F. Bounds throughout the shock

It is now possible to construct upper and lower bounds for the temperature through the shock process. The construction is shown in Fig. 4, where the curves are those computed for a 0.8 Mbar shock in 2024 Al, with the approximation $\tau_H = 0$. The inviscid fluid curve is the $\tau = 0$ partial solution [Theorem 2 and Eqs. (27)–(31)]; it reaches T_H at ϵ^* and so, because $dT/d\epsilon \geq 0$ for $0 < \epsilon < \epsilon_H$ by

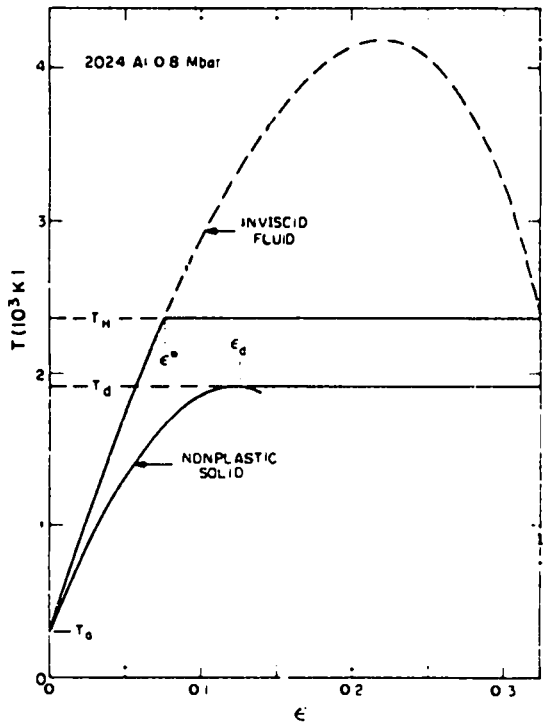

FIG. 4. Solid lines show upper and lower bounds for $T(\epsilon)$ on the Rayleigh line. Curves plotted are for a 0.8 Mbar shock in 2024 Al, where $\tau_H = 0$ has been taken for approximation ($\epsilon_H = 0.324$, $T_H = 2365$ K).

Theorem 4, an upper bound for $T(\epsilon)$ on $\epsilon^* \leq \epsilon \leq \epsilon_H$ is T_H. The nonplastic solid curve is the $\psi = 0$ partial solution [Theorem 3 and Eqs. (32)–(35)]; it has a maximum of T_d at ϵ_d and so, because $dT/d\epsilon \geq 0$ for $0 < \epsilon < \epsilon_H$, a lower bound for $T(\epsilon)$ on $\epsilon_d \leq \epsilon \leq \epsilon_H$ is T_d.

For the real shock process in a solid with heat conduction and dissipative plastic flow, the $T(\epsilon)$ curve must lie within the bounds illustrated in Fig. 4, must be a nondecreasing function of ϵ, and must reach T_H at ϵ_H. Further, with the upper bound for $T(\epsilon)$ prescribed as in Fig. 4, a partial solution of the Rayleigh-line equations can be found, in which $S(\epsilon)$, $\psi(\epsilon)$, $J(\epsilon)$ are upper bounds and $\tau(\epsilon)$ is a lower bound. Also for the lower bound $T(\epsilon)$ shown in Fig. 4, another partial solution can be found, in which $S(\epsilon)$, $\psi(\epsilon)$, $J(\epsilon)$ are lower bounds and $\tau(\epsilon)$ is an upper bound. This gives a great deal of information about the shock process.

G. Necessity of plastic dissipation

With reference to Fig. 4 and with $\tau_H = 0$ for approximation, we consider the possibility that the

inviscid fluid solution for $T(\epsilon)$ remains less than T_H for $0 \leq \epsilon < \epsilon_H$ and reaches T_H at ϵ_H. In his classic paper on shocks in gases, Rayleigh[12] has shown that this is the case for sufficiently weak shocks, but not for shocks stronger than a certain limit. We express this limit in the form $D = (1+x)c_B$, where c_B is the "bulk sound velocity," given by $\rho c_B^2 = B$. For dense systems such as $\rho_a \gtrsim 1$ g/cm^3, and corresponding values of γ_a and C_v, we find $x \sim 10^{-2}$. This value of D is certainly less than the longitudinal sound velocity, so we conclude that for overdriven shocks the inviscid fluid curve of $T(\epsilon)$ passes above T_H at some $\epsilon^* < \epsilon_H$, as shown in Fig. 4. It is therefore possible to establish the following theorem.

Theorem 5. For an overdriven shock in a solid with heat conduction, no solution is possible without plastic dissipation.

The theorem is most easily proved from Fig. 4. The inviscid fluid $T(\epsilon)$ corresponds to $\tau = 0$; therefore, in order to have $T(\epsilon) \leq T_H$ for $\epsilon > \epsilon^*$, we must have $\tau(\epsilon) > 0$ for $\epsilon > \epsilon^*$. The nonplastic solid $T(\epsilon)$ corresponds to $\psi = 0$; therefore, in order that $T(\epsilon) \geq T_d$ for $\epsilon > \epsilon_d$, we must have $\psi(\epsilon) > 0$ for $\epsilon > \epsilon_d$. Thus in the last part of the shock process, for $\epsilon > \epsilon^*$ and $\epsilon > \epsilon_d$, the plastic dissipation $dW^p = 2V\tau d\psi$ is greater than zero.

This result is approximately the counterpart for solids of Rayleigh's theorem[12] for viscous heat-conducting gases. Physically it arises because the heat which must be transported to the initial region of an overdriven shock, in order to bring σ up to the Rayleigh line according to Theorem 1, has to be generated by plastic dissipation in the later stage of the shock.

IV. SUMMARY AND DISCUSSION

We have studied the irreversible thermodynamic process of overdriven shocks in an isotropic solid with heat transport and dissipative plastic flow. Shock-induced macroscopic inhomogeneities and shock-induced phase changes are not considered. The theory developed is expected to apply to polycrystalline metals, and possibly to ductile nonmetals as well. Arguments can be given for the neglect of polycrystalline effects (the Appendix), but more experimental information on this question is needed.

Some comments can be made concerning the steady-wave assumption. When a shock is initiated, for example by a plate impact, the wave front presumably evolves as it moves. The assumption is that it approaches a steady wave (evolution approaches zero), and that for all practical purposes the real shock is well approximated by the limiting steady wave, after a distance of travel of many shock widths. The steady-wave assumption does not hold for weak shocks in solids[2,3] because the elastic precursor travels faster than the plastic wave and the entire shock continues to spread indefinitely. Also, for overdriven shocks a phase change could split the wave into two components traveling at different velocities. Obviously, then, the steady-wave assumption implies some restrictions on the dynamic response of a material. We note that heat transport according to the steady conduction equation is compatible with a steady wave.

The concept of the family of partial solutions is quite useful in analyzing the shock process because these solutions depend only on the best-known material properties, namely, the thermoelastic coefficients. For a given material, with thermoelastic coefficients known as functions of the thermoelastic state, the family contains all continuous solutions with the proper initial and final values, which are consistent with the thermoelastic coefficients and consistent with arbitrary (unspecified) dynamic response properties. Members of the family are ordered by observing that given a partial solution functional variation leads to a new partial solution with $\delta S(\epsilon)$, $\delta T(\epsilon)$, $\delta\psi(\epsilon)$, $\delta J(\epsilon)$ of the same sign everywhere, and $\delta\tau(\epsilon)$ of the opposite sign everywhere. Then because τ must be non-negative, $\tau(\epsilon) = 0$ defines a unique partial solution which gives upper bounds for $S(\epsilon)$, $T(\epsilon)$, $\psi(\epsilon)$, $J(\epsilon)$ (Theorem 2). And because ψ must be non-negative, $\psi(\epsilon) = 0$ defines a partial solution, unique up to ϵ_d where $dT/d\epsilon = 0$, which gives lower bounds for $S(\epsilon)$, $T(\epsilon)$, $\psi(\epsilon)$, $J(\epsilon)$, and an upper bound for $\tau(\epsilon)$, for $0 \leq \epsilon \leq \epsilon_d$ (Theorem 3). Further, the condition that the solution be continuous and single valued in z, coupled with the steady heat-conduction equation, requires $J(\epsilon)$ to be non-negative and $T(\epsilon)$ to be a nondecreasing function of ϵ (Theorem 4). This theorem then narrows the bounds on $T(\epsilon)$ and on the other variables as well (Fig. 4). Finally, it is established that for an overdriven shock in a solid no solution is possible without the operation of *both* dissipative mechanisms, heat transport and plastic flow (Theorems 1 and 5).

An observation is in order on the use of thermodynamics in the theory of shocks. In the present work, irreversible thermodynamics is assumed

valid; this means thermodynamic functions are defined throughout the shock, and they are related by irreversible-thermodynamic relations. It is then possible to solve for, or at least to estimate, the space and time dependence of the shock process, and from this solution it is possible to determine whether or not irreversible thermodynamics is in fact valid. We will pursue this line of investigation in the future. In the following paper, the present theory is used as basis for numerical calculations for some representative metals, and it is found that the Rayleigh-line solution is narrowly bounded and the nature of the shock process is revealed in some detail.

ACKNOWLEDGMENT

Sincere appreciation is expressed to Galen Straub and to James N. Johnson for encouragement and helpful discussions.

APPENDIX: POLYCRYSTALLINE EFFECTS

The question is, for overdriven shocks in solids, is the shock width (or rise time) influenced by polycrystalline effects: more specifically, does the polycrystal structure give rise to a significant dissipation in the shock process. Such dissipation could result if the shock velocity is different in different crystallographic directions and if the shock thickness is small compared to the grain size. Then in any two neighboring grains of different orientation, the shock will move faster in one and will transfer energy sideways to the other grain ahead of the shock front there; this is dissipative, and it broadens the shock front. We note that different shock velocities in different crystal directions can result if there is a noticeable shear stress in the shocked state, and especially if that shear stress is different for the different directions. On the other hand, if the Hugoniot shear stress is insignificant for shocks in all crystal directions, and if the shock is a steady wave, then the Hugoniot lies in isotropic thermodynamic space (stress system is isotropic pressure) and the shock velocity must also be isotropic.

As for experimental data, there is very little to help resolve the question. Grains in metals range nominally from 10^{-3} to 10^{-2} cm. According to the present theory, the width of overdriven shocks in metals is of order 10^{-6} cm, so the shock thickness is small compared to the grain size. The same should be true for any nonmetals to which the present theory might apply. For very weak shocks in NaCl (3 – 15 kbar), a large difference in plastic wave velocities in different crystal directions has been observed.[13] This has been explained by attributing the plastic flow entirely to primary slip.[14] For stronger shocks, driving higher order slip, dependence on crystal orientation is expected to become weaker. Shock velocity-particle velocity measurements for NaCl in different crystal directions all lie on the same curve up to 230 kbar (Ref. 15); a phase change which begins at 230 kbar introduces effects with which we are not concerned here. This result suggests that polycrystal effects should not be important in NaCl up to 230 kbar. For metals we might speculate that $\tau_{II} << \sigma_{II}$ for shocks in the Mbar range, so that shock velocity is insensitive to crystal direction and polycrystal effects are correspondingly negligible. Any experimental information which bears on this question would be welcome in the future.

---

[1]D. C. Wallace, Phys. Rev. B 22, 1477 (1980).
[2]D. C. Wallace, Phys. Rev. B 22, 1487 (1980).
[3]D. C. Wallace, Phys. Rev. B 22, 1495 (1980).
[4]A weak shock is an underdriven shock, i.e., a shock in which the plastic wave velocity is not greater than the elastic precursor velocity. For a given material the elastic precursor velocity is a constant, and is equal to or slightly greater than the longitudinal sound velocity. In an overdriven shock, the shock velocity is greater than the elastic precursor velocity, so there is no elastic precursor.
[5]L. C. Chhabildas and J. R. Asay, J. Appl. Phys. 50, 2749 (1979).
[6]D. C. Wallace, *Thermodynamics of Crystals* (Wiley, New York, 1972).
[7]Neglecting melting, this holds for shocks in solids up to several Mbar, hence it holds generally for shocks to the vicinity of melting, above which $G \rightarrow 0$.
[8]J. M. Ziman, *Electrons and Phonons* (Oxford University Press, Oxford, 1960).
[9]R. E. Peierls, *Quantum Theory of Solids* (Clarendon, Oxford, 1955).
[10]D. Pines, *Elementary Excitations in Solids* (Benjamin, New York, 1963).

[11]J. M. Ziman, *Principles of the Theory of Solids* (Cambridge University Press, Cambridge, 1972).
[12]Lord Rayleigh, Proc. R. Soc. London, Ser. A 84, 247 (1910).
[13]W. J. Murri and G. D. Anderson, J. Appl. Phys. 41, 3521 (1970).
[14]J. N. Johnson, J. Phys. Chem. Solids 35, 609 (1974).
[15]J. N. Fritz, S. P. Marsh, W. J. Carter, and R. G. McQueen, Natl. Bur. Stand. (U.S.), Spec. Publ. 326, 201 (1971).

Nature of the process of overdriven shocks in metals

Duane C. Wallace
Los Alamos Scientific Laboratory, Los Alamos, New Mexico 87545
(Received 6 February 1981)

Within the bounds established by the formal theory of overdriven shocks in solids, an approximate solution is constructed, and a consistent set of approximations for the thermodynamic coefficients is described. Numerical calculations of the temperature, entropy, shear stress, and plastic strain, as functions of compression, are shown for shocks up to 0.8 Mbar in 2024 Al, and up to 3.0 Mbar in Pt. For well-overdriven shocks in metals the shock entropy is generated by heat conduction in the front part of the shock, the heat is generated by plastic flow in the last part of the shock, and the shock rise time is of order 10^{-12} s.

I. INTRODUCTION

We have obtained extensive theoretical information about the irreversible-thermodynamic process of overdriven shocks in solids.[1] This theory was developed for an isotropic solid with heat transport and dissipative plastic flow, and a steady-wave shock which does not induce phase changes or macroscopic inhomogeneities in the solid. The purpose of the present work is to carry out numerical calculations to see what can be learned about the details of the shock process, without assuming anything about the plastic flow behavior. Calculations are done for 2024 Al for shocks of 0.4 and 0.8 Mbar, and for Pt for shocks of 0.5 – 3.0 Mbar. Information is obtained on temperature, entropy, shear stress, plastic strain, and heat current, as functions of compression, and the space and time dependence of the process is estimated.

All the approximations used in the numerical evaluations are described in Sec. II, and their physical bases and implications are discussed. Results are tabulated and [illegible] in Sec. III, and the salient features of ove[illegible] shocks in metals are summarized in Sec. IV. [illegible]tatus of an investigation into the validity of irreversible thermodynamics in shock theory is mentioned in Sec. IV. For the two metals studied here, properties on the Hugoniot are tabulated in the appendixes.

II. AN APPROXIMATE SOLUTION

A. The conduction front

In general, except for shocks not far above the overdriven threshold, the shock process is narrowly bounded by the theory of Ref. 1. The bounds for the temperature $T(\epsilon)$ for a 2.5 Mbar shock in Pt are shown by the solid lines in Fig. 1. Our aim is to construct an approximate $T(\epsilon)$ curve within these bounds, thus defining a partial solution, and then to solve as far as possible the Rayleigh-line equations for the other functions of this partial solution, the entropy per unit mass $S(\epsilon)$, the heat

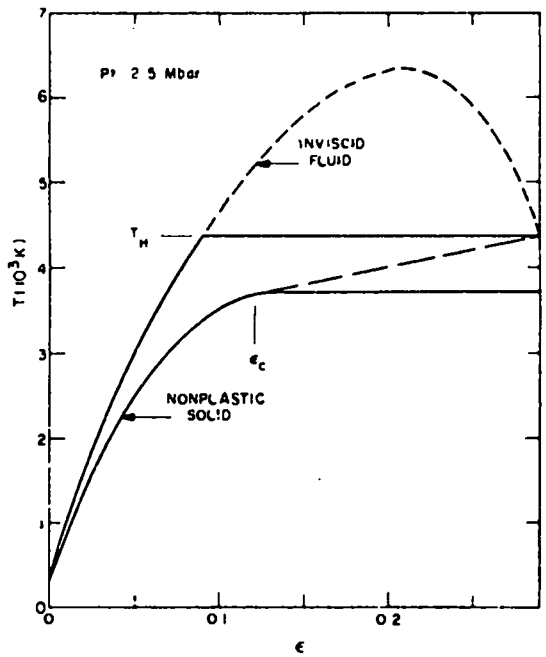

FIG. 1. Solid lines show upper and lower bounds for $T(\epsilon)$ for a 2.5 Mbar shock in Pt. Our approximate solution takes the lower bound (nonplastic solid curve) up to point c, and the linear interpolation (dashed line) from $T_c(\epsilon_c)$ to $T_H(\epsilon_H)$.

current $J(\epsilon)$, the plastic strain $\psi(\epsilon)$, and the shear stress $\tau(\epsilon)$.

At the beginning of the shock, in state a, τ and ψ are zero. As the uniaxial compression begins, τ increases due to elastic response of the material but ψ remains zero unitl τ reaches the static yield value. When τ increases above the static yield, plastic flow proceeds. However, since the shock process is quite fast, its timescale being governed by heat conduction, the plastic flow will be of negligible importance until τ rises high enough to drive ψ at a very high rate, a rate commensurate with the shock rise time. Thus in the leading part of the shock we should have $d\psi=0$ to a good approximation, i.e., we have nearly the response of an elastic solid with infinite yield strength, as described in Theorem 3.[1] We take this approximation to hold up to a point c, at ϵ_c, to be determined later. The region $0\le\epsilon\le\epsilon_c$ is called the conduction front because heat must be transported to this region, according to Theorem 1.[1] The Rayleigh-line equations for the conduction front as function of ϵ are Eqs. (32) – (35) of Ref. 1. These equations are accurately represented by their leading terms in the small-anisotropy expansion, and this representation is used in the present calculations.

B. The flow region

After the point c the plastic flow gets going at a high rate, and the temperature rises significantly above the nonplastic solid curve. From ϵ_c to ϵ_H, $T(\epsilon)$ goes from the nonplastic solid curve to T_H, increasing monotonically with ϵ, as illustrated by the dashed line in Fig. 1. The region $\epsilon_c\le\epsilon\le\epsilon_H$ is called the flow region, because here the dissipative plastic flow is essential to the process. Before approximating $T(\epsilon)$ in the flow region, we will study the Rayleigh-line equations here in some detail.

In the flow region, it is necessary to keep both dissipative mechanisms in the equations. First consider the equation for $d\tau$; in the small-anisotropy expansion this is written

$$d\tau=-G(d\ln V+\tfrac{3}{2}d\psi)+\cdots . \tag{1}$$

The leading terms in $d\tau$ are thus of order $Gd\epsilon$. There are a host of first-order terms, indicated by $+\cdots$ in (1), of relative order τ/G, which means of order $(\tau/G)Gd\epsilon$ in $d\tau$. These terms involve the third-order elastic constants, the anisotropic Gruneisen parameters, and so on. From Eq. (1) we learn two things:

(a) Since $d\tau$ is of order $\tau d\epsilon$, the leading terms must cancel to relative order τ/G, which implies

$$d\psi\approx-\tfrac{3}{2}d\ln V . \tag{2}$$

(b) $d\tau$ depends *essentially* on the first-order terms in (1).

In practice it is not possible to make respectable estimates of *all* the coefficients appearing in the first-order terms in $d\tau$ along the Rayleigh line for overdriven shocks in solids. If we cannot estimate all the coefficients in the first-order terms in $d\tau$, we cannot make a meaningful evaluation of $d\tau$ in the flow region. We conclude that we cannot use Eq. (1) in the flow region.

There are three equations which couple the normal stress $\sigma(\epsilon)$, and $T(\epsilon)$, $S(\epsilon)$, $\psi(\epsilon)$ on the Rayleigh line, namely Eqs. (5), (9), and (11) of Ref. 1. When $\sigma(\epsilon)$ is eliminated, the results can be written as two equations for $S(\epsilon)$ and $\psi(\epsilon)$ in terms of $T(\epsilon)$. Neither of these equations depends critically on the terms of relative order τ/G; meaningful evaluations of both are obtained in zeroth order in the small-anisotropy expansion. In this order the equations are the following:

$$TdS=C_V(dT-\rho\gamma V_a T d\epsilon) , \tag{3}$$

$$d\psi=(2G)^{-1}\{\rho\gamma T dS - [\rho_a D^2-\rho V_a(B+\tfrac{4}{3}G)]d\epsilon\} . \tag{4}$$

Thus if we have an acceptable approximation for $T(\epsilon)$ in the flow region, (3) can be integrated to find $S(\epsilon)$, then (4) can be integrated to find $\psi(\epsilon)$. The coefficients in (3) and (4) can be evaluated with respectable accuracy on the Rayleigh line for real metals.

Finally there is the equation for the entropy production,[1]

$$TdS=dJ/\rho_a D+2V\tau d\psi . \tag{5}$$

This cannot be solved because it contains two unknowns, J and τ. However, because of the initial and final conditions $J_a=J_H=0$, we have an integral condition on dJ, namely $\int_a^H dJ=0$. Hence $\int_a^H T\,dS=\int_a^H 2V\tau\,d\psi$, and this is $\int_c^H 2V\tau\,d\psi$ because $d\psi=0$ on $0\le\epsilon\le\epsilon_c$. This last integral is used to define a mean shear stress $\langle\tau\rangle$ in the flow region:

$$\int_c^H 2V\tau\,d\psi=(V_c+V_H)\langle\tau\rangle\int_c^H d\psi . \tag{6}$$

Then $\langle\tau\rangle$ can be evaluated from

$$\langle\tau\rangle=\frac{\int_a^H T dS}{(V_c+V_H)\psi_H} \quad (7)$$

To emphasize an important point, this estimate of $\langle\tau\rangle$ is not based on Eq. (1) for $d\tau$, which is essentially a first-order equation and hence is extremely difficult to evaluate, but is based on an integral condition for TdS, namely the requirement that the shear stress must do the correct amount of work in the flow region to generate the correct amount of heat, so the material reaches the correct Hugoniot state at the end of the shock. A reasonably accurate evaluation of $\langle\tau\rangle$ can be made for real metals.

The above results for $S(\epsilon)$ and $\psi(\epsilon)$ in the flow region and for $\langle\tau\rangle$ do not depend strongly on the curve of $T(\epsilon)$ in the flow region. We take simply a straight line interpolation for $T(\epsilon)$ from $T_c(\epsilon_c)$ to $T_H(\epsilon_H)$, and define c as the point on the nonplastic solid $T(\epsilon)$ curve which is tangent to the straight line drawn from $T_H(\epsilon_H)$. This approximation is shown for a 2.5 Mbar shock in Pt by the dashed line in Fig. 1. There is a technical point which should be mentioned: The approximation for $T(\epsilon)$ in the flow region should be consistent with the physical requirement that $d\psi/d\epsilon$ be non-negative. Now $dJ/d\epsilon=0$ at ϵ_b, and for the nonplastic solid partial solution both terms on the right side of (4) are zero at ϵ_b, and ϵ_c is close to ϵ_b so $d\psi/d\epsilon$ is always small at ϵ_c, but it can be negative. In the numerical calculations of the present work, $d\psi/d\epsilon$ is found to be essentially zero at ϵ_c.

C. The Hugoniot

We are studying shocks upwards from a few hundred kbar, where nothing is known of the shear stress on the Hugoniot. While the shear stress during the shock becomes large, driving plastic flow at a high rate, all strain rates go to zero at the end of the shock, and the final-state shear stress is the static yield stress on the Hugoniot. For overdriven shocks in metals τ_H/σ_H should be at most a few percent, so neglecting τ_H should not introduce a significant error in the present calculations. We therefore set $\tau_H=0$, which reduces σ_H to an isotropic pressure P_H.

The Hugoniot jump conditions are the first integrals of the equations for conservation of mass, momentum, and energy, evaluated at the final state H [see, e.g., Ref. 1, Eqs. (3) – (5)].

Since our approximate Hugoniot lies in isotropic thermodynamic space, the thermoelastic coefficients on the Hugoniot are reduced to isotropic coefficients, e.g., $\gamma_1=\gamma_2=\gamma$, where

$$\rho\gamma=\left|\frac{\partial P}{\partial U}\right|_V . \quad (8)$$

Equations for calculating T and S on the Hugoniot and the adiabatic bulk modulus on and off the Hugoniot are well known.[2] A well-established experimental result for shocks in solids up to a few Mbar, and excepting cases where phase changes occur, is that the shock velocity is a linear function of the final-state particle velocity[2–4]:

$$D=c+sv_H . \quad (9)$$

The constant c and s are commonly measured for overdriven shocks in solids.

D. Thermodynamic coefficients

In the small-anisotropy expansions,[1] anisotropic coefficients on the anisotropic Rayleigh line at V,S,τ are given in lowest order by isotropic coefficients at V,S; for example,

$$C_\eta(V,S,\tau)=C_V(V,S)+\cdots . \quad (10a)$$

This relation is to be understood when we say "C_V on the Rayleigh line." In the present work we will need γ, C_V, B, and G on the Rayleigh line. Further, because the relation between T and S is evaluated to lowest order in the small anisotropy expansion, which is Eq. (3), the T,V,S relation on the Rayleigh line is in fact the isotropic-space T,V,S relation, so (10a) can also be written

$$C_\eta(V,T,\tau)=C_V(V,T)+\cdots . \quad (10b)$$

For the Grüneisen parameter we use the approximation[5] $\rho\gamma=$ const:

$$\rho\gamma=\rho_a\gamma_a . \quad (11)$$

The heat capacity is the sum of a lattice part C_l and an electronic part C_e. The lattice part is described in terms of a characteristic temperature Θ, e.g., the Debye temperature, where for most metals Θ is less than or equal to room temperature at $P=0$. If $T_a\gtrsim\Theta$, then the Hugoniot and Rayleigh lines all lie in the region $T\gtrsim\Theta$, where $C_l\approx 3Nk$, with $k=$ Boltzmann's constant. For the conduction electrons, degenerate electron theory gives $C_e=\Gamma T$. We will neglect the explicit temperature-dependence of Γ,[6] and use low-temperature measurements for Γ.[7] The volume-

dependence is[8] $g = d\ln\Gamma/d\ln V \approx 1-2$, and we take $g =$ const for a given metal. The total heat capacity is then approximately

$$C_V = 3Nk + \Gamma T , \tag{12a}$$

$$\Gamma = \Gamma_a (V/V_a)^g . \tag{12b}$$

The shear modulus is entirely unknown in the moderate shock region. The common behavior of polycrystalline materials at $P=0$ is $G/B \approx$ constant in T, except near melting. We will assume this holds for shocks in the solid phase, and calculate G on the Rayleigh line from B,

$$G/B = G_a/B_a . \tag{13}$$

As a point of curiosity we calculated B and G for Al from ultrasonic data,[9] in the form of expansions linear in T and P from state a, and found the remarkable results that B(ultrasonic) $\approx B$(shock), and G/B(ultrasonic) $\approx$ const, up to 2 Mbar (neglecting melting) on the Hugoniot. These calculations are tabulated in Appendix B.

The thermal conductivity κ is needed only to compute the explicit space and time dependence of the shock process, from the equation[1]

$$dZ = \frac{-\kappa dT}{(1-\epsilon)J} , \tag{14}$$

where $Z = X - Dt$. For electronic conduction in the region $T/\Theta \gtrsim 1$, we expect κ to be nearly independent of T, and to have a density dependence of order ρ to ρ^2.[1] This density dependence is negligible for the present purposes, and we simply take $\kappa =$ constant and use the measured value of κ at $T/\Theta \gtrsim 1$, $P=0$.

E. Shock thickness and plastic strain rate

The Lagrangian shock thickness ΔZ, the same as ΔX at a fixed time, is usually defined in terms of the compression $\epsilon(Z)$ (Ref 10); we call this the compression thickness $\Delta Z(\epsilon)$:

$$\frac{\Delta\epsilon}{\Delta Z(\epsilon)} = \left|\frac{d\epsilon}{dZ}\right|_{\max} . \tag{15}$$

The temperature profile $T(Z)$ is noticeably broader than the compression, so we define also the temperature thickness $\Delta Z(T)$:

$$\frac{\Delta T}{\Delta Z(T)} = \left|\frac{dT}{dZ}\right|_{\max} . \tag{16}$$

Either derivative $|d\epsilon/dZ|$ or $|dT/dZ|$ is near its maximum at point c, and this gives a simple approximation for the right sides of (15) and (16). For example,

$$\Delta Z(T) \approx \frac{\kappa_i (T_H - T_a)}{(1-\epsilon_c)J_c} .$$

The Lagrangian rise time is then $\Delta t_\chi = \Delta Z/D$.

The plastic strain rate $\dot\psi$ is approximated as follows: $d\psi$ is given by (4), dJ is approximated in the flow region by (5) with $2V_T d\psi \approx (V_c + V_H)(\tau) d\psi$, then dZ is given by (14), and

$$\dot\psi = \left|\frac{\partial\psi}{\partial t}\right|_\chi = -D\frac{d\psi}{dZ} . \tag{17}$$

A useful measure of plastic strain rate in the shock is the average of $\dot\psi$ in the flow region, defined by

$$\langle\dot\psi\rangle = \frac{\int_c^H \dot\psi\, d\epsilon}{\epsilon_H - \epsilon_c} . \tag{18}$$

F. On the electronic contributions

There are several important points to note regarding the electronic contribution to thermodynamic coefficients.

(a) For shocks in the Mbar range, electronic contributions to thermal energy and thermal pressure are not always negligible and should at least be estimated. This was pointed out by Al'tshuler.[11]

(b) In shock analysis, if the electronic heat capacity $C_e = \Gamma T$ cannot be neglected, then the volume dependence of Γ also cannot be neglected because of the significant compression. Including $C_e = \Gamma T$ with a constant value of Γ seriously overestimates C_e.

(c) The Grüneisen parameter γ is not simply the sum of a lattice part γ_l and an electronic part γ_e (Ref. 6, p. 287). Specifically, Eq. (8) can be transformed to $\rho\gamma = -C_V^{-1}(\partial^2 F/\partial V\partial T)_{TV}$, where F is the Helmholtz free energy, the sum of a lattice and an electronic part, $F = F_l + F_e$, from which it follows:

$$\gamma = (C_l/C_V)\gamma_l + (C_e/C_V)\gamma_e .$$

It is γ we want for shock analysis, to calculate *total* P,U relations from Eq. (8), and it is γ which satisfies $\rho\gamma \approx$ const in Neal's[5] compilation.

(d) Degenerate electron theory is satisfactory for kT/ϵ_F is less than or equal to a few tenths, where ϵ_F is the Fermi energy. For sufficiently strong shocks, which may be above the melting tempera-

ture on the Hugoniot, the temperature will rise so high that the electrons are no longer degenerate.

III. RESULTS AND DISCUSSION

The experimental information for the present shock calculations for 2024 Al and Pt is listed in Table I. The Hugoniot was calculated first, and results are tabulated in Appendix A. Several observations follow from the Hugoniot calculations.

(a) The elastic precursor velocity c_p is very close to the longitudinal sound velocity c_l, so the overdriven threshold at $D=c_p$ is close to $D=c_l$; we find

$$P_H(D=c_l)=0.145 \text{ Mbar for 2024 Al},$$
$$P_H(D=c_l)=0.308 \text{ Mbar for Pt}. \quad (19)$$

(b) From the Kraut-Kennedy melting rule,[13] melting on the Hugoniot is found to occur at

$$T_M=2715 \text{ K}, \quad P_M=0.88 \text{ Mbar for 2024 Al},$$
$$T_M=5800 \text{ K}, \quad P_M=3.04 \text{ Mbar for Pt}. \quad (20)$$

To the extent this approximation is in error, we expect it to be low for T_M, P_M.

(c) Neglecting the electronic heat capacity gives a calculated temperature on the Hugoniot too high by about 4% at 0.9 Mbar for 2024 Al, and too high by about 33% at 3 Mbar for Pt. For details see Appendix A.

The approximate solution for the shock process was computed for 2024 Al for shocks of 0.4 and 0.8 Mbar, and for Pt for six shocks of strength 0.5 – 3.0 Mbar. The main results are listed in Table

TABLE I. Input data for shock calculations. Shock measurements (c,s) are from McQueen *et al.* (Ref. 2) for 2024 Al and from Morgan (Ref. 12) for Pt: G_a/B_a are from the poly-crystal averages of Simmons and Wang (Ref. 9); and g are from White and Collins (Ref. 8).

Quantity	2024 Al	Pt
T_a (10^4 K)	0.293	0.293
ρ_a (g/cm^3)	2.785	21.44
c (cm/μs)	0.533	0.363
s	1.338	1.472
γ_c	2.05	2.66
G_a/B_a	0.34	0.23
Γ_a (10^{-4} cal/mole K^3)	3.30	16.4
g	1.8	2.28
κ (cal/cm s K)	0.48	0.20

II. The shape of the shock process as a function of the compression ϵ, and as a function of shock strength, is shown by the Pt sequence in Figs. 2–4. Note that as the shock strength increases, the width ϵ_c of the conduction front becomes larger compared to the width ϵ_H of the entire shock. In the weakly overdriven shock at 0.5 Mbar, only about a quarter of the shock temperature rise T_H-T_a occurs in the conduction front, and the entropy continues to increase in the flow region. In the well-overdriven shocks, 1 Mbar and stronger, at least three quarters of the shock temperature rise occurs in the conduction front, and the entropy decreases in the flow region. The results for 2024 Al show the same qualtitative behavior. We conclude that for well-overdriven shocks, in the present calcultions at shock pressure around three times the overdriven threshold or greater, heat conduction is a major part of the process, and most of the shock temperature rise occurs in the conduction front. For weaker shocks the effect of heat conduction becomes smaller as the shock strength decreases toward the overdriven threshold. In fact since the initial compression of the solid is presumably elastic, in the small ϵ region $J(\epsilon)\to 0$ as $D\to c_l$, and for $D\le c_l$ a solution can be obtained without heat transport. We consider the effect of heat transport to be generally negligible for underdriven shocks in solids.[14]

Because of the shape of $T(\epsilon)$ on the Rayleigh line, it appears that for shocks near melting on the Hugoniot, but still in the solid phase there, $T(\epsilon)$ will rise above the equilibrium melting temperature for a time in the center of the shock. When T passes the melting temperature, the material should begin to respond as a fluid after a time of order t_s, the shear relaxation time of the fluid phase. For most monatomic fluids, $t_s\sim 10^{-13}$ s at zero pressure, and should decrease roughly as $(V/V_a)^\gamma$ in compression. However, fluid behavior depends on the presence of vacancies, and during the shock there may not be time to develop the equilibrium concentration of vacancies, since this is presumably a diffusion process. The time required for fluid response to occur during a shock is an interesting open question.

As mentioned before, our approximate solution for $T(\epsilon)$ is reasonably accurate because of the narrow bounds imposed by the formal theory[1] (see, e.g., Fig. 1; also Fig. 4 of Ref. 1). In the flow region, these bounds limit $T(\epsilon)$ to within a deviation from the mean of $\pm 20\%$ for the two weakest shocks in Table II, namely 0.4 Mbar for 2024 Al

TABLE II. Results of the shock process calculations.

Quantity	2024 Al		Pt					
P_H (Mbar)	0.4	0.8	0.5	1.0	1.5	2.0	2.5	3.0
ϵ_H	0.2363	0.3241	0.1200	0.1863	0.2311	0.2642	0.2903	0.3114
D (cm/μs)	0.779	0.941	0.441	0.500	0.550	0.594	0.634	0.670
T_H (10^3 K)	0.930	2.365	0.534	1.132	2.032	3.138	4.374	5.697
$S_H - S_a$ (cal/mole K)	4.10	8.83	1.84	5.79	9.29	12.1	14.5	16.5
ϵ_c	0.0565	0.1130	0.0155	0.0544	0.0825	0.1044	0.1210	0.1355
$J_c/\rho_a D$ (10^3 cal/mole)	1.81	8.17	0.34	3.61	8.77	15.0	21.9	29.2
T_c (10^3 K)	0.648	1.903	0.359	0.919	1.755	2.699	3.685	4.680
$S_c - S_a$ (cal/mole K)	4.15	10.19	1.06	6.79	11.23	14.5	17.1	19.3
τ_c (Mbar)	0.019	0.048	0.011	0.044	0.075	0.107	0.136	0.167
ψ_H	0.162	0.226	0.081	0.126	0.158	0.182	0.202	0.219
$\langle\tau\rangle$ (Mbar)	0.027	0.064	0.021	0.053	0.086	0.121	0.16	0.19
$\langle\dot{\psi}\rangle$ (10^{12}/s)	0.06	0.27	0.011	0.12	0.32	0.43	0.48	0.51
$\Delta Z(\epsilon)$ (10^{-6} cm)	1.30	0.48	2.47	0.32	0.18	0.17	0.18	0.19
$\Delta Z(T)$ (10^{-6} cm)	2.23	1.41	2.90	0.90	0.71	0.65	0.61	0.58

and 0.5 Mbar for Pt, and to within a deviation of $\pm 10\%$ for the other shocks. The $T(\epsilon)$ bounds can be transformed to bounds on $\tau(\epsilon)$, from the variational relation[1]

$$\delta\tau(\epsilon) = -\tfrac{3}{4}\rho\gamma C_V \delta T(\epsilon) .$$

From this we estimate that our computed values of $\langle\tau\rangle$ have error bounds of $\pm 23\%$ for the two weakest shocks in Table II, and of $\pm 10-15\%$ for the other shocks.

The space-time dependence of the Pt 2.5 Mbar shock is shown in Fig. 5, where $Z=0$ is at point c in the shock. The difference in behavior of the temperature and entropy, as compared with the compression, is clearly seen: Because of the massive long-range transport of heat in the conduction front, the profiles of T and S extend far ahead of point c, and the increases of T and S are large

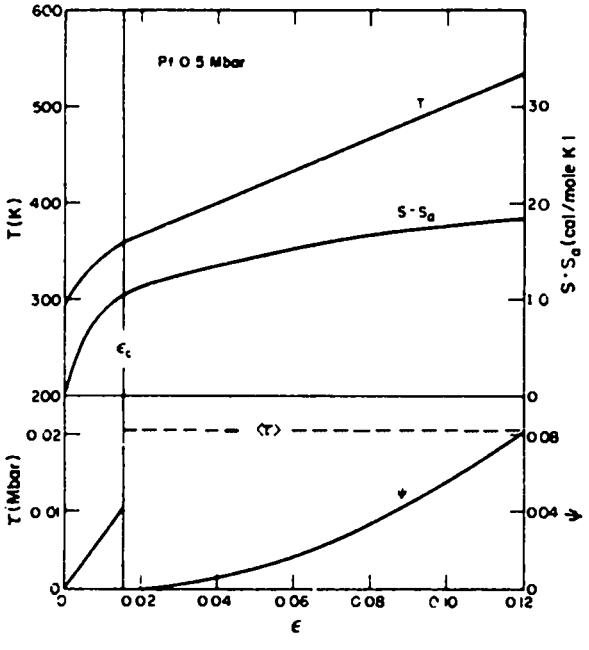

FIG. 2. Shape of the shock process for a 0.5 Mbar shock in Pt.

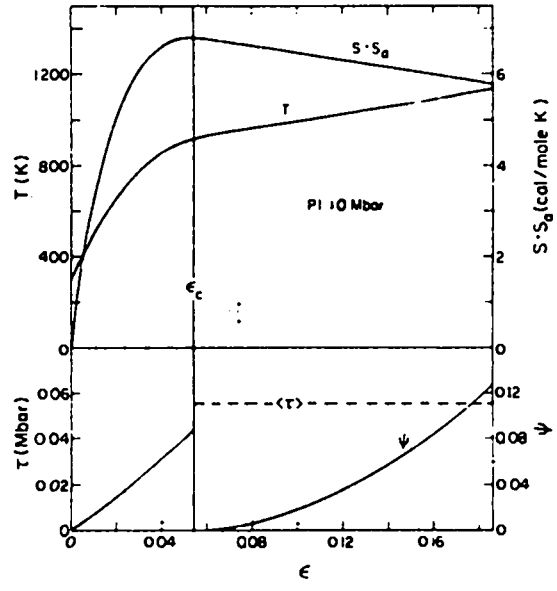

FIG. 3. Shape of the shock process for a 1.0 Mbar shock in Pt.

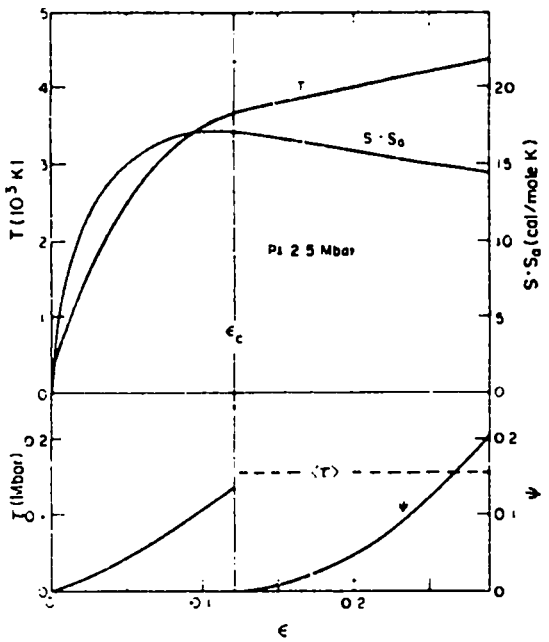

FIG. 4. Shape of the shock process for a 2.5 Mbar shock in Pt.

there; then behind point c, T and S change little while most of the compression takes place. Note, however, that in the limits $Z \to \pm\infty$, all three functions T,S,ϵ have formally the same Z dependence. In particular, for $Z \to \infty$, $T-T_a$, $S-S_a$, and ϵ all approach zero as $e^{-\alpha Z}$, with α a constant; and for $Z \to -\infty$, $|T-T_H|$, $|S-S_H|$, and $|\epsilon-\epsilon_H|$ all approach zero as $e^{\beta Z}$, with β another constant. In the same way, $\psi \to \psi_H$ and $\dot{\psi} \to 0$ behind the shock.

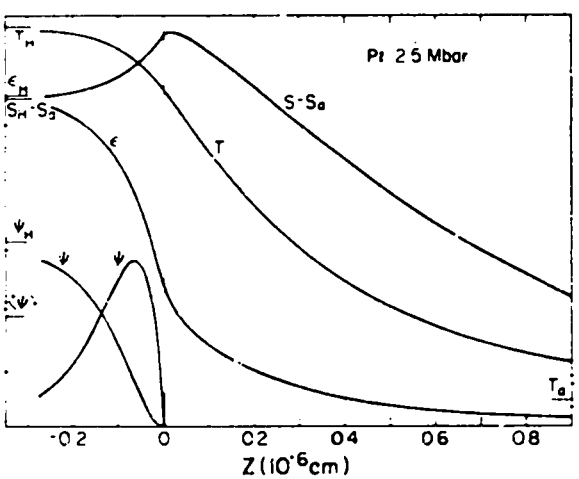

FIG. 5. Shock process as function of Z for a 2.5 Mbar shock in Pt.

Concerning the plastic constitutive behavior through the shock process, we note that $\langle\tau\rangle$ is larger than τ_c for all the shocks. This is consistent with setting $\dot{\psi}=0$ up to point c. In a real solution, of course, plastic flow will start at a much lower value of τ than τ_c, but $\dot{\psi}$ should still be small in the conduction front, and should increase significantly around point c, so the qualitative behavior of ψ and $\dot{\psi}$ should be still as shown in Figs. 2–5. Since the total ψ is small in a planar shock, strain hardening should be correspondingly small, and the high shear stress we find in the flow region is presumably due to the high strain rate $\dot{\psi}$. Finally, while we expect our estimates of $\langle\tau\rangle$ and $\psi(\epsilon)$ to be reasonably accurate, it is difficult to establish bounds for $\psi(\epsilon)$, and only order-of-magnitude meaning can be claimed for our values of $\langle\dot{\psi}\rangle$. For all but the weakest Pt shock in Table II, the ratio $\langle\tau\rangle/\langle\dot{\psi}\rangle$ lies in the range 0.2–0.4 g/cm s.

IV. NATURE OF THE SHOCK PROCESS

We review the nature of shocks in solids, for different ranges of shock strength. Recall that the elastic line is the $\sigma(\epsilon)$ relation corresponding to isentropic uniaxial elastic compression of the solid (see, e.g., Fig. 1 of Ref. 1). In a weak (underdriven) shock, the initial compression is on the elastic line; this signal travels as the elastic precursor. Following this initial elastic compression, the normal stress σ falls *below* the elastic line; hence a solution can be obtained by allowing plastic flow to occur, to relax σ below the elastic line.[14] The effect of heat transport on the shock process is presumably negligible. Since the elastic precursor travels faster than the plastic wave, the entire shock is not a steady wave.

For an overdriven shock, we *assume* the shock is a steady wave. The normal stress rises above the elastic line at small ϵ, so heat transport is necessary to obtain a solution in the leading edge. As the shock strength increases from the overdriven threshold, the quantity of heat which must be transported to the conduction front increases from zero. Also in the vicinity of the overdriven threshold, as shock strength increases, there is a dramatic decrease in the shock rise time, a decrease of a factor of order 10^3 for metals.

As a qualitative definition, a well-overdriven

TABLE III. Hugoniot for 2024 Al. Units are the following: P (Mbar), T (K), S (cal/mole K).

ϵ	P	T	$S-S_a$	T_{ion}
0	0	293	0	293
0.04	0.035	319	0.018	319
0.08	0.079	354	0.157	354
0.12	0.135	411	0.56	411
0.16	0.205	507	1.35	509
0.20	0.295	675	2.59	679
0.24	0.412	962	4.27	974
0.28	0.566	1446	6.30	1474
0.30	0.662	1799	7.41	1842
0.32	0.774	2252	8.58	2319
0.34	0.905	2835	9.79	2938
0.36	1.060	3583	11.04	3741

shock is one in which most of the shock temperature rise occurs in the conduction front. For well-overdriven shocks in solids, the theory we have developed is characterized by the following properties:

(a) Essentially all of the shock entropy is generated in the conduction front, by heat conduction.

(b) The heat is generated in the flow region, by plastic flow.

(c) For metals the shock thickness is $\Delta Z \sim 10^{-6}$ cm, the risetime is $\Delta t \sim 10^{-12}$ s.

(d) For shocks near melting on the Hugoniot, but still in the solid phase there, $T(\epsilon)$ rises above the equilibrium melting temperature for a time in the center of the shock.

Once the detailed space and time dependence of the shock process is found, it is possible to examine conditions on the validity of irreversible thermodynamics, in terms of the relaxation times and the mean free paths of electrons and phonons. The preliminary conclusion from this study, for steady-wave shocks in solid or liquid metals, is that the present theory is a valid approximation for shocks up to a definite limit and is invalid for all stronger shocks. The breakdown of irreversible thermodynamics results from the massive demand for heat transport and the consequent inability of electrons and phonons to remain near equilibrium. The limit is in the range of a few Mbar for metals.

TABLE IV. Hugoniot for Pt. Units are the following: P (Mbar), T (K), S (cal/mole K).

ϵ	P	T	$S-S_a$	T_{ion}
0	0	293	0	293
0.04	0.128	329	0.067	329
0.08	0.290	395	0.56	398
0.12	0.500	534	1.84	546
0.16	0.773	816	4.00	859
0.20	1.135	1348	6.81	1478
0.24	1.621	2282	10.03	2646
0.26	1.928	2967	11.7	3557
0.28	2.289	3839	13.5	4782
0.30	2.718	4942	15.4	6427
0.32	3.231	6327	17.3	8630

TABLE V. Elastic moduli calculated on the Hugoniot for Al, neglecting melting. Units are the following: P (Mbar), T (K), B (Mbar), G (Mbar).

P_H	T_H-T_a	B_H	B_u/B_H	G_u/B_u
0	0	0.79	0.96	0.345
0.2	207	1.55	1.04	0.37
0.4	637	2.20	1.10	0.37
0.6	1274	2.80	1.15	0.37
0.8	2072	3.37	1.18	0.36
1.2	4015	4.47	1.21	0.35
1.6	6270	5.54	1.23	0.34
2.0	8730	6.58	1.25	0.33

ACKNOWLEDGMENTS

The author appreciates helpful discussions with R. G. McQueen, B. R. Suydam, and R. A. Axford.

APPENDIX A: THE HUGONIOT

Thermodynamic functions on the Hugoniot for 2024 Al and for Pt are listed in Tables III and IV, respectively. The effect of neglecting the electronic contribution to C_V is shown by the column T_{ion}, which is computed by taking for C_V only the ion vibrational part, $3Nk$ per mole.

APPENDIX B: ELASTIC MODULI ON THE HUGONIOT

A linear expansion of B from state a ($P=0$, $T=T_a$) is

$$B = B_a + (\partial B/\partial P)_T P + (\partial B/\partial T)_P (T - T_a) ,$$

where the coefficients are to be evaluated at state a.

A similar equation may be written for G. Evaluations of these equations from ultrasonic data are denoted B_u, G_u. For single crystal Al, Thomas[15] measured variations in ultrasonic transit times due to variations in anisotropic stresses up to ~ 25 bar, variations in P up to ~ 50 bar, and variations in T of ~ 10 K. Polycrystalline averages[9] of Thomas's results give

$$B_u = 0.759 + 4.42P - 0.16(10^{-3})(T - T_a) ,$$

$$G_u = 0.262 + 1.82P - 0.14(10^{-3})(T - T_a) ,$$

in Mbar, with P in Mbar, T in K, and $T_a = 293$.

The bulk modulus computed on the Hugoniot from shock data is denoted B_H. We ignore melting and the presence of the liquid phase, and we also ignore the difference between pure Al and 2024 Al in order to compare the ultrasonic and shock results, Table V. It is seen that $B_u \approx B_H$ and $G_u/B_u \approx$ const to 2 Mbar on the Hugoniot.

[1]D. C. Wallace, preceding paper. Phys. Rev. B 24, 5597 (1981).
[2]R. G. McQueen, S. P. Marsh, J. W. Taylor, J. N. Fritz, and W. J. Carter, in *High-Velocity Impact Phenomena*, edited by R. Kinslow (Academic, New York, 1970), p. 293.
[3]L. V. Al'tshuler, N. N. Kalitkin, L. V. Kuz'mina, and B. S. Chekin, Zh. Eksp. Teor. Fiz. 72, 317 (1977) [Sov. Phys.—JETP 45, 167 (1977)].
[4]W. M. Isbell, F. H. Shipman, and A. H. Jones, Report No. MSL-68-13 (General Motors, Warren, Michigan).
[5]T. Neal, Phys. Rev. B 14, 5172 (1976).
[6]D. C. Wallace, *Thermodynamics of Crystals* (Wiley, New York, 1972).
[7]C. Kittel, *Thermal Physics* (Wiley, New York, 1969).
[8]G. K. White and J. G. Collins, J. Low-Temp. Phys. 7, 43 (1972); G. K. White, J. Phys. F 2, L30 (1972).
[9]G. Simmons and H. Wang, *Single Crystal Elastic Constants and Calculated Aggregate Properties* (MIT, Cambridge, Mass., 1971).
[10]Ya. B. Zel'dovich and Yu. P. Raizer, *Physics of Shock Waves and High-Temperature Hydrodynamic Phenomena* (Academic, New York, 1966), Vol. 1, p. 82.
[11]L. V. Al'tshuler, Usp. Fiz. Nauk 85, 197 (1965) [Sov. Phys.—Uspekhi 8, 52 (1965)].
[12]J. A. Morgan, High Temp. High Pressures 6, 195 (1974).
[13]E. A. Kraut and G. C. Kennedy, Phys. Rev. 151, 668 (1966).
[14]D. C. Wallace, Phys. Rev. 22, 1477, 1487 (1980).
[15]J. F. Thomas, Jr., Phys. Rev. 175, 955 (1968).

Erratum: In eq. (17), the second equals sign was incorrectly omitted in the original Physical Review publication.

Theory of the shock process in dense fluids

D. C. Wallace
Los Alamos Scientific Laboratory, Los Alamos, New Mexico 87545
(Received 23 November 1981)

A shock is assumed to be a steady plane wave, and irreversible thermodynamics is assumed valid. The fluid is characterized by heat conduction and by viscous or viscoelastic response, according to the strain rate. It is shown that setting the viscosity zero produces a solution which constitutes a lower bound through the shock process for the shear stress, and upper bounds for the temperature, entropy, pressure, and heat current. It is shown that there exists an upper bound to the dynamic stresses which can be achieved during shock compression, that this bound corresponds to a purely elastic response of the fluid, and that solution for the shock process along this bound constitutes lower bounds for the temperature and entropy. It is shown that a continuous steady shock is possible only if the heat current is positive and the temperature is an increasing function of compression almost everywhere. In his theory of shocks in gases, Rayleigh showed that there is a maximum shock strength for which a continuous steady solution can exist with heat conduction but without viscosity. Two more limits are shown to exist for dense fluids, based on the fluid response in the leading edge of the shock: for shocks at the overdriven threshold and above, no solution is possible without heat transport; for shocks near the viscous fluid limit and above, viscous fluid theory is not valid, and the fluid response in the leading edge of the shock is approximately that of a nonplastic solid. The viscous fluid limit is estimated to be 13 kbar for water and 690 kbar for mercury.

I. INTRODUCTION

The nature of the shock process in a viscous heat-conducting gas was clarified in detail by Rayleigh in 1910.[1] He examined the conditions under which a compressive shock can propagate as a continuous steady wave. When the gas has heat conduction but no viscosity, this is possible only for weak shocks, with shock compression $\lesssim 1.4$. With viscosity but no heat conduction, the continuous steady wave is always possible, and the same is presumably true with both viscosity and heat conduction.

For dense fluids, say with density $\gtrsim 1$ g/cm^3, there are two main differences from a gas: (a) thermodynamic characteristics are markedly different, and (b) at sufficiently high frequencies a dense fluid exhibits elastic solidlike response. When these properties are taken into account, we discover that the nature of shocks in dense fluids is quite different from that in gases.

In the present paper we examine the consequences of an irreversible-thermodynamic theory of shocks in dense fluids. The theory considers simple fluids, characterized by viscous and viscoelastic responses at the appropriate frequencies, and by heat conduction. We neglect ionization, radiation, chemical reactions, and any *other* degrees of freedom which might be excited by the shock; such topics are treated in detail for gases by Zel'dovich and Raizer.[2]

The question arises as to whether or not irreversible thermodynamics is valid, i.e., whether or not the temperature and other thermodynamic functions can be defined through the shock process. One might expect that thermodynamics is valid for shocks up to some critical strength, and not valid for stronger shocks. In a recent study of Lennard-Jones systems, Hoover[3] has shown that Navier-Stokes theory agrees with molecular-dynamics calculations for shocks of approximately 12 and 30 kbar in liquid Ar. Holian and coworkers[4] have further shown that for a shock of 400 kbar in liquid Ar, just below the strength of shock which ionizes the Ar, Navier-Stokes still provides a qualitatively correct representation of the process but gives a slightly narrower shock profile than does molecular dynamics. The molecular-dynamics technique is promising because it can in principle treat problems where irreversible thermodynamics fails. In the present paper, we simply assume irreversible thermodynamics is valid because there are still some new results which can be learned from this theory.

II. VISCOUS FLUID SHOCKS

A. Viscous fluid theory

We summarize the irreversible-thermodynamic flow theory for a compressible viscous heat-conducting fluid. The complete system of equations is organized into three subsets: continuum mechanics, the viscous stress, and thermodynamics.

Location in the laboratory reference frame is $\vec{x}$, and the Lagrangian coordinate of an infinitesimal mass element of the fluid is $\vec{X}$. The fluid velocity is $\vec{v}$, the density is ρ, the stress tensor is $\tau_{ij}=\tau_{ji}$, subscripts $i,j,\ldots$ are Cartesian indices and repeated indices are to be summed. The continuum-mechanic conservation equations are[5]

Conservation of mass:

$$\left.\frac{\partial \rho}{\partial t}\right|_{\vec{X}} = -\rho \left.\frac{\partial v_i}{\partial x_i}\right|_t . \tag{1}$$

Conservation of linear momentum:

$$\rho \left.\frac{\partial v_j}{\partial t}\right|_{\vec{X}} = \left.\frac{\partial \tau_{ij}}{\partial x_i}\right|_t . \tag{2}$$

To write conservation of energy we define the velocity gradients v_{ij} and their symmetric parts $\dot{\epsilon}_{ij}$:

$$v_{ij} = \left|\frac{\partial v_i}{\partial x_j}\right|_t , \tag{3a}$$

$$\dot{\epsilon}_{ij} = \tfrac{1}{2}(v_{ij}+v_{ji}) . \tag{3b}$$

The rate at which work is done by the stresses on a unit mass of fluid is

$$\dot{W} = \rho^{-1}\tau_{ij}\dot{\epsilon}_{ij} , \tag{4}$$

and the rate at which heat flows into a unit mass of fluid is $\dot{Q}$. Then subtracting out the translational kinetic energy of the fluid leaves only the center-of-mass energy U per unit mass, and there results[5]

Conservation of energy:

$$\dot{U} = \dot{W} + \dot{Q} . \tag{5}$$

The total stress tensor is

$$\tau_{ij} = -P\delta_{ij} + \tau^{v}_{ij} , \tag{6}$$

where P is the pressure, determined by equilibrium thermodynamics, and τ^{v}_{ij} is the viscous stress, presumed to be linear in velocity gradients[6]:

$$\tau^{v}_{ij} = 2\eta_s\dot{\epsilon}_{ij} + (\eta_v - \tfrac{2}{3}\eta_s)\dot{\epsilon}_{ll}\delta_{ij} . \tag{7}$$

The shear and bulk viscosities, η_s and η_v, respectively, are functions only of the thermodynamic state and are non-negative. From conservation of mass, the sum $\dot{\epsilon}_{ll}$ is given by

$$\dot{\epsilon}_{ll} = -\dot{\rho}/\rho = \dot{V}/V , \tag{8}$$

where $V=\rho^{-1}$ is the volume per unit mass. While the conservation equations are valid for any dissipative continuum flow, including plastic flow in a solid[7] or viscoelastic flow (Sec. III below), the stress (6) represents specifically a viscous fluid, and the combination of (6) and (2) is the Navier-Stokes equation.

To complete the system of equations we assume the variables U,V,S,P,T are related by equilibrium thermodynamic relations, where S is entropy per unit mass and T is temperature. There are different (but equivalent) ways to proceed. One can take V,U as independent state variables, eliminate S from the system, and determine P and T from the equations of state, which are formally $P=P(V,U)$ and $T=T(V,U)$. Or one can take V,S as independent state variables and generate a hierarchy of differential equations as follows.

Zeroth order:

$$dU = -P\,dV + T\,dS . \tag{9}$$

First order:

$$dP = -\rho B\,dV + \rho\gamma T\,dS , \tag{10}$$

$$dT = -\rho\gamma T\,dV + C_V^{-1}T\,dS , \tag{11}$$

where B is the adiabatic bulk modulus, γ is the Grüneisen parameter, and C_V is the heat capacity at constant volume. We generally break the hierarchy at this point by assuming the second-order coefficients B,γ,C_V are known functions of V,S. We also eliminate U by combining (5) and (9) to give

$$T\,dS = dQ + dW^{v} , \tag{12}$$

where

$$dW^{v} = V\tau^{v}_{ij}d\epsilon_{ij} . \tag{13}$$

Hence the work done by the viscous stress is entirely dissipated.

The heat flux $\vec{J}$ is assumed to be given by the steady conduction equation, $\vec{J} = -\kappa\vec{\nabla}T$, where κ is the thermal conductivity, with $\kappa=\kappa(V,S)$ and $\kappa>0$. It is convenient to eliminate Q in favor of $\vec{J}$ by the relation $\rho\dot{Q} = -\vec{\nabla}\cdot\vec{J}$.

B. Rayleigh-line equations

The shock is a plane wave traveling in the x direction, fluid mass elements are planar slabs normal to the x direction, and edge effects are neglected. Quantities in the initial state (before the shock) are denoted by subscript a, the initial time is $t_a = -\infty$, and the compression from the initial state is measured by ϵ:

$$\epsilon = 1 - V/V_a \ . \tag{14}$$

In the following, ε, V, and ρ are used interchangeably as a single independent variable. Compressive stresses in the normal and transverse directions are, respectively, σ and $\sigma - 2\tau$, so the shear stress is τ. The stress equations (6) and (7) simplify to

$$\sigma = P + \tfrac{4}{3}\alpha\tau \ , \tag{15}$$

$$\tau = -\eta_s(\dot{V}/V) \ , \tag{16}$$

where

$$\tfrac{4}{3}\alpha = \tfrac{4}{3} + \frac{\eta_v}{\eta_s} \ . \tag{17}$$

The shock is assumed to be a steady wave with velocity D. Any fluid property $F(x,t)$ within the shock is a function only of the variable z:

$$\begin{aligned} z &= x - Dt \ , \\ F(x,t) &= F(z) \ . \end{aligned} \tag{18}$$

The steady-wave condition allows partial derivatives to be transformed to total derivatives. The heat flux lies in the x direction and is

$$J = -\kappa \frac{dT}{dz} \ , \tag{19}$$

while the Lagrangian time derivative $\dot{V}/V$ becomes

$$\frac{1}{V}\left|\frac{\partial V}{\partial t}\right|_X = D\frac{d\epsilon}{dz} \ . \tag{20}$$

Then the shear stress (16) may be written

$$\tau = \frac{\eta_s DJ}{\kappa(dT/d\epsilon)} \ . \tag{21}$$

With the steady-wave condition, the conservation equations can be integrated along the shock process. The initial conditions are that the fluid ahead of the shock has zero stress, zero velocity, and is in thermodynamic equilibrium. Thermodynamic equilibrium requires $\dot{V}/V = J = 0$, so the initial conditions can be written

$$\sigma_a = \tau_a = v_a = J_a = 0 \ . \tag{22}$$

First integrals of conservation of mass and momentum give the equations $\epsilon = v/D$ and $\sigma = \rho_a D v$, respectively. Hence the Rayleigh line, which is the $\sigma(\epsilon)$ relation, is

$$\sigma = \rho_a D^2 \epsilon \ . \tag{23}$$

This and five more coupled equations describe the shock process for the case of V,S variables; they are (12) for the entropy production, which becomes

$$T\,dS = dJ/\rho_a D + \tfrac{4}{3}\alpha\tau V_a d\epsilon \ , \tag{24}$$

the thermodynamic equations (10) and (11), and the stresses (15) and (21). We call this set the Rayleigh-line equations. They are six equations in the six variables σ,P,τ,T,S,J and they can be solved in principle for these variables as functions of ϵ. From this solution, the space and time dependence of the process can be computed with (19). The final state of the shock is the Hugoniot state, denoted by subscript H. This is also a thermodynamic equilibrium state, so the final conditions are

$$(\dot{V}/V)_H = J_H = 0 \ . \tag{25}$$

The Hugoniot state is presumed known as a function of D.

C. Family of partial solutions

Consider a viscous heat-conducting fluid, with given values of the thermodynamic coefficients $B,\gamma,C_V,\alpha,\eta_s/\kappa$ as functions of V,S and a given shock velocity D, with corresponding value of ϵ_H. There is presumably a unique solution of the Rayleigh-line equations, for which the six variables σ,P,τ,T,S,J are continuous functions of ϵ, $0 \le \epsilon \le \epsilon_H$, and for which the initial and final conditions are satisfied Consider the subset of equations obtained by omitting (21) for τ. This subset is five equations in the same six variables, and the subset does not contain the coefficient η_s/κ. Any solution of this subset for which σ,P,τ,T,S,J are continuous functions of ϵ, $0 \le \epsilon \le \epsilon_H$, and for which the initial and final conditions are satisfied, is called a partial solution. The family of partial solutions is infinite. It is a one-variable family because if one of the six variables is specified on $0 \le \epsilon \le \epsilon_H$, the subset of equations can be solved for the remaining five variables, and the solution is unique. The family can be viewed as solutions for a family of fluids, each fluid having the given values of B,γ,C_V,α as functions of V,S and having its own characteristic η_s/κ as a function of V,S.

Among the family of partial solutions, some are unacceptable on physical grounds, as will be shown below. This will allow us to find bounds for the correct solution for the shock process, independent of the coefficient η_s/κ.

For illustration, take $T(\epsilon)$ as the generating variable for partial solutions. For any prescribed $T(\epsilon)$ continuous on $0\le\epsilon\le\epsilon_H$, and taking on the values T_a at $\epsilon=0$ and T_H at ϵ_H, there corresponds a unique partial solution. From one partial solution, to generate another one infinitesimally removed, we add to $T(\epsilon)$ the infinitesimal variaton $\delta T(\epsilon)$, which is continuous on $0\le\epsilon\le\epsilon_H$, and which vanishes at $\epsilon=0$ and at ϵ_H. Continuing in this way, all partial solutions can be generated from one initial partial solution. From the defining subset of Rayleigh-line equations, relations can be found among the variations $\delta T(\epsilon)$, $\delta S(\epsilon)$, and so on, at a fixed ϵ. These relations are

$$\delta\sigma(\epsilon)=0\,, \tag{26a}$$

$$\delta S(\epsilon)=(C_V/T)\delta T(\epsilon)\,, \tag{26b}$$

$$\delta J(\epsilon)=\rho_a D C_V\delta T(\epsilon)\,, \tag{26c}$$

$$\delta P(\epsilon)=\rho\gamma C_V\delta T(\epsilon)\,, \tag{26d}$$

$$\tfrac{4}{3}\delta(\alpha\tau(\epsilon))=-\delta P(\epsilon)\,. \tag{26e}$$

Now $\rho\gamma>0, C_V>0, D>0$, so $\delta S(\epsilon)$, $\delta J(\epsilon)$, and $\delta P(\epsilon)$ are everywhere of the same sign as $\delta T(\epsilon)$, and $\delta(\alpha\tau)$ is everywhere of the opposite sign.

The shear stress cannot be negative during shock compression, hence $\tau=0$ is a lower bound for physically acceptable values of $\tau(\epsilon)$ on the Rayleigh line. Since the constant $\tau(\epsilon)=0$ is continuous in ϵ and takes on the correct initial and final values for a fluid, this condition defines a partial solution. Since $\alpha>0$ for a viscous fluid, the $\tau=0$ partial solution is also a lower bound for $\alpha\tau$ on the Rayleigh line; hence from the variational relations (26b)–(26e), the $\tau=0$ partial solution constitutes upper bounds for $T(\epsilon)$, $S(\epsilon)$, $P(\epsilon)$, and $J(\epsilon)$.

In the subset of Rayleigh-line equations which defines partial solutions, if one sets $\tau=0$, one has five equations in the five variables σ,P,T,S,J. These are precisely the Rayleigh-line equations for an inviscid heat-conducting fluid, which is a fluid with the properties $\eta_s=\eta_v=0$ and $\alpha=$ finite, $\kappa>0$. The properties of the $\tau=0$ partial solution are summarized in the following theorem.

Theorem 1. For a viscous heat-conducting fluid, the $\tau=0$ partial solution represents the same fluid made inviscid, and the $\tau=0$ partial solution gives a lower bound for $\tau(\epsilon)$, and upper bounds for $T(\epsilon),S(\epsilon),P(\epsilon),J(\epsilon)$, on $0\le\epsilon\le\epsilon_H$.

D. Solutions continuous in space and time

In a continuous steady wave, the material state must be a continuous single-valued function of space and time, or equivalently of z, and the inverse function must also be continuous and single valued. The Rayleigh-line equations ensure that the material state is continuous and single valued in ϵ, and ϵ is continuous and single valued in the material state. Hence we require $\epsilon(z)$ and $z(\epsilon)$ to be continuous and single valued. Since ϵ increases in the shock, as z decreases, then ϵ must be a nonincreasing function of z:

$$-\infty\le\frac{d\epsilon}{dz}\le 0\,, \tag{27}$$

where either equality can hold on a finite number of points at most. In fact, for a viscous fluid we can rule out the possibility $d\epsilon/dz=-\infty$, because by (16) and (20) this makes τ infinite.

With finite D, the variables σ,P,τ,T,S,J, and their first derivatives with respect to ϵ, are finite on $0\le\epsilon\le\epsilon_H$. From (24) and (11) it follows

$$\frac{dJ}{d\epsilon}<0 \text{ if } \frac{dT}{d\epsilon}\le 0\,. \tag{28}$$

The heat-conduction equation (19) can be written

$$J=-\kappa\frac{dT}{d\epsilon}\frac{d\epsilon}{dz}\,. \tag{29}$$

Equations (27) and (29) require that J and $dT/d\epsilon$ must have the same sign, except possibly on a finite number of points. This result, together with (28) and the final condition $J(\epsilon_H)=0$, rules out the possibility $dT/d\epsilon\le 0$, except possibly on a finite number of points. Hence we have the following theorem.

Theorem 2a. For a viscous heat-conducting fluid, a continuous steady-wave shock is possible only under the conditions $J\ge 0, dT/d\epsilon\ge 0$, on $0\le\epsilon\le\epsilon_H$, where either equality can hold on a finite number of points at most.

The above argument was used by Rayleigh[1] to show that for shocks beyond a certain strength, a continuous steady-wave solution is not possible for an inviscid heat-conducting gas.

III. VISCOELASTICITY

An important physical property of viscous fluid response is that, at least under some conditions of flow, including shock compression, viscous flow is a relaxation process, which can only act to reduce the stress that drives it. At sufficiently high strain rates, there is not time for significant relaxation to take place; under this condition the stresses are supported by elastic forces, and are strain-rate independent. Thus, viscous stresses cannot rise arbitrarily high. In order to include this behavior, approximately, in the theory of shocks in dense fluids, we will construct Rayleigh-line equations for steady-wave shocks in a viscoelastic fluid.

A. Viscoelastic stress (Ref. 8)

In the low-frequency (low strain rate) region, a viscoelastic fluid is characterized by the adiabatic bulk modulus $B_0 = B$, the shear modulus $G_0 = 0$, and ordinary viscous stresses are supported by velocity gradients, with shear and bulk viscosities η_s and η_v, respectively. At high frequencies (high strain rates), the fluid exhibits adiabatic bulk modulus $B_\infty > B_0$, adiabatic shear modulus $G_\infty > 0$, and stresses are supported elastically. Crossover between the two types of response occurs at strain rates around t_s^{-1} or t_v^{-1}, where t_s and t_v are, respectively, the shear and bulk relaxation times and are defined by[8]

$$\eta_s = t_s G_\infty \ , \tag{30}$$

$$\eta_v = t_v (B_\infty - B_0) \ . \tag{31}$$

Litovitz and Davis[8] find many fluids satisfy the approximate relations, including temperature dependence,

$$t_v \approx t_s \ . \tag{32}$$

$$B_\infty - B_0 \approx \tfrac{4}{3} G_\infty \ . \tag{33}$$

These relations imply η_v/η_s is approximately temperature independent. An estimate which we might expect to hold crudely for monatomic fluids, e.g., liquid metals, at arbitrary temperatures and pressures is $t_s \approx t_v \approx$ one atomic vibration time.

The viscoelastic stress tensor is

$$\tau_{ij} = -P\delta_{ij} + \tau_{ij}^{\bullet} \ . \tag{34}$$

Here P is the pressure, determined by equilibrium thermodynamics, and $\tau_{ij}^{\bullet}$ is the dynamic stress, which vanishes at equilibrium and is determined by the constitutive equation

$$\tau_{ij}^{\bullet} + t_s \dot{\tau}_{ij}^{\bullet} + \tfrac{1}{3}(t_v - t_s)\dot{\tau}_{ll}^{\bullet}\delta_{ij} = 2\eta_s \dot{\epsilon}_{ij} + (\eta_v - \tfrac{2}{3}\eta_s)\dot{\epsilon}_{ll}\delta_{ij} \ . \tag{35}$$

Under appropriate conditions, this equation can reduce to the ordinary viscous stress, or to an elastic stress-strain relation, or it can display stress-relaxation behavior, or strain-relaxation behavior. The equation for P is

$$dP = -B_0 d\ln V + \rho\gamma T\, dS \ , \tag{36}$$

the same as (10) because B_0 here is the same as the viscous fluid B. Note (36) has no rate dependence, which means P is always instantaneously in equilibrium with elastic and thermal forces. This approximation will fail at sufficiently high strain rates, where irreversible thermodynamics fails.

B. Plane-wave geometry

For uniaxial motion in a viscoelastic fluid, there are two independent components of the dynamic stress tensor, namely, the shear stress τ and the dynamic pressure $P^{\bullet}$, where

$$P^{\bullet} = -\tfrac{1}{3}\tau_{ll}^{\bullet} \ . \tag{37}$$

The constitutive equation for each component is obtained from (35):

$$\tau + t_s \dot{\tau} = -\eta_s (\dot{V}/V) \ , \tag{38}$$

$$P^{\bullet} + t_v \dot{P}^{\bullet} = -\eta_v (\dot{V}/V) \ . \tag{39}$$

The normal stress is

$$\sigma = P + P^{\bullet} + \tfrac{4}{3}\tau \ . \tag{40}$$

Let us examine the viscoelastic stresses in plane-wave geometry under limiting conditions of slow and fast response. For slow response we have

Viscous response limit:

$$t_s \dot{\tau} << \tau \ , \quad t_v \dot{P}^{\bullet} << P^{\bullet} \ . \tag{41}$$

With these conditions, Eqs. (38) and (40) are reduced to the viscous fluid stresses. Eqs. (16) and (15), respectively. In the opposite extreme we have

Elastic response limit:

$$\tau << t_s \dot{\tau} \ , \quad P^{\bullet} << t_v \dot{P}^{\bullet} \ . \tag{42}$$

With these conditions, $\dot{\tau}$ and $\dot{P}^{\bullet}$ become proportional to $\dot{V}/V$. We write the relations as differentials for $d\tau$ and $dP^{\bullet}$ and include (40) and (36) to express $d\sigma$ as well:

$$d\tau = -G_\infty d\ln V , \tag{43}$$

$$dP^* = -(B_\infty - B_0) d\ln V , \tag{44}$$

$$d\sigma = -(B_\infty + \tfrac{4}{3}G_\infty) d\ln V + \rho\gamma T\, dS . \tag{45}$$

The expressions for $d\tau$ and $d\sigma$ are the same as for an elastic solid with infinite yield strength (a nonplastic solid), when for the solid the thermoelastic coefficients $B_{\alpha\beta}$ and γ_β are evaluated to lowest order in the small-anisotropy expansion, and B,G are then replaced by B_∞, G_∞.[9] The variable P^* does not appear in elastic-solid theory.

C. Rayleigh-line equations

The dynamic stress is linear in variables which measure the departure from the fluid equilibrium state; in the viscous regime it is linear in strain rates and in the elastic regime it is linear in strains. Nonlinear effects are not included. In uniaxial motion, the viscoelastic fluid has elastic tetragonal symmetry and the elastic anisotropy is measured by the small quantity τ/G_∞. The small-anisotropy expansion for a solid consists of expanding the thermoelastic coefficients in powers of τ/G_∞; the corresponding expansion for a viscoelastic fluid is in powers of both τ and P^*. Consistent with the neglect of nonlinear effects in the dynamic stress, we evaluate the transport coefficients and the second-order thermoelastic coefficients at $\tau = P^* = 0$. This reduces all the adiabatic stress-strain coefficients to combinations of B_∞, G_∞, as in (43)–(45), reduces the anisotropic γ_β to γ as in (36), and allows us to use the fluid equation (11) for dT.

Another point should be mentioned. If there is an elastic precursor in a viscoelastic fluid, it will travel at (or near) the longitudinal sound velocity c_l given by

$$\rho c_l^2 = B_\infty + \tfrac{4}{3}G_\infty .$$

For shocks with $D < c_l$ the present theory, by assuming a steady wave, neglects the elastic precursor. To include precursor effects, the theory has to be generalized along the lines of the theory of weak shocks in solids.[10]

We continue under the assumption that the shock is a steady wave. For the viscoelastic Rayleigh-line equations we list seven equations in the seven variables $\sigma, P, P^*, \tau, T, S, J$, although some of the equations can be easily combined with the elimination of variables. The Rayleigh line, Eq. (23), remains the same. The entropy production is

$$T\, dS = \frac{dJ}{\rho_a D} + dW^* , \tag{46}$$

where dW^* is the work dissipated. dW^* is complicated because in a given time increment only part of the work done by the dynamic stresses τ and P^* is dissipated, and the rest is stored elastically and dissipated later. However, an important property can be observed:

$$dW^* \geq 0 . \tag{47}$$

There are four equations in P, τ, P^*, σ, namely, Eqs. (36) and (38)–(40), and the last equation is (11) for dT.

Just as in the viscous fluid case, we can define the family of partial solutions for a viscoelastic fluid. These are solutions of the viscoelastic Rayleigh-line equations with (38) and (39) omitted; the remaining subset is five equations in the six variables $\sigma, P, P^* + \frac{4}{3}\tau, T, S, J$. Given one variable, say $T(\epsilon)$, continuous on $0 \leq \epsilon \leq \epsilon_H$ and taking on the correct values T_a at $\epsilon = 0$ and T_H at ϵ_H, the equations can be solved for the remaining five variables, giving a partial solution. A new partial solution is generated by the infinitesimal variation $\delta T(\epsilon)$, continuous on $0 \leq \epsilon \leq \epsilon_H$ and vanishing at $\epsilon = 0$ and at ϵ_H. Corresponding to $\delta T(\epsilon)$ are the variations $\delta S(\epsilon)$ given by (26b), $\delta P(\epsilon)$ given by (26d), and

$$\delta P^*(\epsilon) + \tfrac{4}{3}\delta\tau(\epsilon) = -\delta P(\epsilon) . \tag{48}$$

Hence $\delta S(\epsilon)$ and $\delta P(\epsilon)$ are everywhere of the same sign as $\delta T(\epsilon)$, and $\delta(P^* + \frac{4}{3}\tau)$ is everywhere of the opposite sign. In the absence of a more detailed specification of dW^*, we are not able to determine the relative sign of the variation $\delta J(\epsilon)$.

Consider Theorem 2a proved for a viscous heat-conducting fluid. We still have (27) and (29) for a viscoelastic heat-conducting fluid, and (28) holds because dW^* is non-negative, so the proof goes through as before.

Theorem 2b. For a viscoelastic heat-conducting fluid, a continuous steady-wave shock is possible only under the conditions $J \geq 0, dT/d\epsilon \geq 0$, on $0 \leq \epsilon \leq \epsilon_H$, where either equality can hold on a finite number of points at most.

D. The elastic bound

During shock compression of a viscoelastic fluid, the dynamic stresses must be non-negative; also because of (20) and (27), $\dot{V}/V$ is nonpositive:

$$\tau \geq 0, \quad P^* \geq 0 .$$
$$\dot{V}/V \leq 0 . \tag{49}$$

With these conditions it is possible to show that there are upper bounds for τ and P^* during shock compression. Rewrite (38) in the form

$$\tau + t_r[\dot{\tau} + G_\infty(\dot{V}/V)] = 0 . \tag{50}$$

$\dot{\tau}$ can be positive or negative. If $|\dot{\tau}| << G_\infty |\dot{V}/V|$ we have viscous fluid behavior, and we also have $|d\tau| << G_\infty |d \ln V|$, which means $d\tau$ is small. On the other hand, for (50) to have a solution with $\tau \geq 0$, we must have $\dot{\tau} \leq -G_\infty(\dot{V}/V)$. Hence $-G_\infty d \ln V$ is always an upper bound for $d\tau$ during shock compression. Note that as long as $\tau > 0$, $d\tau$ never reaches this upper bound. Also, (39) can be written

$$P^* + t_r[\dot{P}^* + (B_\infty - B_0)(\dot{V}/V)] = 0 . \tag{51}$$

It follows that $-(B_\infty - B_0)d \ln V$ is always an upper bound for dP^* during shock compression, and as long as $P^* > 0$, dP^* never reaches this upper bound. These upper bounds are just the expressions (43) and (44) for $d\tau$ and dP^* in the elastic-response limit.

As noted above, the entropy generation during viscoelastic flow is complicated in general. However, in the elastic response limit there is not time for viscous flow to occur, so there is no viscous dissipation; $dW^* = 0$, and the entropy generation is

$$TdS = \frac{dJ}{\rho_0 D} . \tag{52}$$

We make the following definition.

Definition. The elastic bound is the solution of the Rayleigh-line equations for a viscoelastic fluid in the elastic-response limit.

This set of equations reduces to six equations in the six variables $\sigma, \tau, P^*, T, S, J$. The equations are (23) for the Rayleigh line, (52) for TdS, (43)–(45) for $d\tau, dP^*, d\sigma$, and (11) for dT. Since the solution gives upper bounds for $\tau(\epsilon)$ and $P^*(\epsilon)$, it gives lower bounds for $T(\epsilon)$ and $S(\epsilon)$. Omitting the equation for dP^*, the remaining five equations are the same as the Rayleigh-line equations for a nonplastic solid,[9] evaluated to lowest order in the small-anisotropy expansion and with B, G replaced by the high-frequency moduli B_∞, G_∞. The results are summarized as follows.

Theorem 3. For a viscoelastic heat-conducting fluid, the elastic bound is an upper bound for $\tau(\epsilon)$ and $P^*(\epsilon)$ and a lower bound for $T(\epsilon)$ and $S(\epsilon)$, and the elastic bound represents a nonplastic solid in lowest order in the small-anisotropy expansion with B, G given by B_∞, G_∞.

It should be noted that the elastic bound cannot constitute a partial solution of the Rayleigh-line equations because it does not reach the correct Hugoniot state at ϵ_H. In other words, the nonplastic solid does not possess a steady-wave shock solution.[9] However, just as in the theory for solids, we will be interested in the elastic bound only in the initial part of the shock, up to the point where the $T(\epsilon)$ curve has a maximum.

E. Bounds for fluid shocks

A real fluid will display viscous response when the strain rates are not too high. Under this condition we refer to the fluid as a *viscous fluid*, and use the *viscous fluid theory* of Sec. II. At sufficiently high strain rates, a real fluid will display approximately elastic response. When it is necessary to include this behavior we work with a *viscoelastic fluid*, as represented by the theory of this section. An important property of viscoelastic fluid theory is that it establishes a limit on the range of validity of viscous fluid theory, at least in the treatment of the shock process. This follows from the existence and properties of the elastic bound. Denote by $\tau_E(\epsilon)$ the elastic-bound shear stress. Now suppose we solve the viscous fluid Rayleigh-line equations, and find T, S, τ, and so on. We then know that, viscous-fluid theory is valid when $\tau(\epsilon) << \tau_E(\epsilon)$, or strictly when $\dot{\tau} << \dot{\tau}_E$; that viscous-fluid theory is in error when $\tau(\epsilon)$ is near $\tau_E(\epsilon)$; and that viscous-fluid theory is strictly invalid if it gives $\tau(\epsilon) \geq \tau_E(\epsilon)$.

It is possible to construct curves of the thermodynamic variables which are bounds for physically acceptable fluid shock solutions. We construct in particular the bounds for $T(\epsilon)$; curves representative of a Mbar shock in a liquid metal are shown in Fig. 1. The lower bound is the elastic bound for $0 \leq \epsilon \leq \epsilon_d$, where the elastic-bound $T(\epsilon)$ curve has a maximum at ϵ_d. Since $T(\epsilon)$ is a nondecreasing function of ϵ, according to Theorem 2b, a lower bound in the region $\epsilon > \epsilon_d$ is T_d. For ϵ well beyond ϵ_d, $T(\epsilon)$ has to be much higher, and $\tau(\epsilon)$ has to be much lower than the corresponding values on the elastic bound; we therefore must have viscous-fluid behavior in the final part of the shock. A viscous fluid partial solution is defined by $J(\epsilon) = 0$. From Theorem 2a, $J(\epsilon)$ is nonnegative, so from the ordering of the viscous fluid family of partial solutions, the temperature corre-

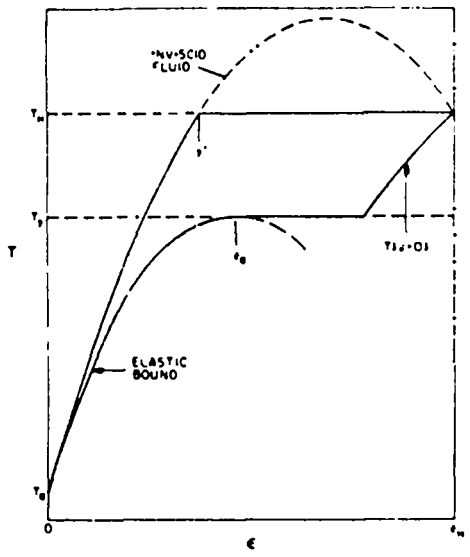

FIG. 1. Solid lines show upper and lower bounds for $T(\epsilon)$ through the shock process. Shape of the curves represents qualitatively a 1-Mbar shock in a liquid metal.

sponding to $J(\epsilon)=0$, denoted by $T(J=0)$, is a viscous fluid lower bound. As shown in Fig. 1, $T(J=0)$ lies above T_d in the last part of the shock, and passes through T_H and ϵ_H.

From Theorem 1, the solution for an inviscid heat-conducting fluid gives an upper bound for $T(\epsilon)$. This solution has the following properties, as shown by Rayleigh[1] for gases: for sufficiently weak shocks, $T(\epsilon)\leq T_H$ on $0\leq\epsilon\leq\epsilon_H$; for shocks stronger than some limit, $T(\epsilon)$ passes above T_H at some $\epsilon'<\epsilon_H$. The latter case is shown in Fig. 1. For dense fluids, the inviscid solution has $T(\epsilon)\leq T_H$ only for very weak shocks, as shown in Sec. IV A below. The complete upper bound for $T(\epsilon)$ is the inviscid fluid curve for $0\leq\epsilon\leq\epsilon'$, and T_H for $\epsilon>\epsilon'$, as shown by the solid line in Fig. 1.

IV. BEHAVIOR AT SMALL ϵ

Much information can be obtained by studying the Rayleigh-line equations in the small-ϵ region. The results will apply to weak shocks, where ϵ_H is small, and also to the leading edge of arbitrarily strong shocks. We write the shock-velocity–particle-velocity relation as

$$D=c+s_1v_H+\tfrac{1}{2}s_2v_H^2+\cdots, \tag{53}$$

where c,s_1,s_2 are experimentally determined quantities. This can be converted to the following expansion in ϵ_H:

$$D=c[1+s_1\epsilon_H+(s_1^2+\tfrac{1}{2}cs_2)\epsilon_H^2+\cdots]. \tag{54}$$

Relations which hold at state a, for fluids, are

$$B_a=\rho_a c^2, \tag{55}$$

$$\left(\frac{\partial\ln B}{\partial\ln V}\right)_S=1-4s_1. \tag{56}$$

Formal expansions of the thermodynamic variables on the Rayleigh line are

$$T=T_a+T_1\epsilon+\tfrac{1}{2}T_2\epsilon^2+\cdots, \tag{57a}$$

$$S=S_a+S_1\epsilon+\tfrac{1}{2}S_2\epsilon^2+\cdots, \tag{57b}$$

$$J=J_1\epsilon+\cdots, \tag{57c}$$

$$\tau=\tau_1\epsilon+\cdots. \tag{57d}$$

From (43), τ_1 on the elastic bound is

$$\tau_1=G_{\infty a}, \tag{58}$$

and this is an upper bound for τ_1.

A. Inviscid fluid

Definition. The inviscid limit is the maximum shock strength for which a continuous steady-wave solution is possible for a fluid with heat conduction but without viscosity.

The inviscid limit was shown to exist by Rayleigh,[1] who calculated it numerically for gases. For dense fluids, the inviscid limit corresponds to very weak shocks and so it can be estimated analytically. For the $\tau=0$ partial solution, which represents an inviscid fluid, the Rayleigh-line equations can be solved for dT to give

$$dT=[\rho\gamma V_aT+(\rho\gamma C_V)^{-1}(\rho_aD^2-\rho V_aB)]d\epsilon. \tag{59}$$

The procedure is to expand the right side in powers of ϵ and ϵ_H, then find the coefficients $T_1,T_2\ldots$ of (57a), each coefficient as a power series in ϵ_H.

The quantity $\rho_aD^2-\rho V_aB$ is of first order in ϵ,ϵ_H. From this together with (11) it follows that $S-S_a$ is of second order in ϵ,ϵ_H. Hence in expansions of thermodynamic coefficients on the Rayleigh line, the entropy change does not contribute in first order. We have the general expansion

$$B(V,S)=B_a+(V-V_a)\left(\frac{\partial B}{\partial V}\right)_S+(S-S_a)\left(\frac{\partial B}{\partial S}\right)_V+\cdots.$$

On the Rayleigh line for an inviscid fluid this becomes

$$B(\epsilon)=B_a[1+(4s_1-1)\epsilon+\cdots]\,. \tag{60}$$

In the same way,

$$\rho\gamma=\rho_a\gamma_a(1+\zeta\epsilon+\cdots)\,, \tag{61}$$

where $\zeta=-(\partial\ln\rho\gamma/\partial\ln V)_S$ is evaluated at state a. Magnitudes of the various parameters for dense fluids are commonly

$$\gamma_a\sim s_1\sim cs_2\sim\zeta\sim 1\,. \tag{62}$$

The natural small parameter of the theory is

$$\xi=\frac{\gamma_a^2 T_a C_{Va}}{c^2}<<1\,. \tag{63}$$

The range of interest for the inviscid fluid is $\epsilon_H<\xi$, and in this range the following magnitudes hold:

$$\begin{aligned} &T_1\sim T_a\,,\\ &\epsilon_H T_2\lesssim T_1\,,\\ &T_3\sim T_2\,. \end{aligned} \tag{64}$$

From these results it follows that expansion of (59) to first order in ϵ,ϵ_H is sufficient to find the inviscid limit to the leading order in ϵ_H.

A continuous steady-wave solution requires $dT/d\epsilon\geq 0$ for $0\leq\epsilon\leq\epsilon_H$. For a fixed D, hence fixed ϵ_H, we find $dT/d\epsilon>0$ at $\epsilon=0$, and $dT/d\epsilon$ decreases as ϵ increases, and so is minimum at ϵ_H. For variable ϵ_H, $dT/d\epsilon\,|_H>0$ at $\epsilon_H=0$, and decreases as ϵ_H increases. Hence a continuous steady-wave solution is possible for $\epsilon_H\leq\epsilon_I$, and is not possible for $\epsilon_H>\epsilon_I$, where $dT/d\epsilon\,|_H=0$ at $\epsilon_H=\epsilon_I$. The inviscid-limit shock pressure, corresponding to ϵ_I, is P_I. To lowest order the solution is

$$\epsilon_I=\frac{\xi}{2s_1-(\gamma_a+\zeta)\xi}=\frac{\xi}{2s_1}+\cdots\,, \tag{65}$$

$$P_I=\rho_a D^2\epsilon_I=\rho_a c^2\epsilon_I+\cdots\,. \tag{66}$$

B. Fluid without heat transport

The shock strength is now arbitrary; the only expansion parameter is ϵ. The condition of no heat transport is $J=0$. We consider first a viscous fluid and use (24) to show that $S-S_a$ is of order ϵ^2. Then eliminating σ from Eqs. (15), (23), and (10) gives the following condition in leading order:

$$\rho_a D^2=B_a+\tfrac{4}{3}\alpha_a\tau_1\,. \tag{67}$$

Thus for a viscous fluid, τ_1 must increase as D increases. But there is an upper bound for τ_1, given by (58), so (67) implies

$$\rho_a D^2<B_a+\tfrac{4}{3}\alpha_a G_{\infty a}\,. \tag{68}$$

These results of viscous fluid theory are summarized in a definition and a theorem.

Definition. An overdriven shock in a viscous fluid is one for which $\rho_a D^2\geq B_a+\frac{4}{3}\alpha_a G_{\infty a}$.

Theorem 4a. For an overdriven shock in a viscous fluid, no solution is possible without heat transport.

Now consider a viscoelastic fluid. TdS is given by (46). At small ϵ, dW^* must be of order $\epsilon d\epsilon$ at the lowest because dW^* is driven by the dynamic stresses τ and P^*, which are zero in state a. Hence for a viscoelastic fluid with $J=0$, $S-S_a$ is again of order ϵ^2 or higher. Then eliminating σ from Eqs. (23), (36), and (40) gives the following condition in leading order:

$$\rho_a D^2=B_{0a}+P_1^*+\tfrac{4}{3}\tau_1\,. \tag{69}$$

As D increases, the right side must increase. But the right side cannot increase indefinitely because both P_1^* and τ_1 are bounded. From (43) and (44), the elastic bound is

$$P_1^*+\tfrac{4}{3}\tau_1=B_{\infty a}-B_{0a}+\tfrac{4}{3}G_{\infty a}\,. \tag{70}$$

Hence Eq. (69) implies

$$\rho_a D^2<B_{\infty a}+\tfrac{4}{3}G_{\infty a}\,. \tag{71}$$

These results are summarized as follows.

Definition. An overdriven shock in a viscoelastic fluid is one for which $\rho_a D^2\geq B_{\infty a}+\frac{4}{3}G_{\infty a}$.

Theorem 4b. For an overdriven shock in a viscoelastic fluid, no solution is possible without heat transport.

The existence of this theorem for a fluid results from the same physical properties as does the corresponding theorem for a solid.[9] Without heat transport, there is an upper limit to the normal stress σ which can be developed by uniaxial compression of a material; this upper limit corresponds to purely elastic compression, without any plastic flow or viscous flow to relax the shear stress. If σ is required to go above this limit in the leading edge of a shock, it can only be accomplished by carrying heat to the leading edge and increasing the thermal pressure there.

In practice, the viscous overdriven threshold is about the same as the viscoelastic one, since the

right sides of (68) and (71) are about the same. For both a viscoelastic fluid and a solid,[9] the overdriven threshold is at $D=c_l$, with c_l the appropriate longitudinal sound velocity.

C. Viscous heat-conducting fluid

The viscous-fluid Rayleigh-line equations can be reduced to three equations in $\tau(\epsilon)$, $T(\epsilon)$, and $J(\epsilon)$. We expand these functions as in (57a)–(57d), and equate the first-order terms in the three equations to find

$$\tau_1=(\eta_{s\alpha}D/\kappa_\alpha)(J_1/T_1)\,, \tag{72}$$

$$\tfrac{4}{3}\alpha_\alpha\tau_1=\rho_\alpha D^2-B_\alpha-(\gamma_\alpha/D)J_1\,, \tag{73}$$

$$T_1=\gamma_\alpha T_\alpha+(\rho_\alpha DC_{V\alpha})^{-1}J_1\,. \tag{74}$$

This set of equations identifies the minimum shock strength, namely zero, as corresponding to $J_1=0$, $\tau_1=0$, $D=c$. We want to solve under the condition $J_1>0$, which implies $\tau_1>0$, $T_1>\gamma_\alpha T_\alpha$, $D>c$. From (73), the presence of the heat current acts to reduce τ_1; thus for a viscous fluid with heat conduction, the range of shock strengths for which a solution exists (a solution with $\tau_1<G_{\infty\alpha}$) is extended beyond the viscous fluid overdriven threshold. However, J_1 is not arbitrary, and there is still a limit to the range of shock strengths for which a physically acceptable solution exists. To discuss this limit, we will solve explicitly for τ_1.

Equations (72)–(74) produce a quadratic equation for τ_1:

$$\tfrac{4}{3}\alpha_\alpha\tau_1^2-(f+\tfrac{4}{3}\alpha_\alpha g+h)\tau_1+fg=0\,, \tag{75}$$

where

$$f=\rho_\alpha D^2-B_\alpha\geq 0\,, \tag{76}$$

$$g=\rho_\alpha D^2(\eta_{s\alpha}C_{V\alpha}/\kappa_\alpha)>0\,, \tag{77}$$

$$h=\rho_\alpha\gamma_\alpha^2C_{V\alpha}T_\alpha>0\,. \tag{78}$$

The two solutions are denoted τ_1^+ and τ_1^-. They are real and distinct for $D\geq c$ and are positive for $D>c$. We want the branch which approaches zero as $D\to c$; this is τ_1^-, which is called simply τ_1 henceforth. Properties of τ_1 are summarized as follows.

Limit $D\to c$

$$\tfrac{4}{3}\alpha_\alpha\tau_1=\frac{f}{1+(h/\tfrac{4}{3}\alpha_\alpha g)}+\cdots\,. \tag{79}$$

The expansion is in powers of f. As $D\to c$, $\tau_1\to 0$, and $h/\tfrac{4}{3}\alpha_\alpha g\to$ const.

Limit $D\to\infty$

(a) Large-viscosity case: $\tfrac{4}{3}\alpha_\alpha\eta_{s\alpha}C_{V\alpha}/\kappa_\alpha>1$.

This implies $\tfrac{4}{3}\alpha_\alpha g>f$ as $D\to\infty$. Then τ_1 goes as D^2, and the expansion is in powers of D^{-2}:

$$\tfrac{4}{3}\alpha_\alpha\tau_1=f\left|1-\frac{h}{\tfrac{4}{3}\alpha_\alpha g-f}+\cdots\right|. \tag{80}$$

(b) Small viscosity case: $\tfrac{4}{3}\alpha_\alpha\eta_{s\alpha}C_{V\alpha}/\kappa_\alpha<1$.

This implies $\tfrac{4}{3}\alpha_\alpha g<f$ as $D\to\infty$. Again τ_1 goes as D^2, and the expansion is in powers of D^{-2}:

$$\tau_1=g\left|1-\frac{h}{f-\tfrac{4}{3}\alpha_\alpha g}+\cdots\right|. \tag{81}$$

For all $D>c$

$$f-\tfrac{4}{3}\alpha_\alpha\tau_1>0\,, \tag{82}$$

$$g-\tau_1>0\,, \tag{83}$$

$$\tau_1 \text{ is monotone increasing with } D\,, \tag{84}$$

$$\tau_1 \text{ is monotone increasing with } \eta_{s\alpha}/\kappa_\alpha\,. \tag{85}$$

Qualitative behavior of τ_1 as a function of D^2 is shown in Fig. 2, for the two cases of large and small viscosity. Implications of the solution for τ_1 are discussed below.

D. Interpretation

The above results of viscous fluid theory have several important consequences. First, because $\tau_1\to 0$ as $D\to c$, according to (79), viscous fluid theory is always valid for sufficiently weak shocks. On the other hand, suppose we use viscous fluid theory to describe a sequence of shocks of increasing strength in a given fluid. Since τ_1 increases as D increases, by property (84), and τ_1 is not bounded, then τ_1 always reaches the elastic bound at a finite shock strength.

Definition. The viscous fluid limit is the shock strength for which viscous fluid theory gives $\tau_1=G_{\infty\alpha}$.

The significant point is that for shocks of strength near the viscous fluid limit and stronger, viscous fluid theory is not valid at small ϵ. Note that without heat transport, the viscous fluid limit is the same as the viscous fluid overdriven threshold; with heat conduction, the viscous fluid limit is

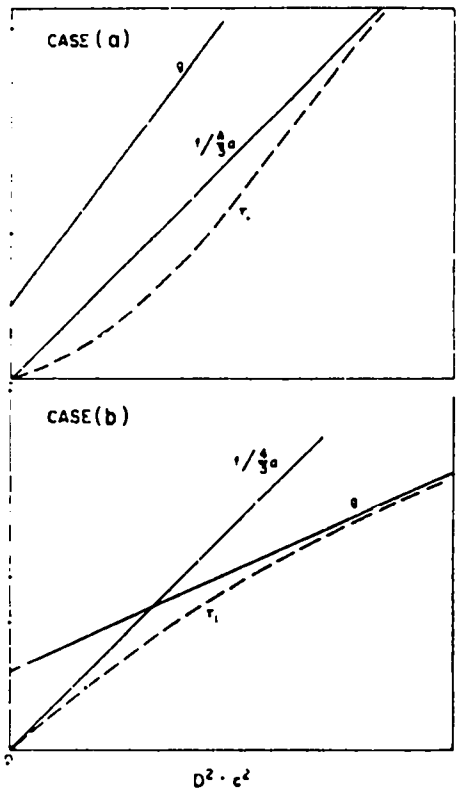

FIG. 2. Qualitative behavior of τ_1 as a function of D^2-c^2. Case (a) is large viscosity, case (b) is small viscosity, as defined in the text.

always greater than the viscous fluid overdriven threshold.

Consider again a sequence of shocks of increasing strength in a given fluid. As the elastic bound is approached, the fluid in the leading edge of the shock will no longer respond as a viscous fluid; τ_1 will not continue to increase strongly with D, but will remain approximately constant somewhat below $G_{\infty a}$, as D increases without limit. For shocks in this region, the initial response of the fluid is approximately that of a nonplastic solid, according to Theorem 3. One has to say "approximately" here, because the elastic bound is never quite reached. We therefore have the theorem:

Theorem 5. For shocks in a viscoelastic fluid, of strength near the viscous fluid limit and above, the fluid behaves approximately as a nonplastic solid in the leading edge of the shock.

It is of interest to consider a fixed shock strength and let the coefficient $\eta_{s\infty}/\kappa_a$ be varied. From property (85), τ_1 increases as $\eta_{s\infty}/\kappa_a$ increases, hence there is a unique elastic-bound value of $\eta_{s\infty}/\kappa_a$, which corresponds to $\tau_1 = G_{\infty a}$. For $\eta_{s\infty}/\kappa_a$ well below the bound we have viscous fluid response in the leading edge of the shock, while for $\eta_{s\infty}/\kappa_a$ near the bound and above it, we have approximately nonplastic solid response. The bound is a function of D. For shocks below the viscous fluid overdriven threshold, i.e., when (68) holds, the bound is infinite. As $D \to \infty$, the condition $\tau_1 = G_{\infty a}$ implies that the solution is case (b), the small viscosity case; then the bound is

$$\eta_{s\infty}/\kappa_a = G_{\infty a}/\rho_a D^2 C_{Va} \,. \tag{86}$$

Hence as $D \to \infty$, the elastic-bound value of $\eta_{s\infty}/\kappa_a \to 0$ as D^{-2}.

TABLE 1. Data needed to calculate the small-ϵ behavior of water and mercury. All quantities are evaluated at state a: $P=0$, $T \approx 293$ K.

Quantity	Water	Mercury
ρ(g/cm^3)	1.00	13.55
C_V(cal/g K)	0.99	0.0290
c(cm/μs)	0.148	0.146
s_1	2.0	2.1
γ	0.11	2.75
κ(cal/cm s K)	0.0014	0.020
η_s(g/cm s)	0.010	0.0155
η_v/η_s	2.8	1.2
G_∞(kbar)	10	50
ξ	0.0067	0.126
$\eta_s C_V/\kappa$	7.1	0.0225
h(kbar)	0.15	36

E. Water and mercury

Data needed to calculate the small-ϵ behavior of water and mercury are collected in Table I. The shock measurements of Walsh and Rice[11] were used to determine s_1. Litovitz and Davis[8] gave values of η_v/η_s, and they also estimated G_∞ for water at 273 K. We used the following method to estimate $G_{\infty a}$ for mercury. In the solid phase, $G/B = \omega$ is nearly independent of temperature for most materials, except near melting. With ω determined from this constant range, $\omega = 0.17$ for mercury, we set $G_{\infty a} = \omega B_a$ in the liquid phase. Such an estimate may be accurate within a factor of 2; the procedure gives 9 kbar for $G_{\infty a}$ in water. To calculate the overdriven threshold, we used the approximation $t_v/t_s = 1$ in state a, so the viscoelastic

overdriven threshold is the same as the viscous fluid overdriven threshold.

For a given fluid, we generally have to solve (75) numerically for τ_1 vs D^2, to find the viscous fluid limit. For water, however, the entire solution range $\tau_1 \leq G_{\infty a}$ is in the $D \to c$ limit, Eq. (79). This circumstance results from a number of factors, the most significant being that $\eta_s C_V/\kappa$ is large compared to 1 for water at 293 K. For water, we find the inviscid limit is at a shock pressure of 0.040 kbar, the overdriven threshold is at 13 kbar, and because the factor $h/\frac{4}{3}\alpha_a g$ in (79) is extremely small, the viscous fluid limit is barely beyond the overdriven threshold; the shock pressure at the viscous fluid limit is 1.0003 times the shock pressure at the overdriven threshold.

For mercury, the inviscid limit is at 9 kbar and the overdriven threshold is at 33 kbar. The solution of (75) for τ_1 when the viscous fluid limit is reached is in the $D \to \infty$ limit, small-viscosity case, Eq. (81). This situation is probably representative of liquid metals in general and is due to a number of factors, the most significant being $\eta_s C_V/\kappa << 1$ in state a. Our calculation gives 690 kbar for the viscous fluid limit of mercury.

As mentioned in Sec. I, we expect irreversible thermodynamics to be valid for shocks up to some critical strength, and not valid for stronger shocks. For metals, solid or liquid phase, our preliminary estimate places this critical limit in the region of a few Mbar.[12] Hence the present computations for liquid mercury should be in the range of validity of irreversible thermodynamics.

ACKNOWLEDGMENTS

The author is grateful to Bill Hoover, Roy Axford, and B. R. Suydam for helpful discussions on shock physics.

[1]Lord Rayleigh, Proc. R. Soc. London, Ser. A 84, 247 (1910).
[2]Ya. B. Zel'dovich and Yu. P. Raizer, *Physics of Shock Waves and High-Temperature Hydrodynamic Phenomena* (Academic, New York, 1966 and 1967), Vols. 1 and 2.
[3]W. G. Hoover, Phys. Rev. Lett. 42, 1531 (1979).
[4]B. L. Holian, W. G. Hoover, B. Moran, and G. K. Straub, Phys. Rev. A 22, 2798 (1980).
[5]W. Prager, *Introduction to Mechanics of Continua* (Ginn, Boston, 1961).
[6]L. D. Landau and E. M. Lifshitz, *Fluid Mechanics* (Pergamon, London, 1959).
[7]D. C. Wallace, Phys. Rev. B 22, 1477 (1980).
[8]T. A. Litovitz and C. M. Davis, in *Physical Acoustics*, edited by W. P. Mason (Academic, New York, 1965), Vol. IIA, p. 281.
[9]D. C. Wallace, Phys. Rev. B 24, 5597 (1981).
[10]D. C. Wallace, Phys. Rev. B 22, 1487, 1495 (1980).
[11]J. M. Walsh and M. H. Rice, J. Chem. Phys. 26, 815 (1957).
[12]Theoretical calculations of the shock process for solid metals are given in Wallace, Phys. Rev. B 24, 5607 (1981).